Characterisation of Chemical Ageing Processes in Encapsulant Materials Used in PV Modules

Master's Thesis

by

Florian Wagner

Work performed at

Polymer Competence Center Leoben GmbH

and

Institute of Material Science and Testing of Polymers

at the Montanuniversitaet Leoben

Supervision: Dr.mont. Gernot Oreski, DI Bettina Hischmann

Academic Advisor: Univ.-Prof. DI Dr.mont. Gerald Pinter

Leoben, June 2015

AFFIDAVIT

I declare in lieu of oath, that I wrote this thesis and performed the associated research myself, using only literature cited in this volume.

EIDESSTATTLICHE ERKLÄRUNG

Ich erkläre an Eides statt, dass ich diese Arbeit selbstständig verfasst, andere als die angegebenen Quellen und Hilfsmittel nicht benutzt und mich auch sonst keiner unerlaubter Hilfsmittel bedient habe.

LEOBEN, June 2015 **(Florian Wagner)**

ACKNOWLEDGMENTS

I would like to express my sincere gratitude to Univ.-Prof. DI Dr.mont. Gerald Pinter and DI Dr.mont. Gernot Oreski for giving me the great opportunity to write my Master's thesis in cooperation of the Institute of Materials Science and Testing of Polymers at the Montanuniversitaet Leoben and the Polymer Competence Center Leoben. It was a huge enrichment for my scientific experience and gave me the possibility to expand my knowledge in the field of chemical analysis of polymers as well as in the planning and structuring of scientific research.

A special thank you goes to my supervisor DI Bettina Hirschmann for her guidance and advises throughout the thesis. She helped me greatly in the planning process of the thesis, handling the testing equipment and provided me always with very helpful information.

I am also very grateful to Dr. Melanie Brasch and the Institute of Chemistry of Polymeric Materials at the Montanuniversitaet Leoben for the measurement and analysis of the HPLC-MS/UV experiments.

In addition I thank DI Marlene Knausz, Astrid Rauschenbach and M.Sc Andrea Wanner of the Polymer Competence Center Leoben that helped me handling the machines, gave me important advises for my experiments and provided helpful literature for my thesis.

ABSTRACT

Polymer films used as encapsulant materials in PV modules are responsible for the optical and mechanical connection of different layers of the module, electric isolation, protection of the solar cell against mechanical damage and work as a barrier against environmental impurities. The application range of PV modules is expected to be up to 25 years with only 20% reduction in the power output during that time. Changing environmental conditions as day-night-cycles, annual thermal changes as well as weather conditions like hail, rain, wind or dust cause high requests in the material properties and demand a sophisticated knowledge on the ageing behaviour of these polymers. In this thesis the focus is laid on the characterisation of the chemical ageing processes of the commercially most applied ethylene-vinyl acetate copolymer (EVA) and an alternaive polyethylene (PE) encapsulant. To simulate conditions found in PV modules the samples were artificially aged using damp heat exposure (85 °C/85 RH) and xenon weathering (90 W/m², 60°C, wet/dry cycles) for 2000 hours. The encapsulant materials were exposed as single films and incorporated in a laminate to observe the ageing processes in different microclimates at the polymer films. Infrared spectroscopy, Raman spectroscopy and differential scanning calorimetry measurements showed the formation of various photo-oxidation products, C=C double bonds, post crosslinking, fluorescence and changes of the polymer structure of the encapsulants. Ultraviolet/Visible/Near-infrared spectroscopy detected discolouration and changes of the reflectance properties of the polymers and with high performance liquid chromatography additives present in the polymers could be determined. It was shown that the exposure of the encapsulant materials as single films or incorporated in a laminate resulted in very different ageing behaviour due to the different microclimates at the polymer films.

KURZFASSUNG

Einkapselungsmaterialien für Photovoltaik Module bestehend aus Kunststofffolien sind verantwortlich für die mechanische und optische Verbindung der einzelnen Schichten des Modules, elektrische Isolation, den Schutz der Solarzelle vor mechanischem Schaden und der Diffusion von Schmutzpartikeln aus der Umwelt. Die Lebensdauer von Solarmodulen soll bis zu 25 Jahren mit höchstens 20% an Leistungsverlust betragen. Wechselnde Umweltbedingungen wie Tag-Nacht-Zyklen, jährliche Temperaturschwankungen und auch Wetterbedingungen wie Regen, Hagel, Wind oder Staub stellen hohe Herausforderungen an diese Materialien. Ein reichhaltiges Wissen über die Alterungsprozesse dieser Polymere ist daher unumgänglich. Der Fokus dieser Arbeit liegt auf den chemischen Alterungsprozessen des kommerziell meist eingesetzten Ethylenvinlyacetat Copolymers (EVA) und eines alternative Einkapselungsmaterials aus Polyethylen. Um die Umweltbedingungen zu simulieren, die auf Einkapselungsmaterialien in einem Photovoltaik Modul wirken, wurden die Materialien mit dem Damp Heat Test (85 °C/85 RH) und der Xenonbewitterung (90 W/m², 60°C, Nass-/Trockenzyklen) für 2000 Stunden künstlich gealtert. Die Einkapselungsmaterialien wurden als einfache Folien und in einem laminierten Verbund ausgelagert um die Alterung bei unterschiedlichen Mikroklimas zu untersuchen. Mit Hilfe von Infrarotspektroskopie, Raman Spektroskopie und dynamischer Differenzkalorimetrie konnte die Formierung diverser Photo-oxidationsprodukte, C=C Doppelbindungen, Nachvernetzung, Fluoreszenz und Veränderungen der Polymerkette in den Einkapselungsfilmen festgestellt werden. Die Ultraviolett/Visible/Nahinfrarot Spektroskopie lieferte Ergebnisse zu Verfärbungen und Veränderungen des Reflexionsverhaltens und mit Hochleistungs-flüssigkeitschromatographie konnten Additive in den Materialien bestimmt werden. Es konnte gezeigt werden dass die Auslagerung der Einkapselungsmaterialien als Folie oder in einem Verbund durch die verschiedenen Mikroklimas ein sehr unterschiedliches Alterungsverhalten aufweisen.

LIST OF CONTENT

ABBREVIATIONS AND ACRONYMS

PV	Photovoltaic
IR	Infrared
NIR	Near-Infrared
ATR	Attenuated Total Reflectance
MS	Mass Spectrometry
HPLC	High Performance Liquid Chromatography
DSC	Differential Scanning Calorimetry
DH	Damp Heat Ageing
XE	Xenon Weathering
VLP	Vacuum Lamination Press
LO	Laboratory Oven
UV	Ultraviolet
Vis	Visible
EVA	Ethylene-vinyl acetate
PE	Polyethylene
PVF	Polyvinly Fluoride
PET	Polyethylene Terephthalate
PVC	Polyvinylchloride
HALS	Hindered Amine Light Stabilizers
RH	Relative Humidity
λ	Wavelength
$\tilde{\nu}$	Wavenumber
Θ	Angle of Incidence
d_p	Depth of Penetration
$\dot{Q}$	Heat Flow

v	Heating Rate
T	Temperature
c_p	Specific Heat Capacity
m	Mass
H	Enthalpy
h	Planck Constant
v_0	Frequency of an Electromagnetic Wave
I_0	Intensity of the Incident Light
I_R	Intensity of the Reflected Light
I_A	Intensity of the Absorbed Light
I_T	Intensity of the Transmitted Light
ESI	Electrospray Ionization
cm	Centimetre
µm	Micrometre
nm	Nanometre
µl	Microlitre
min	Minute
h	Hour
m/z	Atomic Mass Unit/Number of Charges
g/mm	Grooves/Millimetre

1 INTRODUCTION AND OBJECTIVE

The energy demand of the world keeps increasing every year and is covered mainly by fossil energy sources (International Energy Agency, 2014). The non-regenerative nature of these sources itself requires the search for alternative options. Renewable energies make use of natural, sustainable sources as wind, water, geothermal heat or the sun to produce energy (Quaschning, 2010). Every year sunbeams reach the surface of the earth holding 5000 times the energy needed on the entire planet (Klima- und Energiefonds, 2014). Clearly the possible energy output from solar energy has to be relativised and depends on many factors but the potential of this energy source still remains enormous. Photovoltaic (PV) is a climate friendly technology that uses the sunlight to produce electricity and its market has been growing rapidly over the last three decades (Razykov et al., 2011). The equipment used to realise the conversion of sunlight to electrical power is a photovoltaic (PV) module. PV modules have operating times longer than 25 years and are exposed to direct sunlight, rain, temperature changes and other ambient conditions during their application (Czanderna and Pern, 1996; Hasan and Arif, 2014). The request to PV module materials to endure such challenging conditions during the long period of use demands a high knowledge about their stability and their ageing processes to assure a good performance with minimal efficiency loss.

A standard PV module consists of a glass cover, an encapsulant layer, the solar cell, a second encapsulant layer and a backsheet layer. The encapsulant layers are polymeric films responsible for the optical and mechanical connection of the different layers in the PV module, the mechanical protection and isolation of the solar cell as well as for protection against environmental exposure (Hasan and Arif, 2014; Czanderna and Pern, 1996; Kempe et al., 2007). Crossllinked ethylene-vinyl acetate (EVA) copolymer is currently the dominating encapsulant polymer in the industry and many investigations cover physical testing of this material as the delamination from the backsheet layer, diffusion of water in the PV module or the thermal transitions of polymers (Agroui et al., 2012; Hasan and Arif 2014; Oreski and Wallner, 2005; Hülsmann and Weiss, 2015). Apart from physical changes the outdoor environment can also cause chemical changes in the material that result in discoloration and therefore could reduce the efficiency of the PV module, support corrosion of circuit materials due to the separation of acids or lead to a reduction of the lifetime of the whole module (Erzin et al., 1995; Kempe et al., 2007; Klemchuk et al., 1997). It is important to analyse

the chemical ageing processes that may occur during the application of the PV modules to improve the stabilisation and the performance of these materials as well as to get a better understanding of the impact the environmental conditions have on chemical ageing. To simulate outdoor exposure accelerated artificial ageing is used. The big advantages of artificial ageing methods are relatively short exposure times and repetitive laboratory conditions that can be achieved (Ehrenstein and Pongratz, 2007). Xenon weathering simulates the exposure to direct sunlight with dry/rain cycles and damp heat ageing exposes the samples to increased temperatures and humidity that can be found in a PV module (Atlas Material Testing Solutions, 2001; IEC 61215). The exposure to these ageing methods favours different ageing behaviour of the tested material and many investigations have been carried out on the photo-oxidative and thermo-oxidative ageing of PV encapsulants.

When looking at the publications regarding this field of reasearch it can be observed that artificial ageing was carried out with plain films or with films incorporated in PV modules (Erzin et al., 1995; Pern, 1996; Allen et al., 2000). The chemical ageing behaviour of EVA encapsulants has been broadly investigated but no studies focused on the impact of the microclimate at the polymer film (Peike et al., 2011; Klemchuk et al., 1997; Allen et al., 2000; Pern, 1996; Rodríguez-Vásquez et al., 2006). When incorporated in a PV module the environment of the encapsulant film changes compared to the single film. The other layers of the module may work as barriers and influence oxygen and humidity diffusion to the encapsulant layer (Peike et al., 2012; Jorgensen et al., 2006). Thus, the same exposure of the same material may lead to different results due to a different microclimate at the polymer film. Investigations showed that films aged in PV modules showed a stronger discolouration in the centre while on the edge area no discolouration could be observed (Pern, 1996). Allen et al. also described a greater degradation rate and formation of coloured products of EVA in an oxygen atmosphere than in a nitrogen atmosphere (Allen et al., 2000). The oxygen concentration at the encapsulant might have a large influence on the photo- and thermo-oxidation reactions of the polymer. The question to expose application near in a PV module or to investigate the behaviour of the pure material without the influence of surrounding parts depends on the study case. Anyhow, it is crucial to determine the impact the type of exposure has on the investigated ageing behaviour and compare the outcome after the ageing in different microcilmates at the encapsulant materials.

2 PRINCIPLES

2.1 Materials and Application

PV modules play an important role for the generation of energy from renewable energy sources. A standard PV module consists of a glass front, a polymer encapsulant layer, the solar cell, a second encapsulant layer and the polymeric backsheet layer. The structure of a PV module can be seen in Figure 2.1. Additional to the mainly used glass/polymer module type mentioned above there are constructions with glass front and glass backsides and modules with polymeric front and backsides, respectively. The glass/glass type is a heavy construction which is used for application at building fronts due to security regulations. The polymer/polymer module is very light and flexible that makes it easier to mount and opens new possibilities of applications as for instance the incorporation in vehicle roofs (Plessing, 2003; Klemchuk et al., 1997).

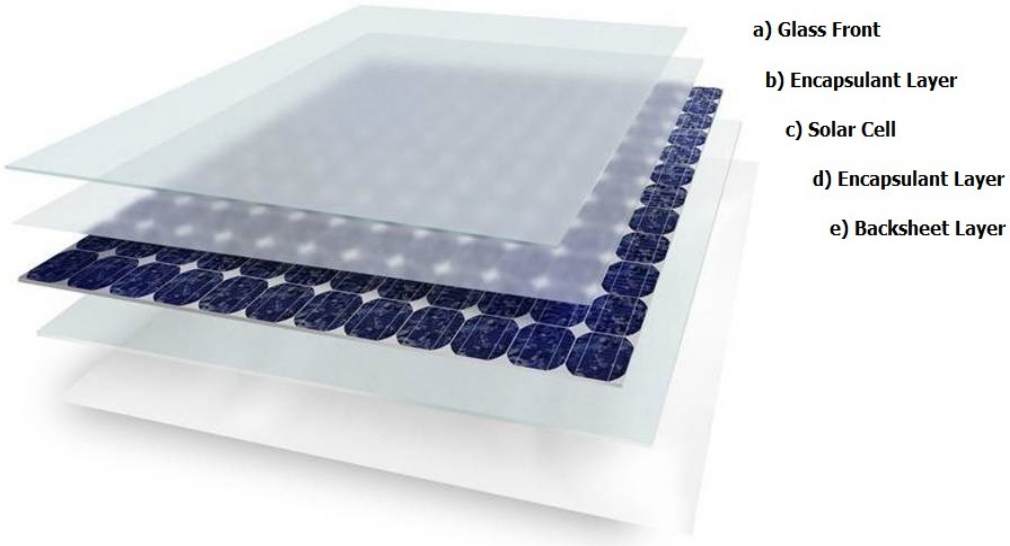

Figure 2.1: Structure of a PV module with a) glass front, b) encapsulant layer, c) solar cell, d) encapsulant layer and e) backsheet layer.

The energy conversion from light into electricity is carried out by the solar cell which is placed in the centre of the PV module. The glass front provides electrical isolation, mechanical stiffness and protection against the diffusion of environmental impurities and moisture in the PV module. Special glasses with low Fe content are applied to assure high transmittance of the cover. An attenuation of the UV portion of the incident light because of the glass cover can still be the case. The result is a lower effieciency of the PV module but a better protection of the encapsulant layer due to a reduced UV radiation

(Klemchuk et al., 1997). The backsheet is typically a polymeric multilayer laminate consisting of fluoropolymers and polyehtylenetherephthalate (Gambogi, 2010). The function of the backsheet is to provide electrical and environmental isolation but no transmittance is required. The backsheet acts as a mechanical barrier against diffusion of oxygen and water in the PV module. Glass provides better diffusion barrier properties than polymers but results in a large weight increase of the PV module. Depending on the laminate applied as backsheet layer different degrees of diffusion can be found (Klemchuk et al., 1997; Peike et al., 2012). The encapsulant layers are needed to mechanically and optically connect the front and back cover with the solar cell. Beyond that the main functions of these layers are to protect the solar cell against mechanical damage and to avoid moisture and foreign impurities to diffuse into the solar cells. Some other necessary properties are a high transmittance of light at wavelengths between 300 and 1100 nm and a good thermal conduction to avoid efficiency loss. The material should further be cheap, easy to process and is needed to have a long operating range due to required lifetimes of PV modules of up to 25 years with only 20% reduction in the power output (Hasan and Arif, 2014). The properties of the encapsulant are critical to the long term stability of the module. Changing environmental conditions as day-night-cycles, annual thermal changes as well as weather conditions like hail, rain, wind or dust, cause high requests in the material properties (Czanderna and Pern, 1996).

Crosslinked ethylene-vinyl acetate (EVA) copolymer has been widely used as an encapsulant material in PV modules since the 1980s and is now the dominant encapsulant polymer in the industry (Pern, 1993; Hasan and Arif, 2014). Initially polyethylene (PE) was chosen because of its simple structure and low cost. However, it has the disadvantage of an opaque appearance due to its semi-crystalline nature. Therefore vinyl acetate content was added (EVA) to reduce the crystallinity and increase the transparency (Hsu et al., 2010). The chemical structures of PE and EVA can be seen in Figure 2.2.

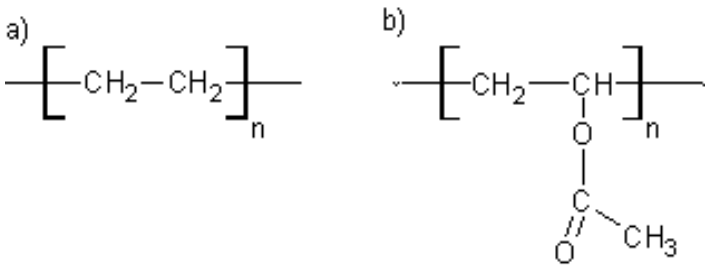

Figure 2.2: Chemical structure of a) polyethylene (PE) and b) ethylene-vinly acetate copolymer (EVA).

EVA is crosslinked with peroxides to increase the stiffness of the material and to allow higher application temperatures. The polymer was mainly chosen because of the low price of the material (Czanderna and Pern, 1996).

The exposure to an outdoor environment for many years demands a good knowledge of possible material changes that occur during application time. Thermal degradation occurs when the material is exposued to temperature without the presence of oxygen. Chain scission or post-crosslinking may be the result of thermal ageing. In the presence of oxygen the ageing reactions may start at lower temperatures and oxidation products can be formed. In practice these thermo-oxidation reactions predominate the thermal degradation. The tendency to degrade may vary depending on the oxygen concentration that can catalyse the reactions. Photo-oxidation reactions are caused by the irraditation with light under the presence of oxygen. The degradation of polymers is mainly caused by the irradiance with light in the UV range between 300 and 400 nm. In a PV module the conditions for photo-oxidations can be found in positions with direct exposure to sunlight and thermo-oxidation is favoured behind the solar cell. The oxygen concentraton that catalyses these reactions may vary in the PV module. The material changes that occur can be differentiated in physical and chemical ageing processes. Physical ageing includes reversible processes as for example post-crystallisation, changes in molecular orientations or internal stresses of the material. Chemical ageing is understood as irreversible processes in the material as for example changes of the molecular structure, the formation of functional groups or the separation of decomposition products (Ehrenstein and Pongratz, 2007). Experience with PV modules shows that physical ageing as delamination of the interfaces, permeation of water through the encapsulant, stresses caused by different thermal expansion coefficients or short circuits are examples of problems that may occur during the application and can lead to failure of the PV module (Czanderna and Pern, 1996). A major problem in the use of EVA is the chemical ageing of the material during the application. Discoloration, diffusion or degradation of additives, the formation of double bonds and degradation products may affect the optical properties of the material and lower the efficiency of the whole PV module. Chemical changes as post-crosslinking or chain scission can have a big impact on the mechanical properties and reduce the lifetime of the module (Pern, 1996; Pern and Czanderna, 1992a). In this thesis the focus is laid on the characterisation of these chemical ageing processes.

The formation of acetic acid is the initial step in EVA degradation and has been reported by Kempe et al. and Allen et al. (Kempe et al., 2007; Allen et al., 2000). EVA will produce

acetic acid when exposed to UV light or water. Beside the remaining double bond, the acetic acid works autocatalytic for further chain degradation. As a result the pH value increases which is very likely to have an impact on the corrosion of circuit materials (Peike et al., 2013b; Kempe et al., 2007). Other degradation products of EVA like lactones, ketones, unsaturated carbonyls, hydroxyl groups and anhydride formation have been reported by Allen et al. and Çopuroğlu and Şen (Allen et al., 2000; Çopuroğlu and Şen, 2004). Figure 2.3 shows three possible degradation reactions (Norrish type I, II and III) due to induced UV irradiation where oxygen radicals, aldehydes (Norrish I), C=C double bonds, acetic acid (Norrish II) and ketones (Norrish III) are formed.

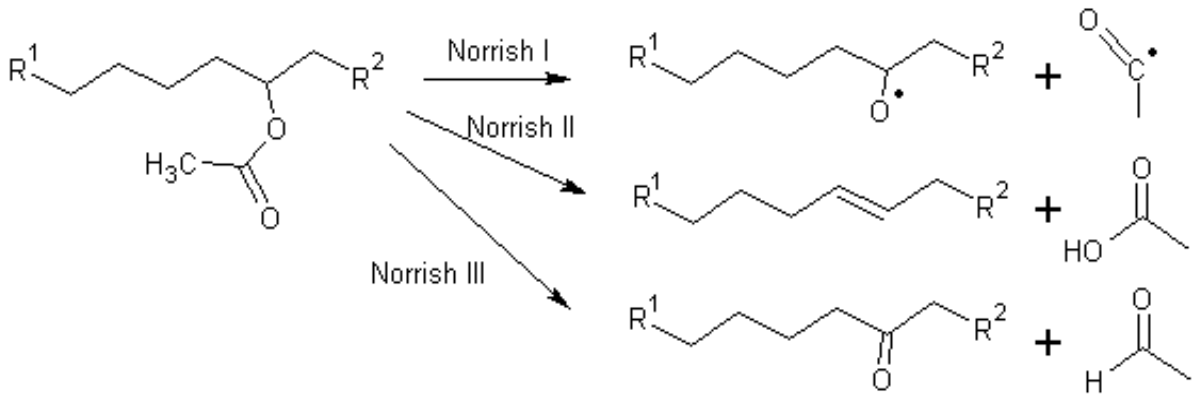

Figure 2.3: Degradation mechanisms of EVA due to UV irradiation (Pern and Czanderna, 1992b).

A big problem of EVA is its tendency to change the colour as a result of chemical ageing. The discolouration is called yellowing due to the yellow appearance of the material after weathering. Early approaches to explain the cause of the yellowing came deriving from polyvinylchloride (PVC) research. It was assumed that the formation of conjugated C=C double bonds in the polymer chain causes the discolouration (Pern and Czanderna, 1992a; Pern, 1993). It can be seen in Figure 2.3 that double bonds can be formed during the formation of acetic acid from the vinyl acetate group (Norrish II). Pern and Czanderna described that a depletion of the UV absorber in the polymer results in yellowing mainly due to polyenes and possible contributions of discolouring elements as photo transformed moieties of for instance stabilizers were not ruled out (Pern and Czanderna, 1992a; Pern, 1996). Allen et al. later distinguished the nature of polyconjugation from PVC and EVA (Allen et al., 2000). The polymers showed different UV absorption spectra for similar discoloured samples and discoloured EVA could not be bleached by the treatment with bromine, maleic anhydride or paracetic acid as observed

for PVC. Further studies showed that the cause of yellowing is more likely due to changes of additives and polymer oxidation. The interaction of stabilizing additives with remaining peroxides was observed to result in the formation of chromophores that appear yellow and also the oxidation of the encapsulant might have an impact on the discolouration (Klemchuk et al., 1997; Ezrin et al., 1995). Rodríguez-Vásquez et al. suggested that the species responsible for the colour formation in EVA is due to polyconjugated carbonyl products (Rodríguez-Vásquez et al., 2006). Morlier et al. reported that the curing state of EVA influences the materials stability towards oxidation when exposed to damp heat ageing (Morlier et al., 2013). Materials with high amounts of curing agents (peroxides and coactivators) showed lower stabilities. The chemical reaction of the UV absorber and the peroxide to form chromophore precursors can be seen in Figure 2.4.

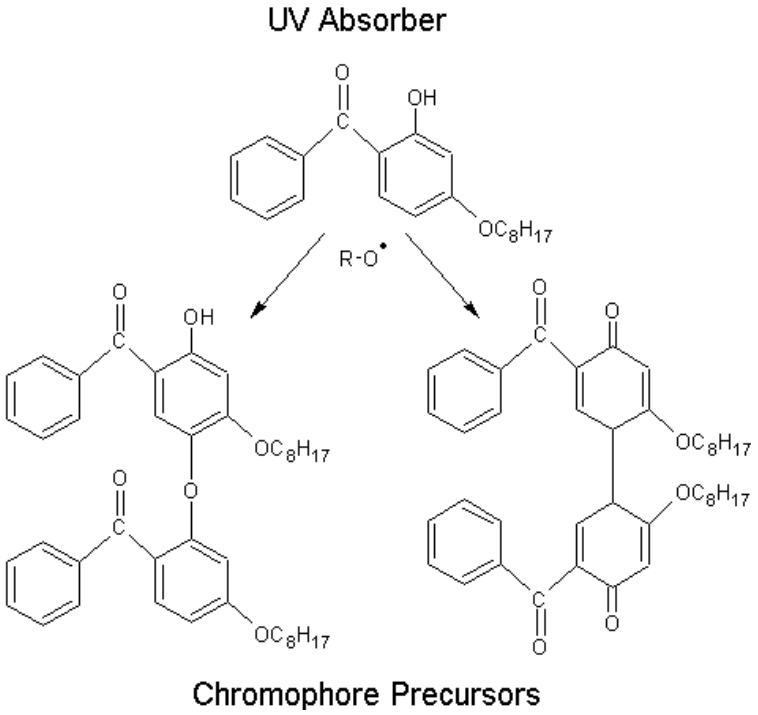

Figure 2.4: Reaction of UV absorber with peroxide to chromophore precursors (Klemchuk et al., 1997).

A recent study from Peike et al. suggests that even though the main thermal and photochemical degradation process of EVA results in the formation of conjugated moieties capable of absorbing visible light it is the formation of chromophores due to additives in the material that is responsible for the yellowing of the material. Highly stabilised EVA foils in this study showed higher discolouration rates and foils with just one additive added showed only minor changes in colour (Peike et al., 2013c).

Beside EVA other polymers as for instance ethylene copolymers based on vinyl acetates or acrylic acids or modified polyethylene might be used as encapsulant materials (Oreski and Wallner, 2009). Usually low density polyethylene is used because it has a more amorphous structure than high density polyethylene. Modifications needed to fit the requests for the PE to be used as a PV encapsulant material are for instance due to the oxidation of the polymer (Hsu et al., 2010). PE consist of a saturated polymer chain with no vinyl acetate groups and therefore shows no formation of acetic acid during ageing. Under the exposure to UV irradiation and oxygen atmosphere the formation of various oxidation products as well as chain scission and the appearance of C=C double bonds is known (Carrasco et al., 2001; Ehrenstein and Pongraz, 2007; Salvalaggio et al., 2006).

2.2 Artificial Ageing

To test how materials and the whole PV module change during application it would be necessary to run experiments on samples that have been applied for several years. The advantage would be material information under the prevailing conditions and influences, but the disadvantage is the extremely long waiting period. This makes material development a very long lasting process and to shorten the testing period it is possible to use artificial ageing. Additionally artificial ageing brings advantages such as the independence of the prevailing climate, air pollutions or seasonal changes. Exact adjustments and setups of artificial ageing conditions make it comparable and repeatable at other testing locations. The correlation between natural and artificial weathering with electromagnetic radiation is given for instance by the calculation of the amount of irradiation. It has to be considered that an increased irradiation also leads to increased sample temperatures and possibly different ageing conditions. An aware choice and control of the sample temperature is therefore a crucial parameter for the correlation. Nevertheless the comparison of natural and artificial weathering has to be interpreted with caution because ageing processes might run differently when exposed to the same amount of irradiation but at stronger rates. Artificial ageing can be applied by various methods. In this thesis damp heat ageing and xenon weathering were chosen. In xenon weathering the source of irradiation is a xenon arc lamp which simulates UV and visible solar irradiation. This method is preferred when the tested material will be exposed to natural sunlight (Ehrenstein and Pongraz, 2007; Atlas Material Testing Solutions, 2001). A comparison of the relative irradiation strengths of a xenon arc lamp and sunlight can be seen in Figure 2.5.

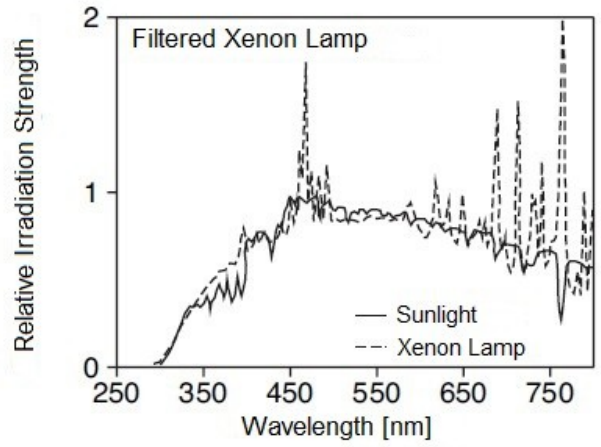

Figure 2.5: Relative irradiation stregth of a xenon arc lamp compared to the irradiation of sunlight (Ehrenstein and Pongratz, 2007).

The samples are positioned in a xenon tester on a rack that rotates around the xenon arc lamp. Water spraying installations in the tester allow the simulation of rain and humidity and different exposure programs with dry and wet cycles can be adjusted. Furthermore conditions as for instance the sample temperature, humidity or amount of irradiation can be controlled (Atlas Material Testing Solutions, 2001). The artificial ageing in a damp heat tester differs from the weathering in a xenon tester. In a damp heat exposure no irradiance with electromagnetic waves is applied. The samples are exposed to increased temperature with a set relative humidity and no direct spraying of water (IEC 61215). The different types of exposure of these ageing methods result in different ageing processes of the material. The xenon arc test favours a photo-oxidative degradation of the material and the damp heat test a thermo-oxidative degradation (Rodríguez-Vásquez et al., 2006).

Additional to the ageing method also the type of exposure may lead to a different degradation. Allen et al. for instance found out that the degradation rate of EVA as well as the formation of coloured products is greater in oxygen than in nitrogen atmosphere. Another observed effect after the ageing of PV modules is the stronger discolouration in the centre of the module than at the edge (Allen et al., 2000). The edges tend to be less discoloured or show no optical changes (Klemchuk et al., 1997). A possible explanation is photobleaching where it is assumed that the reason is the photo-oxidation of chromophores – the parts of the molecules responsible for its colour - at the edge areas of the modules where oxygen can diffuse to (Pern, 1996). The different conditions at the edge of a PV module result in different results regarding discolouration. The microclimate at the encapsulant film has a large impact on the chemical aging behaviour. The chemical

ageing of EVA has been broadly investigated but when looking at publications it can be seen that research was made with films or PV modules but no studies investigate the comparison of the chemical ageing of films and films laminated in a PV module (Erzin et al., 1995; Pern, 1996; Allen et al., 2000).

3 EXPERIMENTAL

3.1 Materials and Preparation

In this thesis four commercially available encapsulant materials were investigated, three ethylene-vinyl acetate copolymer (EVA) types and one polyethylene (PE) type. The EVA types were the fast curing Vistasolar 486.00®, the ultra fast curing Vistasolar 520.78® and the fast curing NovoVellum Optima MF01® (Solutia, 2012a; Solutia, 2012b; Novopolymers NV, 2012). According to literature the vinyl acetate content was 33% of EVA Vistasolar 486.00® and EVA NovoVellum Optima MF01® (Carsson et al., 2006; Novopolymers NV, 2012). The vinyl acetate content of EVA Vistasolar 520.78® could not be found in the literature. The non curing polyethylene encapsulant was PV-FS Z68® (Dnpsolar, 2010). An overview of the investigated materials can be seen in Table 3.1.

Table 3.1: Overview of investigated encapsulant materials.

Name	Company	Material	Type
Vistasolar 486.00	Solutia Inc.	EVA	fast cure
Vistasolar 520.78	Solutia Inc.	EVA	ultra fast cure
NovoVellum Optima MF01	Novopolymers NV	EVA	fast cure
PV-FS Z68	dnpSolar	PE	non curing

Films and glass/encapsulate/backsheet laminates were prepared with dimensions of approximately 7x25 cm. For the laminated samples one layer of encapsulant and a PVF/PET/PVF multilayer-backsheet were used. No sealant was applied on the edges of the laminate. Figure 3.1 schematically displays the cross section of a) a film sample and b) a laminated sample.

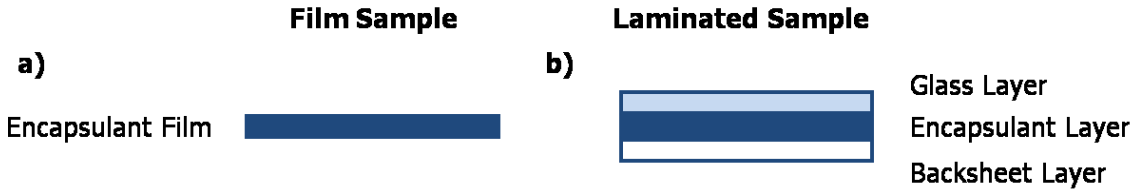

Figure 3.1: Schematic display of the cross section of the a) films and b) the laminated samples.

Film and laminated samples were cured in a vacuum lamination press (VLP). Films were placed between two glass covers with two anti-stick foils inbetween so they would cure under the same conditions as the laminates but would not attach to the glass covers. The

polyethylene type was treated under the same conditions as the EVA types to provide comparability. The lamination process lasted 16:20 minutes at 144 °C and consisted of the evacuation step (6 min, 144 °C) and the following curing step (10:20 min, 144 °C) at a reduced pressure of 850 mbar. The EVA films which were exposed to damp heat ageing were cured in a Heraeus Vakuumtrockenschrank VT 6025 laboratory oven (LO) at 150 °C for 45 min under a pressure of 350 - 500 mbar. The parameters of the LO curing were evaluated by a series of Differential Scanning Calorimetry measurements of different curing times and temperatures of NovoVellum Optima MF01® films. The LO preparation was adjusted to achieve similar degrees of curing as found in the VLP prepared samples to provide comparability. The thickness of the samples was between 0,45±0,03 mm and 0,59±0,04 mm for the films and between 5,69±0,03 and 5,80±0,01 mm for the laminates. The specific thickness values of the EVA and PE films and laminates can be seen in Table 3.2.

Table 3.2: Thickness values of the EVA and PE encapsulant plain film and laminated samples.

Material	Thickness [mm]		
	Film - VLP	Film - LO	Laminate
Vistasolar 486.00	0,50±0,03	0,47±0,01	5,70±0,05
Vistasolar 520.78	0,51±0,03	0,59±0,04	5,80±0,01
NovoVellum Optima MF01	0,45±0,03	0,55±0,04	5,69±0,03
PV-FS Z68	0,56±0,01	-	5,78±0,02

3.2 Artificial Ageing

All film and laminated samples were exposed to artificial ageing. In order to support thermo-oxidative ageing processes damp heat ageing (DH) was chosen according to IEC 61215. This storage of the samples was conducted under 85°C and 85% relative humidity (RH) in a climate chamber (Weiß Umwelttechnik GesmbH, Austria). To evaluate the influence of radiation the second artificial ageing method was xenon arc lamp weathering (XE) to support photo-oxidative ageing processes. Films and laminates were exposed according to ISO 4892-2 in a Xenontest Beta LM (Atlas Material Testing Technology GmbH, Germany) with an increased irradiance of 90 W/m² between 300 and 400 nm. The dry phase of the exposure cycle lasted 102 minutes and the wet (rain) phase lasted 18 minutes, where water was sprayed on the samples. The temperature inside the chamber was 60°C throughout the exposure. All film and laminated samples were

exposed for up to 2000 hours. In the experiments unaged, but cured samples were used for comparison. The unaged laminated samples were the same for both exposure methods and for the DH films reference samples were produced in the LO to provide comparability. An overview of the exposure of the samples can be seen in Table 3.3.

Table 3.3: Overview of the exposure of the samples.

Exposure Time [h]	Damp Heat Ageing 85°C - 85% RH		Xenon Weathering 90 W/m² - 60 °C - wet/dry	
	Film	Laminate	Film	Laminate
0	✓	✓	✓	✓
500	✓	-	-	-
1000	✓	✓	✓	✓
2000	✓	✓	✓	✓

3.3 Characterisation Methods

A well chosen combination of characterisation methods is crucial to provide a comprehensive analysis of the chemical aging processes. In this thesis the encapsulant films and laminates were tested by Infrared (IR) spectroscopy, Raman spectroscopy, Ultraviolet/Visible/Near-infrared (UV/Vis/NIR) spectroscopy, high performance liquid chromatography (HPLC) with mass spectrometry (MS) and ultraviolet (UV) detectors and differential scanning calorimetry (DSC).

3.3.1 Infrared (IR) Spectroscopy

Infrared (IR) spectroscopy is one of the most important methods in analytical chemistry as well as in polymer characterisation. The main applications in polymer analysis are the identification of polymeric materials and the clarification of their chemical structure. The physical principle of this method is the interaction of molecules with IR light where the incident electromagnetic wave provokes oscillations of parts of the molecules. Absorption only occurs when the frequency of the light matches the resonance frequency of a molecular vibration. Functional groups are only IR active – absorb IR light – if the induced oscillation results in a change of the dipolar moment. Polar groups (e.g. CO, OH, CN) for instance have a dipolar moment and can therefore interact with IR light, but also non polar groups such as CH or C=C are IR active if an induced oscillation results in shift of the charges and therefore a change in the dipolar moment. The IR light is found at longer wavelengths λ than visible light in the electromagnetic spectrum. It is categorised in three regions - the near (0,7 – 2,5 µm), the middle (2,5 – 100 µm) and the far IR region (100 –

1000 µm). The setup of an IR spectrometer consists of a radiation source that emits the electromagnetic waves and a spectral device which is needed for the isolation of light of a certain spectral region, a Michelson-interferometer is often used for that propose. The sample gets placed between the spectral device and the detector, which is connected to a computer that calculates the spectra (Günzler and Gremlich, 2003; Schrader, 1995; Grellmann and Seidler, 2011). A general setup of an IR spectrometer can be seen in Figure 3.2.

Figure 3.2: General setup of an IR spectrometer (Günzler and Gremlich, 2003).

The measurements can be conducted in transmittance mode, where the IR light passes through the sample and the transmitted electromagnetic waves are measured by the detector. For non-transparent samples a measuring method called attenuated total reflectance (ATR) spectroscopy can be used. The sample gets placed on a crystal and the light gets reflected on the crystal-sample interface. The light therefore carries information about the surface of the sample. This schematic principle of the beam path in an ATR measurement is displayed in Figure 3.3 (Günzler and Gremlich; 2003, Urban, 1996).

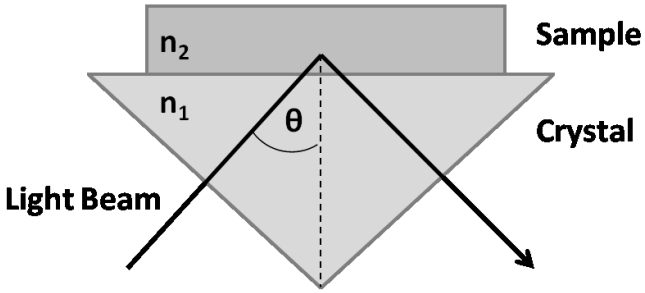

Figure 3.3: Schematic principle of the beam path of an ATR measurement with the refractive index of the crystal n_1, the refractive index of the sample n_2 and the angle of the incident light Θ (Günzler and Gremlich, 2003).

The depth d_p the incident light can enter in the sample surface depends on the wavelength λ, the refractive indices of the sample n_2 and the crystal n_1 as well as on the angle of incidence Θ as shown in formula 3.1 (Urban, 1996).

$$d_{\mathrm{p}} = \frac{\lambda}{2*\pi*\sqrt{({n_1}^2*sin^2\theta - {n_2}^2)}} \qquad (3.1)$$

The depth of penetration of the incident beam can be varied using different angles of incidence. This method is called variable angle ATR and can be used to characterise the material's chemical composition as a function of depth from the surface without the destruction of the sample (Nishikida, 1995; Pocius and Dilliard, 2002; Avadanei, 2012).

The IR spectroscopy measurements were carried out with a FTIR Spektrum GX (PerkinElmer, USA) which was used in ATR mode with a removable Pike Veemax II ATR part (Pike Technologies, USA). A zinc selenide (ZnSe) crystal was used for all materials and the measuring range was between 4000 and 650 cm^{-1} with 16 scans for one spectrum. The sample size needed for the experiments was approximately 3 x 3 cm and the films could be placed on the ATR crystal without further preparation. For the laminated samples the encapsulant material had to be separated from the glass layer and the background layer to allow the IR experiments. For the separation of the encapsulant film a stretching of the material was inevitable. Possible resulting changes in crystallinity or orientation did not affect the peaks used for the characterisation of the material ageing. The Pike Veemax II ATR was controlled by AutoPro 5 software and for every sample variable angles of 45°, 50°, 60° and 70° were measured. For the evaluation of the data the Spectrum 10 software was used and the baseline correction of the software was applied on every spectrum. Normalisation to the 2916 cm^{-1} peak was carried out for the displayed IR spectra. This peak of the CH_2 vibration was chosen due to its stability during ageing. For the depth analysis the spectra were transformed in absorbance and evaluated without normalisation. The parameters of the IR spectroscopy experiments can be seen in Table 9.1 in the appendix.

3.3.2 Raman Spectroscopy

Raman spectroscopy is based on the principle of the scattering of light waves on molecules. An electromagnetic wave is described mathematically as $h*\nu_0$ with h being the Planck constant and ν_0 the frequency of the wave. If light gets scattered the highest probability is that the light gets scattered without the loss or gain of energy. This scattering where the frequency of the electromagnetic wave does not change is called Rayleigh scattering (elastic scattering). In Raman scattering the electromagnetic wave $h*\nu_0$ interacts with the molecule and gets scattered with a higher or lower energy (inelastic scattering). The loss of energy can be explained by the rise of the molecule to a vibrational excited state ν_m and a gain of energy can occur if the molecule is already in a vibrational excited state ν_m so that photons with higher energy get emitted. The principle

of Raman and Rayleigh scattering can be seen in Figure 3.4 (Schrader, 1995; Ferraro and Nakamoto, 2003).

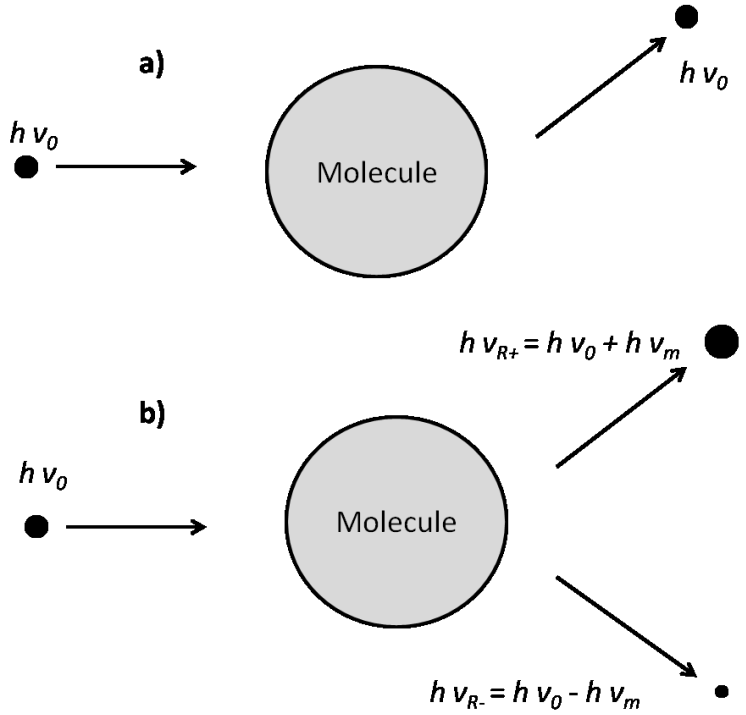

Figure 3.4: Principle of a) Reyleigh (elastic) and b) Raman (inelastic) scattering of an electromagnetic wave $h*v_0$ on a molecule (Schrader, 1995).

In Raman spectroscopy the sample is irradiated by intense light beams in the UV/Vis region and the scattered light is measured in a right angle to the incident beam as seen in Figure 3.5 (Ferraro and Nakamoto, 2003).

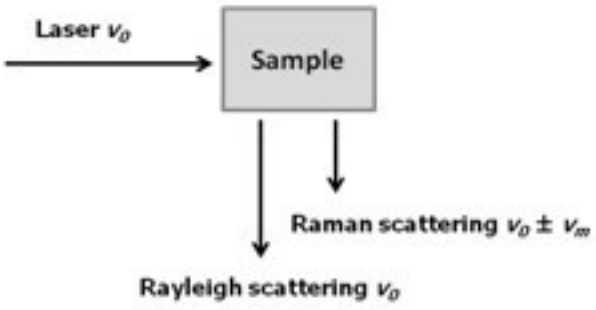

Figure 3.5: Schematic principle of the light scattering measured in a right angle from the incident laser in a Raman measurement (Ferraro and Nakamoto, 2003).

Scattered photons are measured and plotted as a function of intensity over the wave number (Raman shift) and provide information about vibrational frequencies of the

surface of a material. Raman and IR are both spectroscopic methods that provide information about the vibrational frequencies (see chapter 3.3.1). A molecular vibration is Raman-active if the polarisability is changed during the measurement and IR-active if there is a change in the dipole moment. In general a vibration is IR-active or Raman active or active in both and therefore one technique supplements the other one. For instance vibrations of bonds with a covalent behaviour (e.g. C=C, C≡C or S-S) show strong Raman-activity and vibrations of bonds with a more ionic behaviour (e.g. O-H or N-H) show strong IR-activity (Ferraro and Nakamoto, 2003).

The Raman spectra were measured with a confocal spectrometer named LabRAM HR800 (Horiba Jobin Yvon GmbH, Germany). Pieces of approximately 1 x 1 cm² were cut out of the films and the films from the laminates to fit in the spectrometer. For every sample one spectrum was taken in the Raman shift range of 650 – 4000 cm^{-1} with 15 scans. A green laser with a wavelength of 514 nm was chosen after pretests for all materials. The adjustments were 500 µm hole size, 100 µm slit size, 600 g/mm (grooves/millimetre) grating and 5 seconds of irradiation time. To improve the spectra of aged samples the hole size was reduced to 300 µm or a D0,3 laser filter was applied. The baseline correction and the evaluation of the spectra were made with a LabSpec 5 Software. The 1439 cm^{-1} peak was chosen for normalisation because it is found to be least affected by changes in the Raman shift range between 2000 and 650 cm^{-1} (Shimoyama et al., 1997). For Raman measurements the films were taken from the laminate and the tests were carried out in the discoloured centre as well as on the uncoloured edge area. For the DH exposed laminates the same spots where chosen for sample taking even though no visible difference in colour could be observed. All parameters of the Raman spectroscopy measurements can be seen in Table 9.2 in the appendix.

3.3.3 Ultraviolet/Visible/Near-infrared (UV/Vis/NIR) Spectroscopy

Ultraviolet/Visible/Near-infrared (UV/Vis/NIR) spectroscopy is a spectroscopic method which is based on the absorption of ultraviolet and visible light of a material. Usually light with wavelengths between 200 and 2500 nm is used for polymer characterisation. Contrary to the IR spectroscopy, where the absorption is based on the oscillation and rotation of molecules, the absorption in the UV/Vis/NIR spectroscopy can be explained by the raise of electrons to an energetically higher state. If a light beam with an intensity I_0 hits a material, parts of it can be reflected I_R, transmitted I_T and absorbed I_A. The sum of the intensities I_R, I_T and I_A has to result in the intensity of the incident beam I_0

(Gottwald and Heinrich, 1998). The principle of incidence of light on a material is displayed in Figure 3.6.

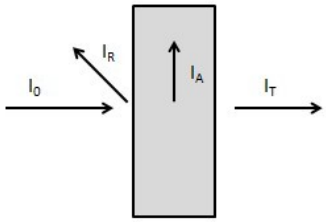

Figure 3.6: Principle of incidence of light I_0 on a material and its division in reflected I_R, absorbed I_A and transmitted I_T beams (Askerland and Phulé, 2006).

Figure 3.7 shows the light beam path of an UV/Vis/NIR spectrometer with an integrating sphere. To measure the light transmittance of a sample it gets mounted in front of the integrating sphere (Figure 3.7 a) and to measure the reflected light it gets mounted at the end of the integrating sphere (Figure 3.7 b) (Perkin Elmer, 2004). The integrating sphere's (Ulbricht sphere) surface is made of a high reflecting material and allows capturing all the diffuse light that has passed the sample or has been reflected by the sample, depending on the type of measurement.

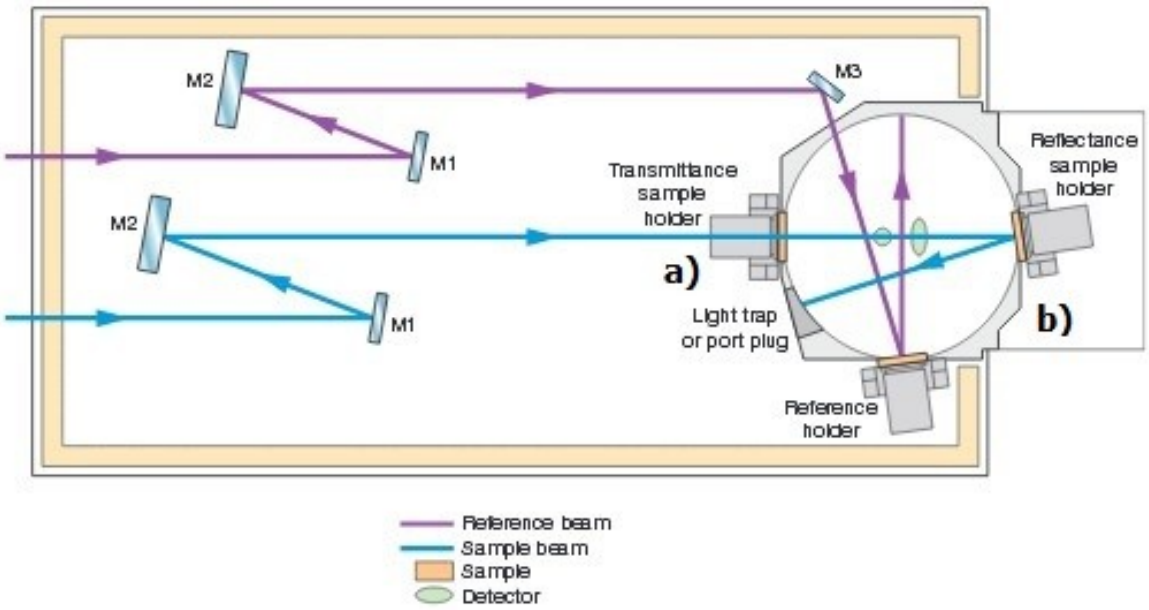

Figure 3.7: Setup of an UV/Vis spectrometer with an integrating sphere and the positions a) for transmittance and b) for reflectance measurements (Perkin Elmer, 2004).

If a light beam is reflected on the surface of a sample it can either be directed reflectance – where the light gets reflected in just one direction – or diffuse reflectance – where the

light gets reflected in various directions – or a mixture of the two types (Figure 3.8). The collected light therefore gives information about the roughness of the surface of the sample (Gottwald and Heinrich, 1998; Ehrenstein and Pongraz, 2007; Perkin Elmer, 2004; Tams and Enjalbert, 2009).

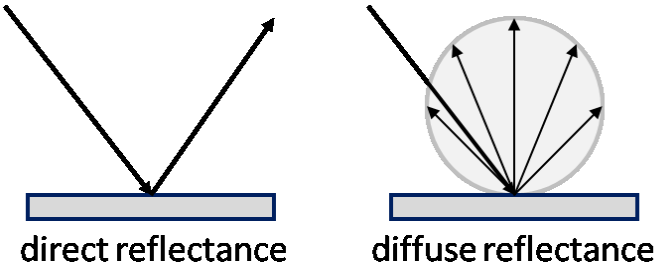

Figure 3.8: Principle of direct and diffuse reflectance on a surface (Grellmann and Seidler, 2011).

Additionally to the measurement of the transmittance or reflectance of light it is also possible to measure the colour of a material with UV/Vis/NIR spectroscopy. For the measurement of colour it is necessary to assign a value to every colour. For that purpose different systems or colour spaces have been developed. One example is the CIELab colour space or Lab system shown in Figure 3.9 (Bastian, 2010). The Lab system consist of a coordinate system with an a*, b* and L* axis with positive and negative values arranged at right angles to each other. The +a*-axis represents red colours and the –a*-axis green colours. Blue colours are expressed by the –b*-axis and yellow colours by the +b*-axis. The L*-axis stands for the lightness of the colours and holds no negative values. The axis is scaled between 0 and 100, where 100 stands for an extremely bright material that reflects all the light and 0 represents an extreme dark material that absorbs all the incident light (Bastian, 2010).

For the UV/Vis/NIR spectroscopy experiments a Lambda 950 of the PerkinElmer company was used with a integrating sphere of Labsphere with spectralon coating and 150 mm diameter. The measuring range was between 250 and 2500 nm wavelength and the spectra were calculated according to AM 1.5 standard weighting from three independent measurements of each sample. The films were measured in reflectance and transmittance mode. Films aged in a laminate could not be removed sufficiently to allow UV/Vis/NIR measurements and were therefore measured with the glass cover and background layer in reflectance mode. It has to be considered in the evaluation of the experiments that a laminated spectrum is the combination of the transmittance of the glass cover and the encapsulant material and the reflectance of the backsheet layer. For every experiment a

hemispheric and a diffuse measurement has been made. The spectra were evaluated with the Spectrum 10 software and the colour values of the spectra were calculated with the WinColor 3.1.6 software. All parameters of the UV/Vis/NIR spectroscopy experiments can be seen in Table 9.3 in the appendix.

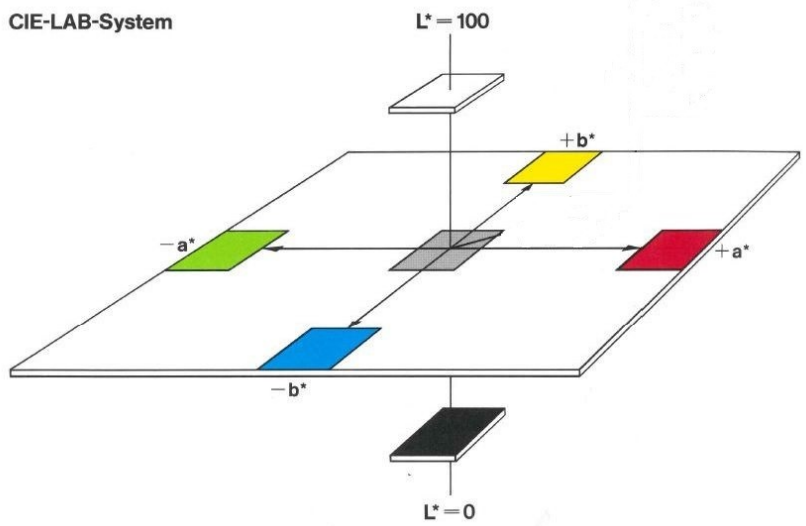

Figure 3.9: CIELab colour space coordinate system with L*, a* and b*-axis and the correlating colours and brightness (www.din.de, 28.05.2014).

3.3.4 High Performance Liquid Chromatography (HPLC) with Mass Spectrometry (MS) and Ultraviolet (UV) Spectroscopy

High performance liquid chromatography (HPLC) is a separation method where a substance is solved in a mobile phase and then passes a capillary or column that holds a stationary phase. Based on the ability of the molecules to interact with the column the residence time differs and the molecules with a stronger interaction leave the column after molecules with lower interaction. The interaction between the solute and the stationary phase can be for instance due to adsorption, ion-exchange or size exclusion. In adsorption chromatography for instance the solutes separate based on their ability to adsorb to a stationary phase. After passing the column the separated molecules in the solvent are analysed by a detector. Common detector principles are ultraviolet (UV) spectroscopy - where the absorption of UV light is measured – or mass spectrometry (MS) (Harvey, 2008; Hanai and Smith, 1999; Pasch and Trathnigg, 1999). Regarding the UV spectroscopy the principle of spectroscopic analysis is explained in the chapters 2.3.1, 2.3.2 and 2.3.3. Mass Spectrometry is an analytic method often used in organic chemistry to identify elements and molecules as well as to study their structure. The principle of MS

is the creation of ions from organic or inorganic substances and the following separation of these ions based on their mass/charge-relation. For the ionization in this thesis a method called electrospray ionization (ESI) was applied. The ESI is often used in combination with HPLC because it transfers ions in solution to ions in a gas phase without the use of heat. The ionization also takes place under atmospheric pressure and continuously transfers the ions to the vacuum conditions of the mass detector. The ions are then sprayed by a capillary and an applied electrical field. Fine electrically charged drops of the ions in solution leave the capillary and are accelerated towards the mass analyzer. The fine drops of sizes in the micrometer range decrease to even smaller ion drops due to vaporization of the solvent. ESI can be used in either positive or negative polarity mode depending on the applied electrical field. The resulting mass spectrum is the display of the mass/charge-relation (m/z) on the x-axis and the y-axis represents the intensity (relative abundance) of the peak (Gross, 2013; Thermo Fischer Scientific, 2007).

The mass spectrometry and high performance liquid chromatography measurements were carried out with a Surveyor MSQ Plus (Thermo Fisher Scientific Inc, USA) with a mass spectrometer in ESI mode. The separation column was reverse phase C18 column (Advanced Chromatography Technologies LTD, UK). The experiments were made in positive and negative mode in the range of 150 – 600 m/z or 150 – 2000 m/z. The flow rate was 300 µl/min with 100% acetonitrile used as a solvent. For the HPCL-MS/UV experiments 250 mg of encapsulant samples were used. The additives were extracted from the polymer matrix by the immersion in dichlormethane for 12 hours and additional immersion in acetonitrile for 12 hours under ambient conditions. All parameters of the HPLC-MS/UV spectrometry experiments can be seen in Table 9.4 in the appendix.

3.3.5 Differential Scanning Calorimetry (DSC)

The differential scanning calorimetry (DSC) is a method for the thermal characterisation of materials. The objective is the measurement of heat that is absorbed or released by the tested material due to physical or chemical changes during a heating or cooling process. The sample gets placed in an oven with a reference material and the heat flow $\dot{Q}$ needed to keep both the sample and the reference material at the same temperature is being measured (Ehrenstein et al., 2003; Frick and Stern, 2006). The schematic setup of a heat flux DSC is displayed in Figure 3.10. The heat flow $\dot{Q}$ is the product of the specific heat capacity c_p – the amount of energy needed to raise the temperature of 1 g of a material

for 1°C – the heating rate v and the mass m of the tested substance (formula 3.2) (Ehrenstein et al., 2003).

$$\dot{\mathbf{Q}} = \mathbf{v} * c_p * \mathbf{m} \qquad (3.2)$$

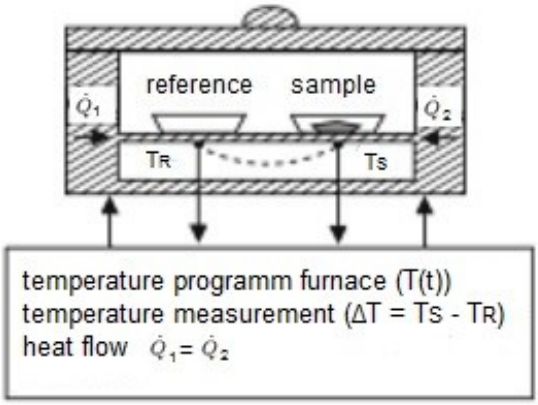

Figure 3.10: Schematic diagram of a heat flux DSC (Ehrenstein et al., 2003).

In endothermic processes (e.g. melting, vaporisation) the temperature of the sample will stop to rise until the required amount of heat for the process is supplied and in exothermic processes (e.g. crosslinking, crystallisation or degradation) the material will release heat. The measured heat flow $\dot{Q}$ will result in a peak in the curve as seen in Figure 3.11 (Ehrenstein et al., 2003; Frick and Stern, 2006). Temperature values of the material such as melting temperature, crystallisation temperature or temperature where a chemical reaction takes place can be received from the curve. Additionally to temperature values the change of the enthalpy ΔH – the change of the inner energy of a material at constant pressure – of the observed thermal processes can be received from the peaks in the curve by measuring the area of a peak to the baseline received from connecting the start and end point of the peak (Ehrenstein et al., 2003; Frick and Stern, 2006).

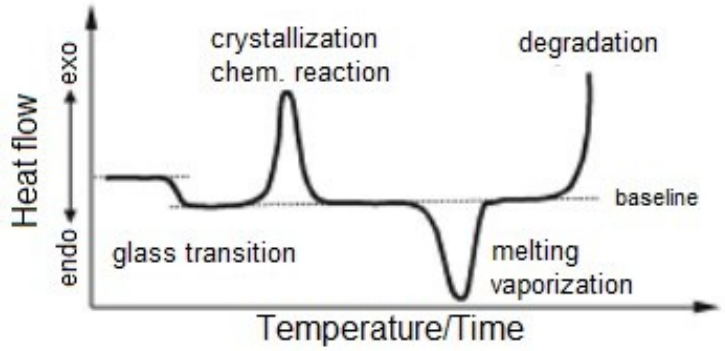

Figure 3.11: Schematic heat flow $\dot{Q}$ over temperature/time curve of a DSC measurment (Ehrenstein et al., 2003).

The degree of curing of a material can be calculated with the curing enthalpy H_C of the material and the curing enthalpy of an uncured material H_0 as shown in formula 3.3 (Ehrenstein et al., 2003).

$$Curing\ Degree\ [\%] = \frac{H_0 - H_C}{H_0} * 100 \qquad (3.3)$$

To gain information about the specific material properties the tested material is heated a second time. The first heating provides information about the thermal history of the material and the cooling between the first and second heating influences the results of the second heating (Ehrenstein et al., 2003; Frick and Stern, 2006).

For the DSC tests a PerkinElmer DSC 4000 (Perkin Elmer, USA) was used. Pieces of 10 to 15 mg were punched out of the films and the encapsulant material removed from the laminated samples. Three independent measurements were made for every experiment. The testing method for the EVA samples contained two heating steps and one cooling step. The first heating was from -40 °C to 230 °C with a heating rate of 10 °C/min. The sample was then cooled down to -40 °C at 10 °C/min and afterwards heated up to 300 °C at the same rate. Nitrogen was used as purge gas throughout the whole experiment. The testing method for all PE samples was adapted to the material and contained the same program as for the EVA samples but with a maximum heating temperature of 150 °C for both heating steps. The evaluation of the received curves was carried out according to ISO 11357 with the Pyris 11 software. All parameters of the DSC experiments can be seen in Table 9.5 in the appendix.

The combination of characterisation methods was chosen to provide a comprehensive analysis of the encapsulants. IR and Raman spectroscopy are suitable methods to analyse the material structure, decomposition products, double bond formation and additives in the polymers. UV/Vis/NIR spectroscopy was used to observe discolouration, the transmittance of the films and information about the UV absorber in the material. HPLC-MS/UV was chosen to analyse the additives in the encapsulants and DSC to characterise thermal behaviour changes and to collect information about the crosslinking of the EVA. Table 3.4 shows the analysis methods chosen to characterise chemical ageing processes of the encapsulant materials. All EVA and PE film and laminate samples were exposed to DH and XE for 2000 hours. Analysis was carried out for all exposure combinations with IR spectroscopy, Raman spectroscopy, UV/Vis/NIR spectroscopy and DSC. For the HPLC-MS/UV experiments only samples exposed to XE weathering were used. Table 3.5 gives

an overview of the film and laminate samples exposed to DH and XE and tested by the analysis methods.

According to the known effect of a stronger discolouration in the centre and uncoloured area around the edge of PV modules the sample taking has been adapted to compare these regions. In the Raman, DSC and HPLC–MS/UV analysis the centre of the EVA and PE laminates was compared to the edge of the laminate. For the other characterisation methods only the centre of the laminate could be measured due to the size of the occurring uncoloured area. In Figure 3.12 the sample taking for the applied characterisation methods is shown on the basis of the unaged and 2000 hours XE weathered laminated samples of EVA Vistasolar 486.00®.

Table 3.4: Combination of characterisation methods chosen for the analysis of chemical ageing processes of the encapsulants.

Characterisation Method	Structure Analysis	Additives	Decomposition Products	Discolouration	C=C Double Bond Formation	Crosslinking	Transmittance
IR Spectroscopy	✓	✓	✓	-	✓	-	-
Raman Spectroscopy	✓	✓	✓	-	✓	-	-
UV/Vis/NIR Spectroscopy	-	✓	-	✓	-	-	✓
HPLC-MS/UV	-	✓	-	-	-	-	-
DSC	-	-	-	-	-	✓	-

Table 3.5: Overview of the film and laminates exposed to DH and XE and tested by the analysis methods.

Analysis Method	Film		Laminate	
	Damp Heat	Xenon	Damp Heat	Xenon
IR	✓	✓	✓	✓
Raman	✓	✓	✓	✓
UV/Vis/NIR	✓	✓	✓	✓
HPLC and MS	-	✓	-	✓
DSC	✓	✓	✓	✓

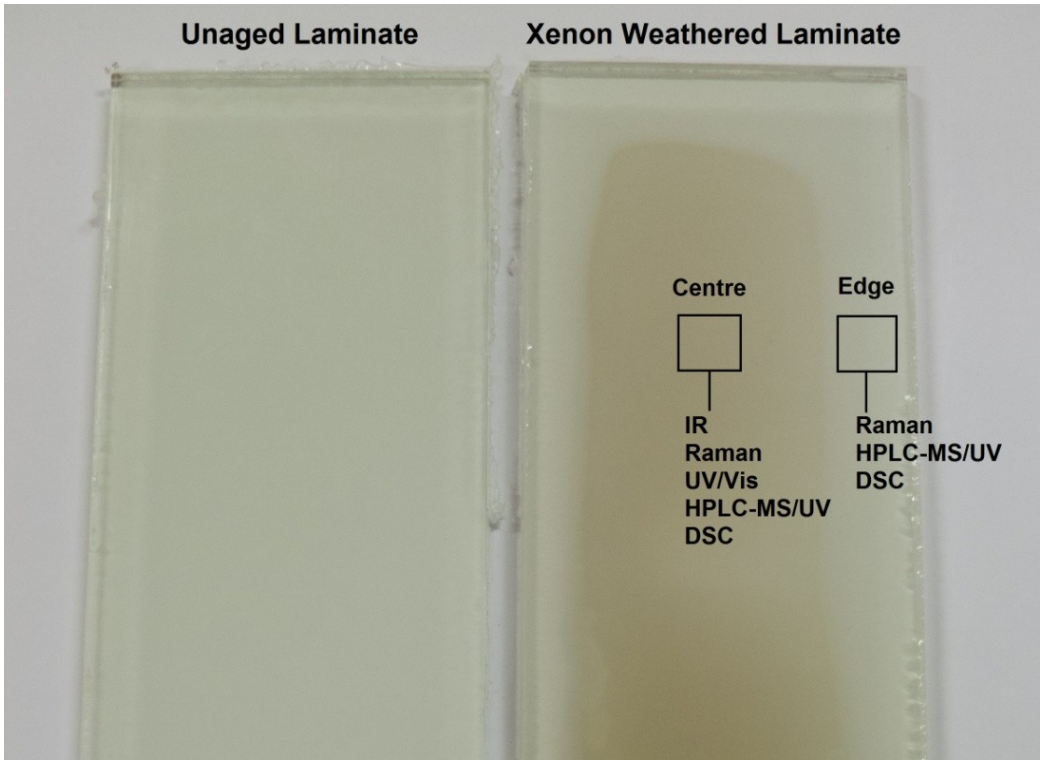

Figure 3.12: Display of the sample taking for the applied characterisation methods based on the example of the unaged and XE weathered EVA Vistasolar 486.00® laminated sample.

4 RESULTS AND INTERPRETATION

First observations with the bare eye showed that the exposure of EVA and PE laminates to XE for 2000 hours resulted in a discolouration of the laminates. While the PE laminates showed an evenly distributed discolouration on the exposed area different colour shades could be observed for the EVA laminates. The samples showed stronger discolouration in the centre of the laminate with fading shades towards the edge area. In some exposed areas around the edge of the laminates no discolouration could be observed. For the laminates exposed to DH as well as for the XE and DH exposed films no significant discolouration could be observed by the bare eye. The difference in discolouration in the XE exposed laminates could be due to the lower oxygen concentrations in the centre than at the edge area. The EVA films exposed to XE where an oxygen rich environment can be found no significant observations regarding discolouration could be made by the bare eye. Chromophores responsible for discolouration might oxidise in the presence of oxygen and reduce the discolouration (Pern, 1996). In Figure 3.12 in chapter 3.3 the discolouration of an EVA Vistasolar 486.00® laminate compared to an unaged sample can be seen.

4.1 Infrared (IR) Spectroscopy

Ethylene-Vinyl Acetate Copolymer

The IR spectra of unaged EVA films were compared to the spectra of samples exposed to DH and XE for 1000 hours and 2000 hours. The curves of unaged and 2000 hours aged EVA Vistasolar 486.00® were chosen to describe the chemical ageing effects found in the three EVA types as shown in Figure 4.1. The peaks at 2918, 2848, 1463, 1370 and 721 cm^{-1} can be assigned to the vibrations of CH_2 and CH_3 groups. The carbon oxygen double and single bond vibrations cause the peaks at 1734, 1232 and 1019 cm^{-1} (Oreski et al., 2009). The peaks at 3300, 1636 and 1556 cm^{-1} found in the DH exposed EVA Vistasolar 486.00® films may appear because of a high additive concentration at the surface of the material. Oreski et al. described that the peak at 1540 cm^{-1} can be assigned to hindered amine light stabilizers (HALS) and Gulmine et al. also suggests that the peaks at 3400 – 3200 cm^{-1} and 1600 cm^{-1} might be caused by additives like Tinuvin® (HALS), Chimasorb® (UV absorber) or Cyasorb® (UV absorber) (Oreski et al., 2009; Gulmine et al., 2002). However, no significant change in the intensity of the EVA peaks or the additive peaks can be observed for films exposed to DH for 2000 hours. Therefore, the additive peaks found in the spectra were not caused by additive diffusion during

ageing and it can be assumed that a film area with a higher concentration of additives on the surface was taken for investigation. Furthermore, no changes of the EVA peaks and no additional peaks after DH exposure (85 °C/85 % RH) of the films for 2000 hours could be observed that would indicate chemical ageing. Wang et al. found hydrolysis indications in EVA via OH group formation after further 1000 hours of DH exposure (Wang et al., 2013). The IR spectra of EVA Vistasolar 520.78® and EVA NovoVellum Optima MF01® films exposed to DH for 2000 hours also showed no significant changes (Figure 9.1 and Figure 9.2 in the appendix).

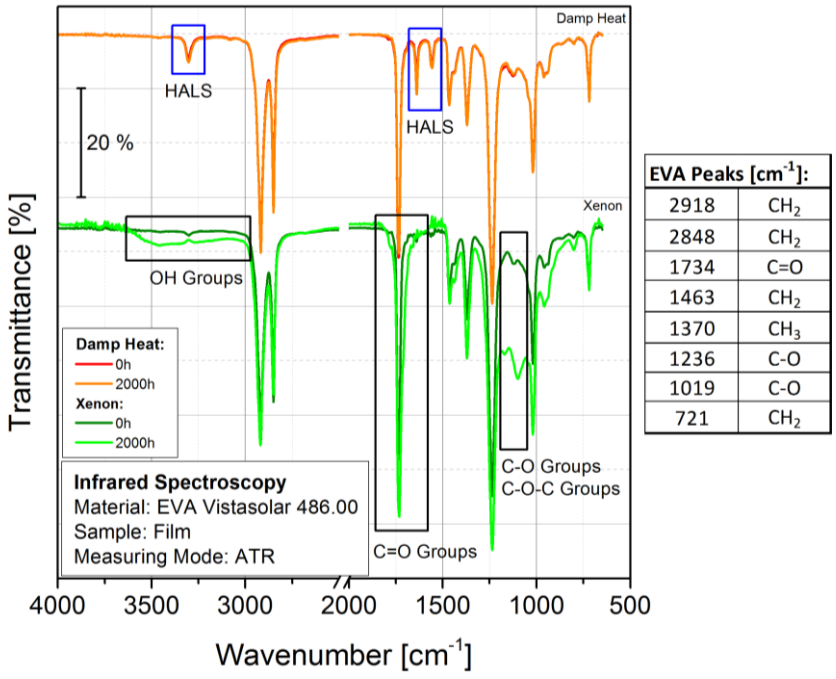

Figure 4.1: IR spectra of EVA Vistasolar 486.00® films unaged and exposed to DH and XE for 2000 hours.

EVA Vistasolar 486.00 unaged films for XE weathering showed the same material peaks at 2918, 2848, 1734, 1463, 1370, 1236, 1019 and 721 cm^{-1} as found in the unaged films for DH ageing. No singificant UV stabiliser peaks at 3300, 1636 and 1556 cm^{-1} were found for these films. When exposed to XE (90 W/m², 60 °C, wet/dry cycles) for 2000 hours, significant changes in the IR spectrum due to polymer oxidation could be observed. Between 3600 and 3000 cm^{-1} and between 1050 and 1200 cm^{-1} broad peaks occured which can be related to hydroxyl formation of alcohols, peroxides or hydroperoxides as described by Oreski et al. (Oreski et al., 2009). At wavenumbers between 1050 and 1200 cm^{-1} the most dominant peak occured at 1100 cm^{-1} caused by a C-O vibration of hydroxyl groups (Günzler and Gremlich, 2003). A less intense peak at 1170 cm^{-1} can be

related to the C=O stretching of formed ketones or possibly to the C-O-C stretch of esters and lactones (Salvalaggio et al., 2006; Allen et al., 2000; Jin et al., 2010). The photo-degraded films also showed changes of the peak at 1734 cm^{-1} with increasing exposure time (Figure 4.2). The shoulder formed at lower wavenumbers (1660–1720 cm^{-1}) might be caused by the C=O stretching of formed ketone structures (1714 cm^{-1}) and the shoulder between 1750 and 1800 cm^{-1} could be caused due to lactone formation (1773 cm^{-1}) in the polymer chain. Not only the broadening of the peak but also an increase in intensity, possibly due to an increase in ester or aldehyde groups, could be measured (Jin et al., 2010; Allen et al., 2000; Gulmine and Acelrud, 2006). No significant peaks around 1412 or 1636 cm^{-1} were found indicating C=C double bonds in the aged EVA films (Liu et al., 2014; Carrasco et al., 2001).

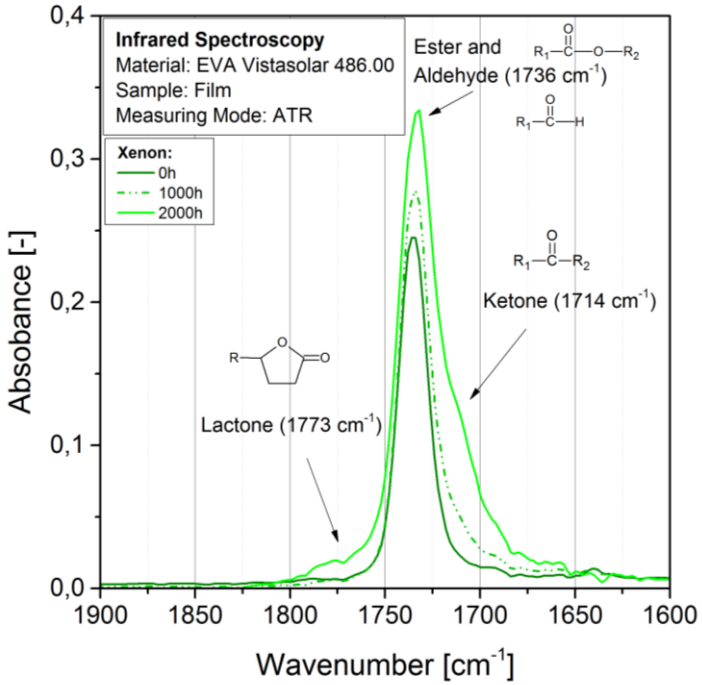

Figure 4.2: Detailed plot of the 1736 cm^{-1} peak of unaged and XE aged EVA Vistasolar 486.00® films.

The described chemical ageing processes after photo-degradation were also observed in the IR spectra of EVA Vistasolar 520.78® and NovoVellum Optima MF01® films (Figure 9.1, Figure 9.2 and Figure 9.3 in the appendix). The Vistasolar 520.78® film after 2000 hours of XE exposure could not be measured with IR spectroscopy due to very advanced degradation. The film had turned into a sticky substance and could not be positioned properly to allow IR measurements. Therefore the film aged for 1000 hours was used for characterisation. The IR results of all EVA copolymers showed that the

encapsulants responded much more sensitive to photo-oxidation than to thermo-oxidation when exposed for the same time.

Due to the variable angle analysis it was possible to determine the observed ageing processes depending on the depth to the material surface. The depth of penetration was calculated according to formula 3.1 with the refractive indices 2.43 for the ZnSE crystal and 1.479 for EVA Vistasolar 486.00® (Avadanei, 2012; Solutia, 2012a). The most dominant peak formed after the exposure to XE for 2000 hours was found at 1100 cm^{-1} (C-O vibration) due to hydroxyl formation in the polymer chain. The formed peak was related to the peak of the CH_2 asymmetric stretching at 2919 cm^{-1} because of its stability during ageing. Figure 4.3 shows the relation of the 1100/2919 cm^{-1} peaks of the films in dependence on the depth to the material surface. For the peak intensity relation 16 scans were made for each angle and combined to one spectrum by the Spectrum 10 software. The peak relation was formed with the values evaluated from that spectrum and therefore no standard deviation could be displayed in the figure.

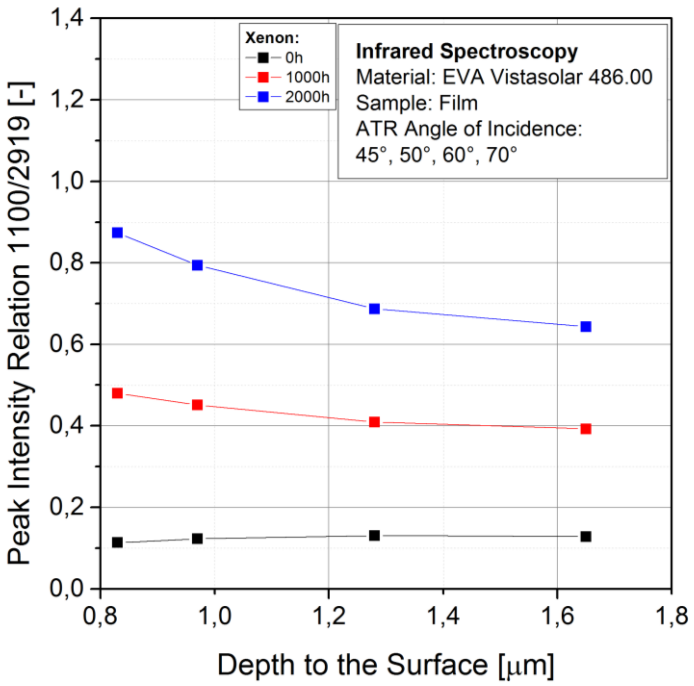

Figure 4.3: Formation of hyxdroxyl groups of EVA Vistasolar 486.00® films exposed to XE in dependence on the depth to the material surface.

The peak relation was measured between 0.83 and 1.65 µm and no significant changes in dependence on the depth could be observed for the unaged sample. The exposure to XE for 1000 hours showed an increase of hydroxyl groups at all depths with the tendency of

stronger increase close to the material surface. After 2000 hours of exposure a further increase of the peak relation was measured. The increase of the hydroxyl groups from the bulk to the surface could be found more pronounced after 2000 hours of XE exposure. The increased oxidation at the surface compared to the bulk material might indicate that photo-oxidation caused the ageing on the surface and with distance to the surface less light entered the material and thermo-oxidation predominanted. EVA Vistasolar 520.78® films also showed increased hydroxyl groups after 1000 hours of exposure with a slight increase in dependence on the depth to the surface of the polymer (Figure 9.4 in the appendix). EVA NovoVellum Optima MF01® films showed hydroxyl formation after 1000 hours of XE exposure but only after 2000 hours a significant dependence on the depth to the surface could be seen (Figure 9.4 in the appendix). The refractive indices used for the calculation of the penetration of depth were 1.485 for EVA Vistasolar 520.78® and 1.4809 for EVA NovoVellum Optima MF01® (Solutia, 2012b; Novopolymers NV, 2014).

EVA Vistasolar 486.00® unaged laminates showed typical EVA material peaks at 2919, 2849, 1735, 1463, 1371, 1236, 1020 and 718 cm^{-1} as found for the film samples. Figure 4.4 shows the IR spectra of unaged EVA Vistasolar 486.00® laminates and after exposure to DH and XE for 2000 hours.

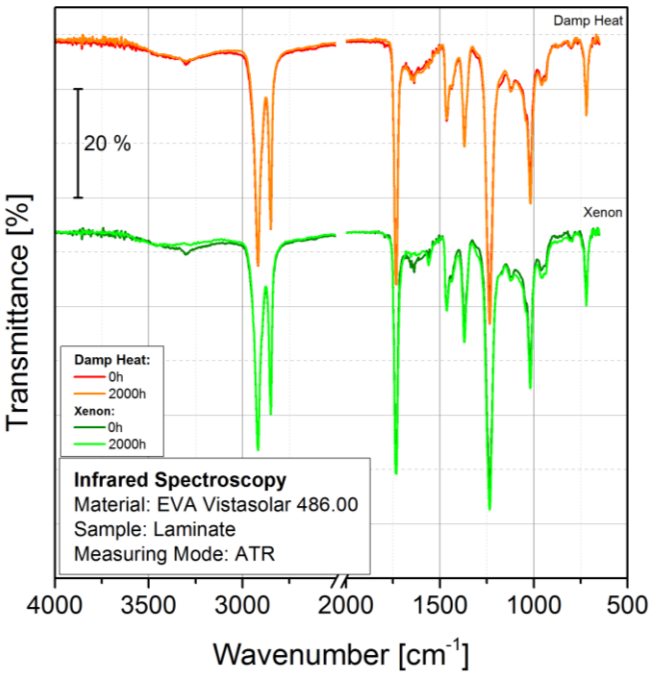

Figure 4.4: IR spectra of EVA Vistasolar 486.00® laminated samples, unaged and exposed to DH and XE for 2000 hours.

The laminates aged under DH conditions for 2000 hours showed no significant changes as also observed for the films aged under the same conditions. The damp heat exposure for 2000 hours at 85 °C with 85 % RH therefore seemed to have no significant influence on chemical ageing processes observable with IR spectroscopy both for the films and laminates. The laminates aged under XE exposure for 2000 hours also showed no observable changes in the IR spectra where films aged under the same conditions showed significant photo-oxidation. The IR spectra of EVA Vistasolar 520.78® and EVA NovoVellum Optima MF01® laminates are shown in Figure 9.1 and Figure 9.2 in the appendix and similar observations made as for the IR spectra of EVA Vistasolar 486.00®. The XE weathering of EVA for 2000 hours only provoked photo-oxidation if the sample was in direct contact with air (oxygen) under the irradiance of UV light. The photo-oxidation could be found to be higher at the material surface. This could be due to a higher irradiation with UV light under the presence of oxygen. With distance to the surface less high-energy light entered the material and the oxidation of the polymer decreased. The lamination between a glass and backsheet layer seemed to protect the encapsulant sufficiently to avoid photo-oxidation, detectable with IR spectroscopy when exposed to XE for 2000 hours. These layers work as barriers against oxygen and moisture diffusion possibly resulting in a lower concentration in the laminate. Additionally the glass cover might have decreased the intensity of the UV irradiation and therefore hindered photo-oxidation.

Polyethylene

The IR spectra of unaged PE PV-FS Z68® films and the spectra after exposure to DH and XE for 2000 hours can be seen in Figure 4.5. The unaged spectra showed strong peaks at 2915 and 2848 cm^{-1} that can be assigned to the asymmetric and symmetric stretching of the CH_2 groups and the weak peak at 2954 cm^{-1} is caused by the CH_3 group (Krimm et al., 1956). Further significant peaks at 1463 and 728/717 cm^{-1} are also main absorption peaks of polyethylene and occur due to CH_2 bending and rocking deformations, respectively. Peaks with low intensity at wavenumbers between 3400 and 3200 cm^{-1} as well as at 1638 cm^{-1} could be observed and may be caused by HALS, as described above for EVA 486.00® (Gulmine et al., 2002). It is also possible that the observed groups were part of the polymer chain due to modifications (carboxylic acid) of the PE encapsulant (Hsu et al., 2010). Considering that these peaks could be found in all unaged PE samples in the same intensity a modification of the material seemed to be more reasonable. The overall intensity of the peaks was poor and various small peaks

could be seen in the spectra that were not assigned to any material vibrations but classified as measurement and environment effects. The PE encapsulant films were harder with a rougher surface compared to the EVA samples possibly resulting in a poor contact of the sample with the crystal.

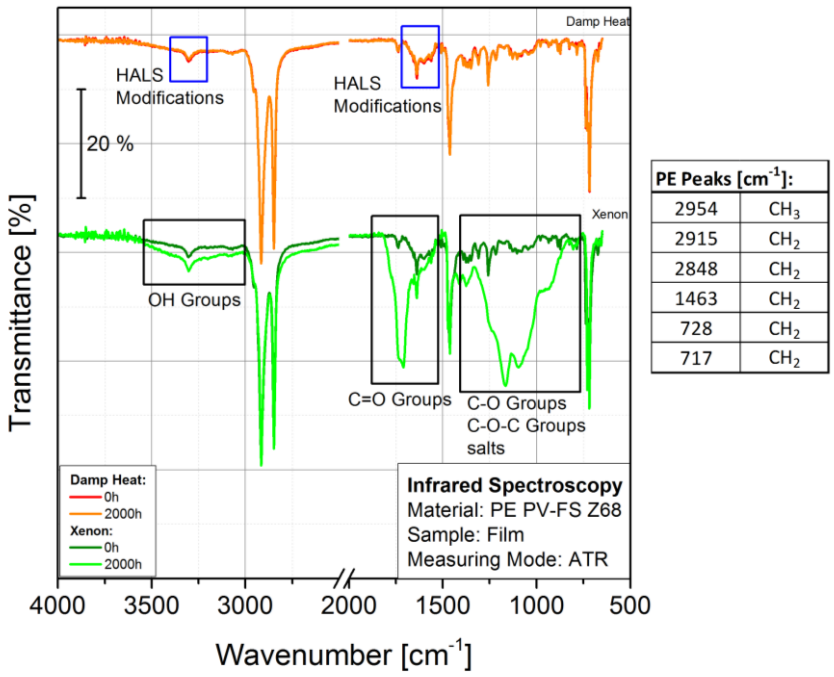

Figure 4.5: IR spectra of PE PV-FS Z68® films, unaged and exposed to DH and XE for 2000 hours.

After the exposure to DH for 2000 hours no significant changes in the IR spectra of the films could be seen. The XE exposure for 2000 hours of PE PV-FS Z68® films resulted in the oxidation of the polymer. A broad peak formed at wavenumbers between 3500 and 3000 cm^{-1} which can be assigned to the OH groups of alcohols and hydroperoxides (Gulmine and Acelrud, 2006). The formation of a C=O peak could be observed between 1800 and 1650 cm^{-1} and is the result of various peaks overlapping at this wavenumbers (Figure 4.6). The peak at 1739 cm^{-1} can already be observed in the spectrum of the unaged PE film and may be caused by ester or aldehyde groups of HALS additive in the material (Hummel, 2002). After XE exposure the development of a strong peak around 1710 cm^{-1} due to carboxylic acid formation in the material could be observed (Salvalaggio et al., 2006; Haillant and Lamaire, 2006). Between these two peaks the formation of ketones is indicated by IR responses around 1720 cm^{-1} (Salvalaggio et al., 2006). The shoulder formed at wavenumbers between 1740 and 1820 cm^{-1} may be caused by isolated carboxylic acids (1767 cm^{-1}), peracids (1750 cm^{-1}),

peresters (1779 cm^{-1}) and lactones (1788 cm^{-1}) formed in the polymer chain (Gulmine and Acelrud, 2006; Gardette et al., 2013; Salvalaggio et al., 2006). The peak at 1639 cm^{-1} was already observed in the unaged material and seemed to increase with exposure time to XE. A possible cause might be C=C double bonds from additives present in the material because isolated C=C double bonds would show a peak at 1650 cm^{-1} (Lin-Vien et al., 1991). The peak at 1368 cm^{-1} can be related to the vibration of $-C(CH_3)_3$ groups (Carrasco et al., 2001).

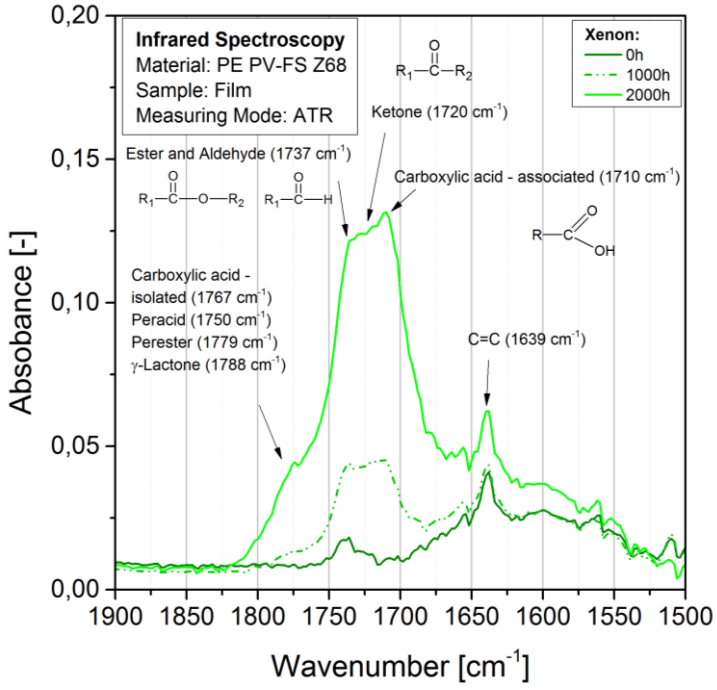

Figure 4.6: Detailed plot of the 1720 cm^{-1} peak of unaged and XE weathered PE PV-FS Z68® films.

The photo-oxidation of the encapsulant also resulted in the formation of a broad peak between 1330 and 800 cm^{-1} as a result of overlapping peaks in this range of wavenumbers. The main cause of this peak might be oxidation of the polymer and the presence of double bonds. The strong peaks at 1166 and 1097 cm^{-1} might be caused by C-O-C groups and C-O groups, respectively (Salvalaggio et al., 2006; Allen et al., 2000; Küpper et al., 2004). According to Carrasco et al. the formation of double bonds would cause peaks at 909, 965 and 990 cm^{-1} (Carrasco et al., 2001). Therefore the shoulder between 1000 and 800 cm^{-1} might be caused by the formation of unsaturated structures in the polymer chain. Gulmine et al. found a similar peak in the area between 1100 and 1300 cm^{-1} after weathering in a xenon chamber and postulate that the peak might be

correlated to an increased salt concentration found in energy disperse spectroscopy measurements on the polymer surface (Gulmine et al., 2003). The salts might come from unpurified water in the spray system of the chamber, supported by their observation that UV aged samples (without the spraying of water) did not show this peak. The peak maxima of 1100 and 1170 cm^{-1} were also observed in the EVA Vistasolar 486.00 films exposed to XE for 2000 hours. Anyhow, a variety of peaks at 1256, 1217, 1171 and 1100 cm^{-1} was found in the PE films exposed to XE for 1000 hours (Figure 4.7). It could be seen that with progressed ageing the peaks did not just increase in intensity but different peaks seemed to overlap and dominate after further exposure. Not excluding the possible present of salts in the spectrum, a change in the spectrum due to the formation of C-O and C-O-C groups therefore appears to be more reasonable.

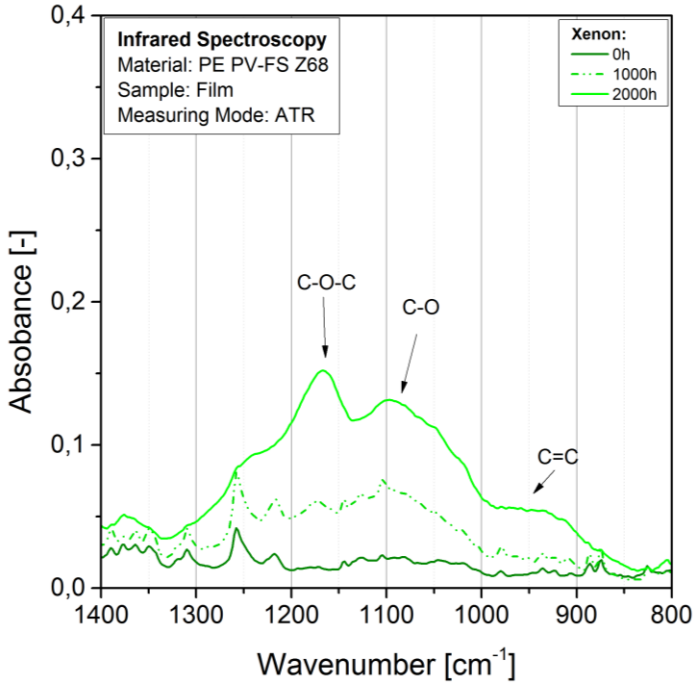

Figure 4.7: Detailed plot of the IR spectra of XE exposed films of PE PV-FS Z68®.

The oxidation of the PE films in dependence on the depth to the sample surface was calculated using the relation of the 1720 cm^{-1} peak (C=O) to the 2917 cm^{-1} peak (CH_2). The peak relations from the variable angle ATR measurements are shown in Figure 4.8. The calculation depth to the sample surface was calculated according to formula 2.1 using the refractive indices of 2,43 for the ZnSe crystal and 1,50 for PE (Gulmine et al., 2003). The unaged PE film showed no oxidation and a steady level of the peak relation between 0.54 and 1.1 µm of depth. After 1000 hours of XE exposure oxidation of the PE film could be observed. The peak relation of the exposed sample increased and showed a steady

level within the measured range of depth. After 2000 hours of XE ageing the peak relation showed further increase but no significant tendency of an increased oxidation in the surface near area could be found as observed for the EVA films. Gulmine et al. investigated in their research the oxidation depth profile of weathered PE (Gulmine et al., 2003). At short exposure time a higher carbonyl content was found near the sample surface and after further exposure the difference in oxidation diminished and a plateau was reached. The unaged PE already showed a C=O peak due to the material modifications. The photo-oxidation resulted in the formation of further C=O groups due to chemical ageing. The presence of these polar groups in the polymer could have favoured the diffusion of the formed C=O groups in the material resulting in an even distribution of these groups at the polymer surface.

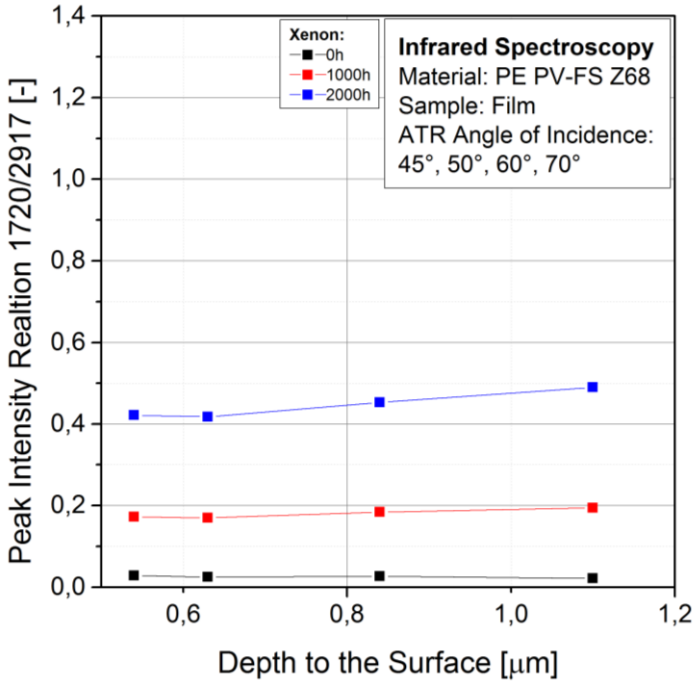

Figure 4.8: Oxidation of PE PV-FS Z68® films exposed to XE in dependence on the depth from the material surface.

The IR spectra of unaged PE PV-FS Z68® laminates showed the typical material peaks at 2915, 2848, 1463 and 717 cm^{-1} as already described for the PE films and can be seen in Figure 4.9. After the exposure of the PE laminates to DH and XE for 2000 hours no significant indicators for chemical ageing could be observed in the IR spectra. The differences in the spectra of the unaged and XE exposed samples in the wavenumber range between 1000 and 1500 cm^{-1} were caused due to the poor contact of the samples with the crystal. The exposure of the PE encapsulant to DH therefore showed no

significant chemical ageing of the films or laminates in IR spectroscopy. DH exposure did not result in material ageing observable in IR spectroscopy after 2000 hours. XE exposure resulted in significant oxidation of the films while laminates showed no indication for material ageing in IR spectroscopy. As described for the EVA samples the reason might be a higher concentration of oxygen and a higher intensity of the UV irradiation at the film samples while the glass cover of the laminates filtered parts of the UV light and avoided oxygen and moisture diffusion.

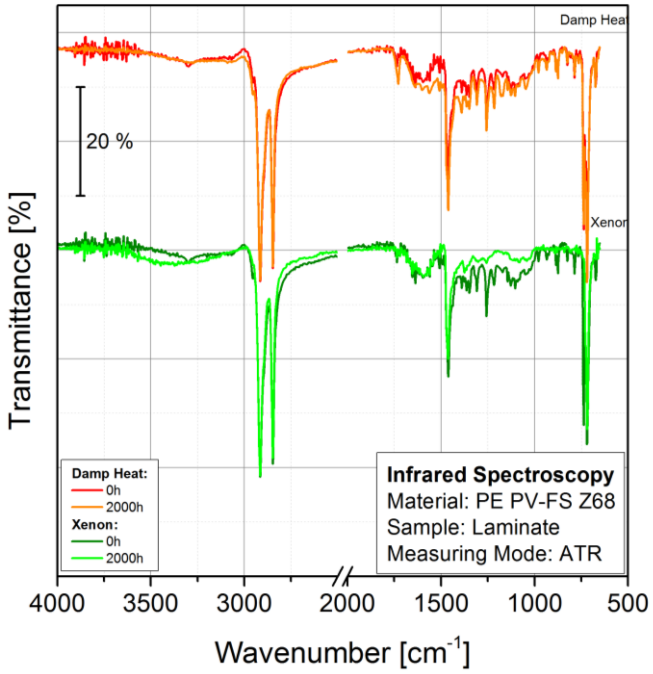

Figure 4.9: IR spectra of PE PV-FS Z68® laminates unaged and exposed to DH and XE for 2000 hours.

4.2 Raman Spectroscopy

Ethylene-Vinyl Acetate Copolymer

The Raman spectrum of an unaged EVA Vistasolar 486.00® film is shown in Figure 4.10 with a detailed plot of the Raman shift area between 650 and 2000 cm^{-1}. The typical EVA peaks at 2936 cm^{-1} of the CH_3 symmetric stretching (ν^sCH_3), at 2883 cm^{-1} of the CH_2 asymmetric stretching ($\nu^{as}CH_2$), at 2851 cm^{-1} of the CH_2 symmetric stretching (ν^sCH_2), at 1737 cm^{-1} of the C=O stretching (νC=O), at 1439 cm^{-1} of the CH_2 scissoring (δCH_2), at 1296 cm^{-1} of the CH_2 twisting (tCH_2), at 1128 cm^{-1} and 1061 cm^{-1} of the C-C stretching (νC-C) could be observed (Shimoyama et al., 1997; Lin-Vien et al., 1991).

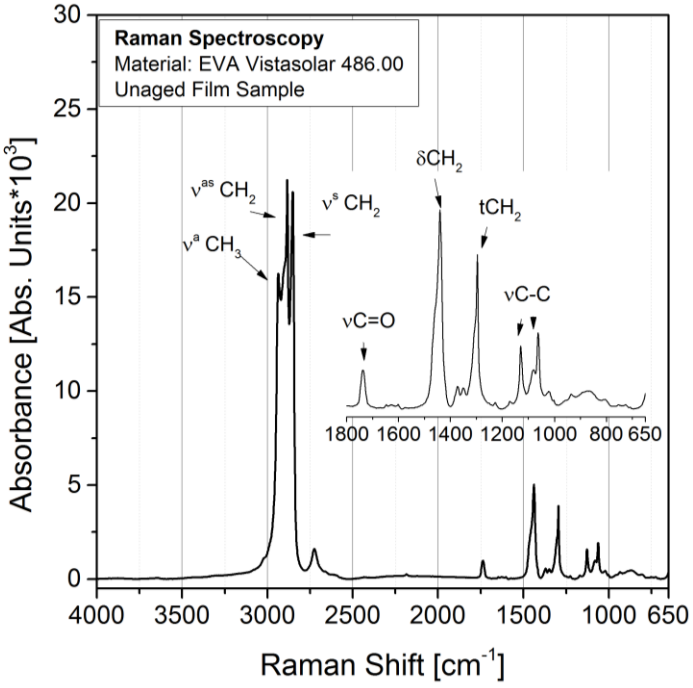

Figure 4.10: Raman spectrum of an unaged EVA Vistasolar 486.00® film.

The normalised Raman spectra between 2000 and 650 cm^{-1} of the EVA Vistasolar 486.00® films exposed to DH and XE can be seen in Figure 4.11. Films exposed to DH for 2000 hours showed no significant changes of the Raman peaks and no additional peaks occurred in the spectra. The exposure of the films to XE for 2000 hours resulted in the formation of C=C double bonds in the Raman shift area around 1650 cm^{-1} (Klemchuk et al., 1997). Further investigation in the spectra to evaluate changes of the vinyl acetate content from the peaks in the Raman shift area between 2800 and 3000 cm^{-1} according to Lin-Vien et al. and the evaluation from the fingerprint area according to Shimoyama et al. led to no analytically conclusive tendency or result (Lin-Vien et al., 1991; Shimoyama et al., 1997). The Raman spectra of Vistasolar 520.78® and NovoVellum Optima MF01® films showed similar results and can be seen in Figure 9.5 and Figure 9.6 in the appendix.

The Raman spectra (2000-650 cm^{-1}) of EVA Vistasolar 486.00® laminates (centre and edge) exposed to DH and XE can be seen in Figure 9.7 in the appendix. The laminates exposed to DH showed whether significant changes in the discoloured centre nor around the uncoloured edge. As described for IR spectroscopy in chapter 4.1 the DH exposure of EVA for 2000 hours seemed to not result in chemical ageing of the encapsulants. The Raman spectra of the EVA Vistasolar 520.78® and NovoVellum Optima MF01® laminates are shown in Figure 9.8 and Figure 9.9 in the appendix. The shift of the spectra of the DH

exposed laminates could be caused due to a different ambient temperature in the laboratory and was not interpreted as an ageing effect. For the XE exposed laminates no significant peak changes or C=C double bond increase could be found on the edges of EVA Vistasolar 486.00® and NovoVellum Optima MF01®. The measurements made in the centre of the laminate could not be evaluated for all three EVA types made due to a strong background increase that could not be corrected sufficiently with the software. For EVA Vistasolar 520.78® also the measurement on the edge of the laminate could not be evaluated properly.

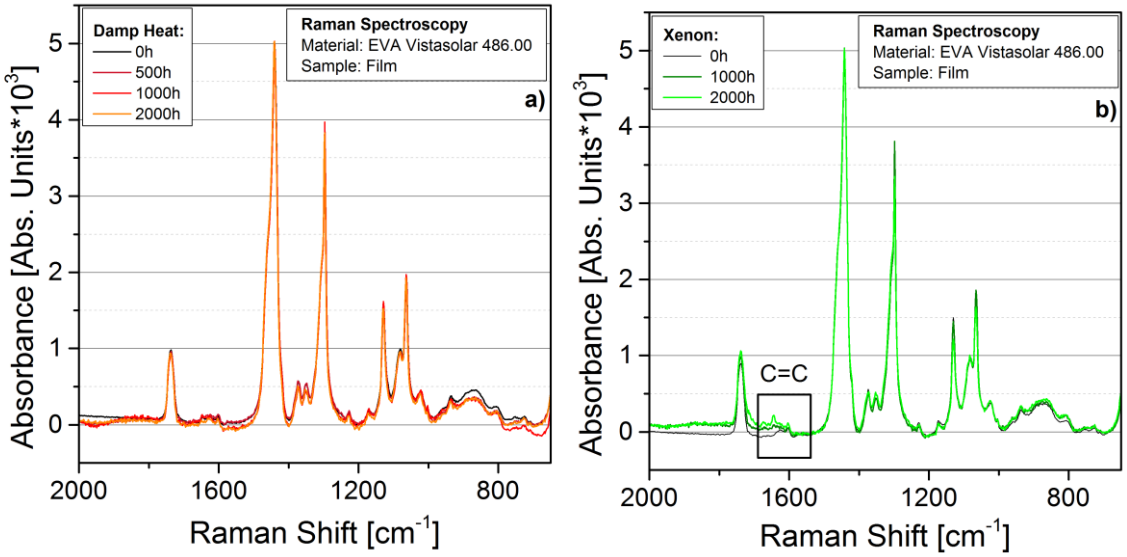

Figure 4.11: Detailed plot of Raman spectra of EVA Vistasolar 486.00® films exposed to a) DH and b) XE for 2000 hours.

When examining the Raman spectra without baseline correction or any normalisation an increase of the baseline could be observed. Figure 4.12 shows the raw Raman spectra of EVA Vistasolar 486.00® films exposed to DH and XE for 2000 hours. The baseline increased for the films exposed to DH while the XE exposed samples showed no higher baselines than the unaged samples. This could also be observed for EVA NovoVellum Optima MF01® films (Figure 9.11 in the appendix). EVA Vistasolar 520.78® films (Figure 9.10 in the appendix) exposed to DH for 2000 hours showed no baseline increase and films exposed to XE for 1000 hours resulted in a formed maximum around 2000 cm^{-1}. The higher baseline could be caused due to an increase of the fluorescence background of the material. Peike et al. described that chromophores can be formed due to material ageing that result in an increase of the fluorescence background of the material (Peike et al. 2011; Peike et al., 2012; Peike et al., 2013a).

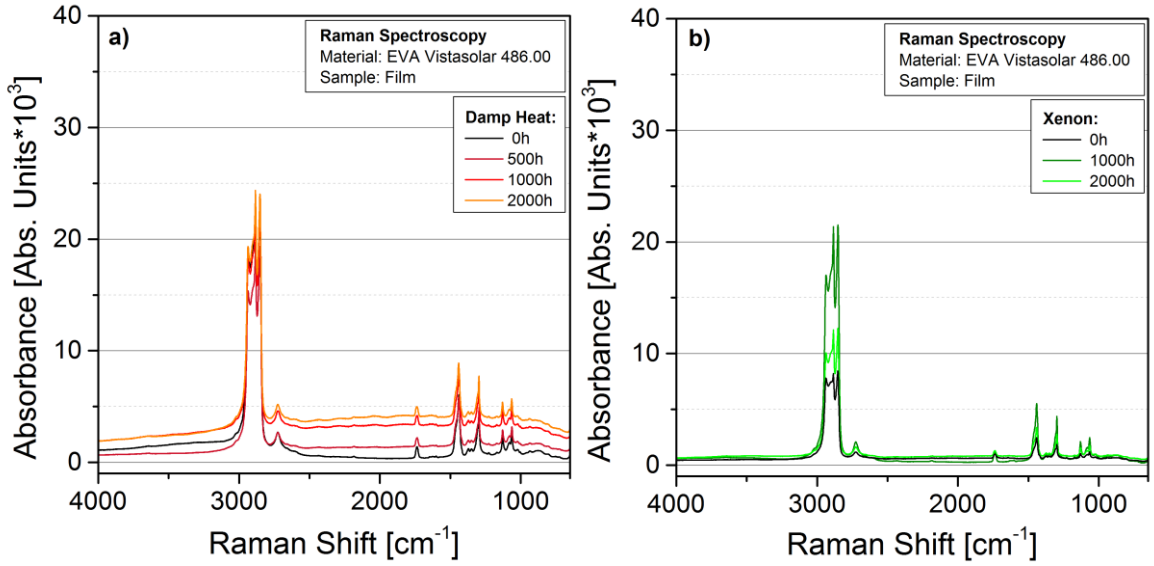

Figure 4.12: Raman spectra of EVA Vistasolar 486.00® films exposed to a) DH and b) XE for 2000 hours.

As seen in Figure 4.13 the spectra of EVA Vistasolar 486.00® laminates showed the same increase in the baseline in the centre as the spectra measured on the edge when exposed to DH. The increase in the 4000 – 3000 cm^{-1} region in the centre of the unaged laminate of EVA Vistasolar 486.00® is caused by a measurement effect and does not represent a material peak. For the XE exposed laminates a very strong increase in the baseline in the discoloured centre of the sample could be seen. The edge of EVA Vistasolar 486.00® laminate showed a higher baseline after 2000 hours, comparable to the DH exposed results. At this point it has to be considered that for most 2000 hours DH exposed samples as well as for most XE weathered samples a reduction in the hole parameter from 500 to 300 has been made to receive spectra with good quality. In pretests the reduction of the hole parameter resulted in a decrease of the baseline of the same sample. The Raman spectra of EVA NovoVellum Optima MF01® laminates showed the same baseline tendencies (Figure 9.13 in the appendix). EVA Vistasolar 520.78® laminates did result in an increased baseline in the centre of the laminated samples between 2000 and 4000 cm^{-1} after DH exposure. This increase was also observed for unaged samples in pretests and is therefore not considered to be caused by material ageing. The edge of the DH exposed laminate showed no such increase. The XE exposed laminates showed a comparable increase in the baseline for measurements made in the centre and on the edge of the laminate (Figure 9.12 in the appendix).

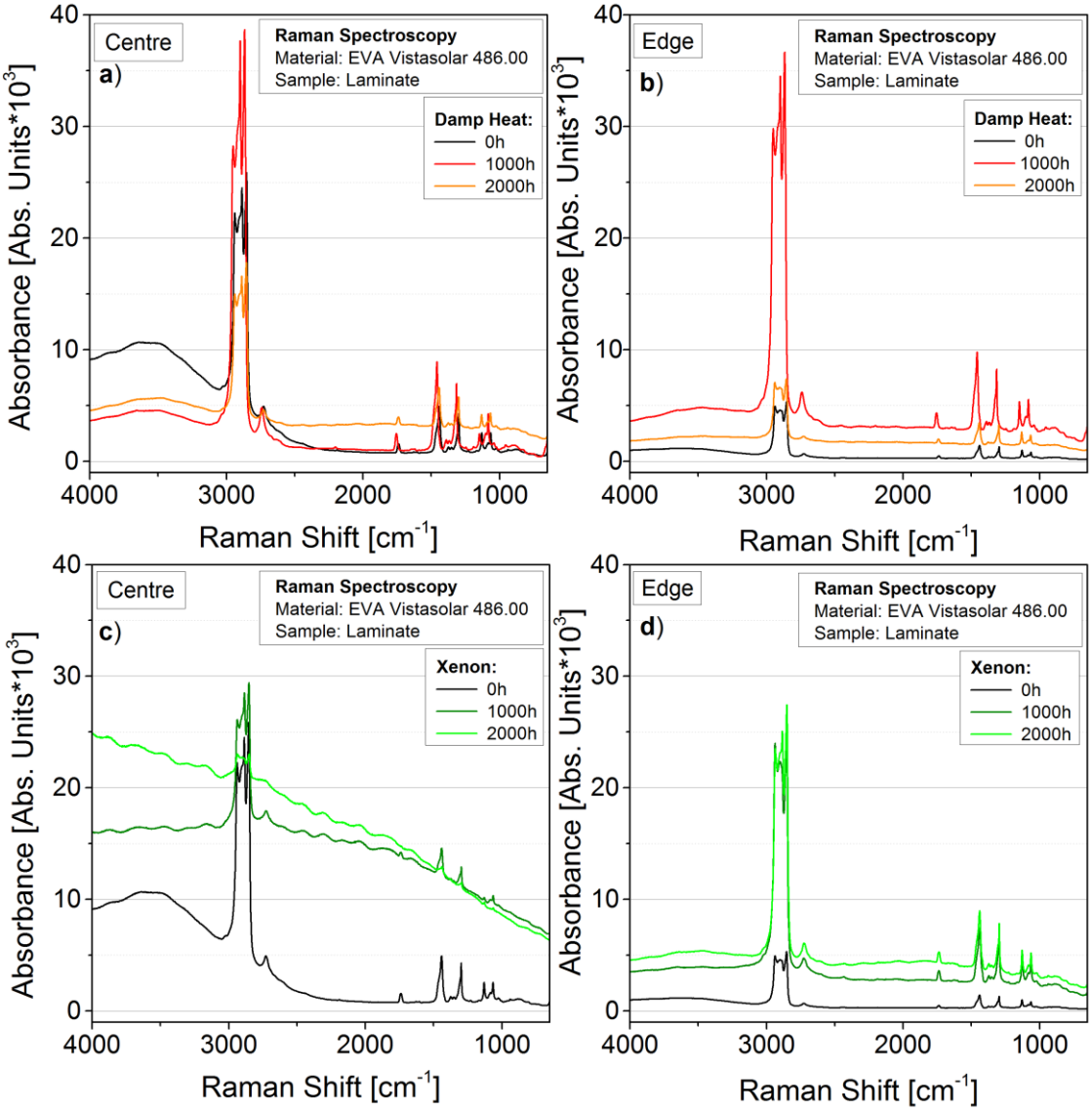

Figure 4.13: Raman spectra of EVA Vistasolar 486.00® laminates exposed to DH ageing a) centre, b) edge and XE c) cetre, d) edge.

Both DH and XE ageing of the EVA encapsulants resulted in an increasing fluorescence background. The laminated encapsulants seemed to develop more fluorescence than the films and fluorescence in the laminates was higher after XE exposure. The formation of chromophores might be stronger under XE exposure but the presence of oxygen and UV radiation might also cause photobleaching of the chromophores and therefore reduce fluorescence. XE exposed films therefore showed lower fluorescence than DH exposed films. The edge area of the XE exposed laminates showed lower fluorescence than the centre due to a higher oxygen concentration for photobleaching. Additionally a hindered

vaporisation or rinse of the chromophores by the glass cover might have caused the stronger fluorescence in laminates compared to the film samples.

Polyethylene

In Figure 4.14 the Raman spectrum of an unaged PE PV-FS Z68® film can be seen with the assignments of the typical polymer peaks. The Raman shift at 2884 cm^{-1} can be assigned to the CH_2 asymmetric stretching ($\nu^{as}CH_2$) and at 2850 cm^{-1} to the CH_2 symmetric stretching ($\nu^{s}CH_2$). Three overlaping peaks due to CH_2 scissoring (δCH_2) at 1463 cm^{-1} and the Fermi resonance and overtones at 1441 and 1418 cm^{-1} could be observed. The peaks at 1372, 1298 and 1174 cm^{-1} could be due to CH_2 wagging (ωCH_2), CH_2 twisting (tCH_2) and CH_2 rocking (ρCH_2), respectively. C-C symmetric stretching (ν^{s}C-C) could be seen at 1129 cm^{-1} and C-C asymmetric stretching (ν^{ss}C-C) at 1064 cm^{-1} (Lu et al., 1998; Sato et al., 2002; Lin-Vien et al., 1991).

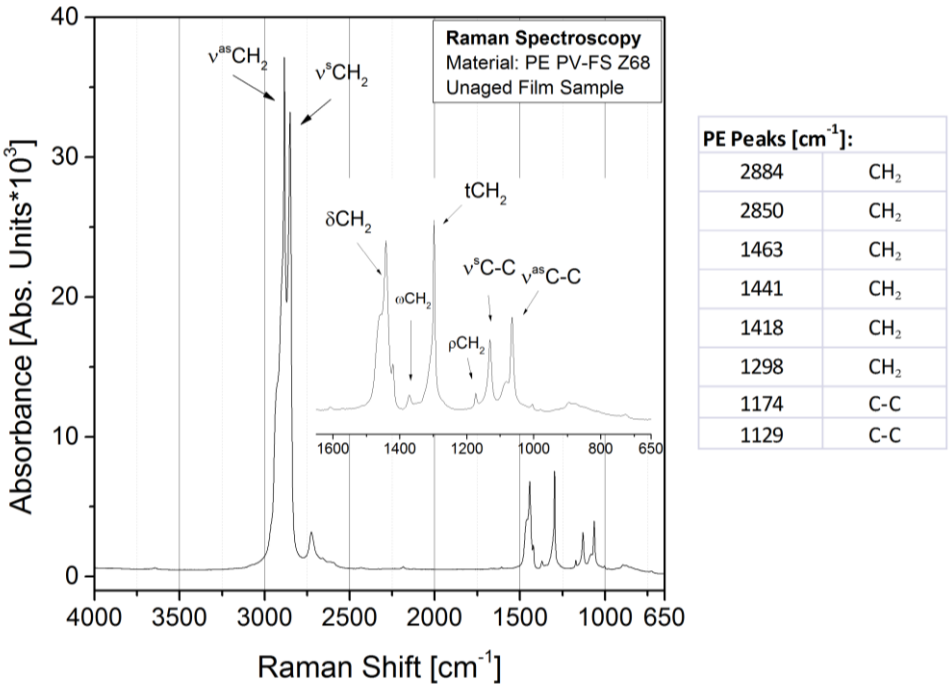

PE Peaks [cm^{-1}]:	
2884	CH_2
2850	CH_2
1463	CH_2
1441	CH_2
1418	CH_2
1298	CH_2
1174	C-C
1129	C-C

Figure 4.14: Raman spectrum of unaged PE PV-FS Z68® film sample.

In Figure 4.15 the Raman spectra of PE PV-FS Z68® films exposed to DH and XE ageing for 2000 hours can be seen without normalisation or the correction of the baseline. After the exposure of the films to DH for 2000 hours an increase of the baseline could be observed. Additional peaks at 1608, 1574, 1515, 1005, 980, 884 cm^{-1} could also be measured for the 500 hours DH exposed film. The peaks may be assigned to aromatic additives present in the material. The peaks between 1500 and 1600 cm^{-1} could be

caused by the CC vibrations of the aromatic rings and the peaks around 1000 cm^{-1} due to C-H out of plane bending (Sokrates, 2001). The same peaks could also be observed for the 2000 hours XE exposed film as well as for unaged spectra of the laminates. The peaks were therefore not considered ageing effects but possibly caused by a higher concentration of additives present in the measured spots. In the 2000 hours XE exposed film a slight indication of a peak around 1720 cm^{-1} could be seen. This peak may be caused by the formation of C=O groups in the material as observed significantly in the IR spectra (chapter 4.1). Raman spectroscopy does not respond as strongly to the C=O vibration as IR spectroscopy and PE degradation reactions resulting in C=O group formation might be detected due to C=C vibrations around 1640 cm^{-1} and hydroperoxide vibrations around 880 cm^{-1} (Sokrates, 2001). However, no peaks around 1640 cm^{-1} could be observed and the peaks around 880 cm^{-1} also occurred for unaged samples peaks are more likely to be caused by material or additive vibrations. No baseline increase could be observed for the XE exposed film samples possibly due to photobleaching of the formed chromophores in an oxygen rich environment while the DH exposed films did show an increased fluorescence.

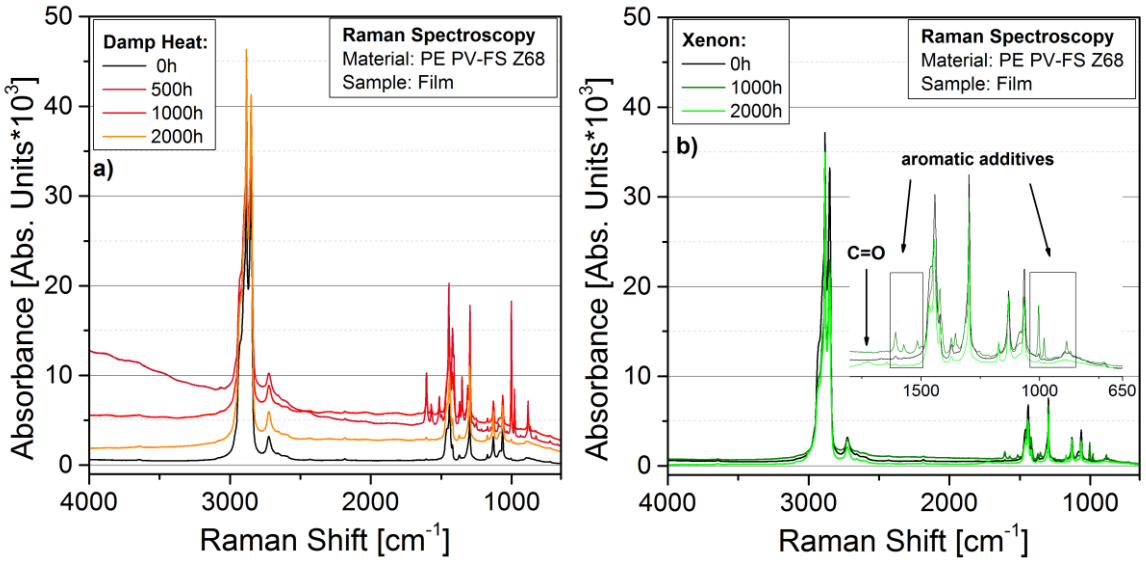

Figure 4.15: Raman spectra of PE PV-FS Z68® films exposed to a) DH ageing and b) XE for 2000 hours.

The Raman spectra of the PE PV-FS Z68® laminates exposed to DH and XE for 2000 hours can be seen in Figure 4.16. Measurements have been carried out in the centre and on the edge of the laminate as for the EVA samples even though the PE laminates showed an evenly distributed discolouration. The spectra showed typical material peaks as discussed for the unaged films. Additional peaks assigned to aromatic additives were

observed on the edge of the unaged laminate as well as on the XE exposed and DH exposed laminate edges. The baseline of the spectra showed a slight increase for all samples but no significant differences between the DH exposed samples and the XE exposed samples also for the measurements made in the centre and on the edge of the sample no significant changes could be observed. The films showed an increased baseline after DH exposure and the formation of C=O groups after XE exposure while the exposure of the laminates did not show any chemical ageing processes in Raman spectroscopy. The PE might have a lower tendency to from chromphores than EVA. Laminates therefore resulted in a lower fluorescence increase than the films due to a low oxygen concentration and possibly reduced UV radiation due to the glass cover and backsheet layer.

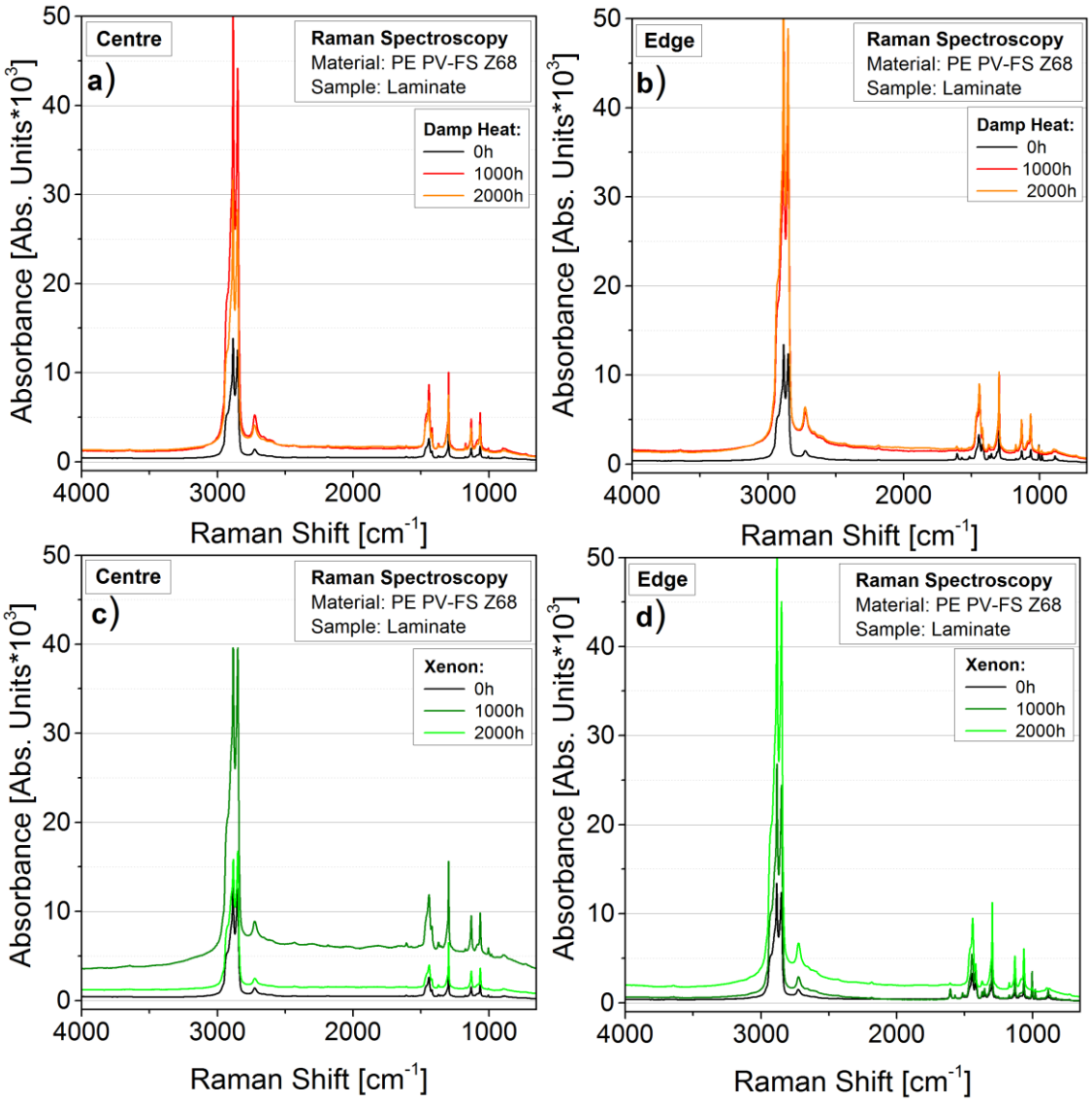

Figure 4.16: Raman spectra of PE PV-FS Z68® laminates exposed to DH ageing a) centre, b) egde and XE c) centre, d) edge.

4.3 Ultraviolet/Visible/Near-infrared (UV/Vis/NIR) Spectroscopy

Ethylene-Vinyl Acetate Copolymer

For the films UV/Vis/NIR measurements in reflectance and transmittance mode were made and the laminates were measured in reflectance mode without the removal of the encapsulant film. In order to evaluate the results from the UV/Vis/NIR experiments it has to be considered that not only the reflected and transmitted light of the films may carry different information but also that the reflectance of light at a laminate has to be distinguished from the reflected light at a film sample. A laminate measured in reflectance mode means that the light transmitted through the glass layer and then through the encapsulant film. The backsheet reflected the light back through the encapsulant layer and glass cover. Additionally reflectance of parts of the light may occur at every layer. The reflectance of the laminate measurements therefore carried a combination of various reflectance and transmittance information of the different layers.

The UV/Vis/NIR spectra were measured between 250 and 2500 nm wavelength but only the range around the cut off (200 to 800 nm) is displayed and discussed because at wavelengths higher than 800 nm (NIR region) no significant tendencies could be observed. The cut off is the point between the UV and the visible region where reflectance/transmittance of the sample drops to values close to zero. In Figure 4.17 the UV/Vis/NIR spectra of the EVA Vistasolar 486.00® films exposed to DH and XE can be seen. The spectra were measured in reflectance and transmittance mode. Both hemispherical and diffuse spectra of the films showed no significant changes in their reflectance after DH exposure. The diffuse spectrum of the 500 hours DH exposed film could not be displayed in the figure because of calculation problems due to missing data points. For the DH exposed films the cut off could be seen between 360 and 400 nm where reflectance dropped from 7.5 % to around 2.7 % (Figure 4.17 a). The XE exposed films showed an increase in the hemispherical reflectance in the UV region between 250 and 350 nm. This could be caused by the decrease of UV absorbers in the material due to the decomposition of the additives or a possible diffusion of the additives out of the film due to the missing backsheet and glass cover (Pern, 1996). The hemispherical reflectance above the cut off was about 7.5 % and differences in the curves could be considered standard deviation of the results. The diffuse reflectance of the XE exposed films increased with the exposure time indicating changes of the polymer surface. While

unaged films had a diffuse reflectance around 2.6 % the XE exposure for 2000 hours resulted in a diffuse reflectance that was almost as high as the total reflected light.

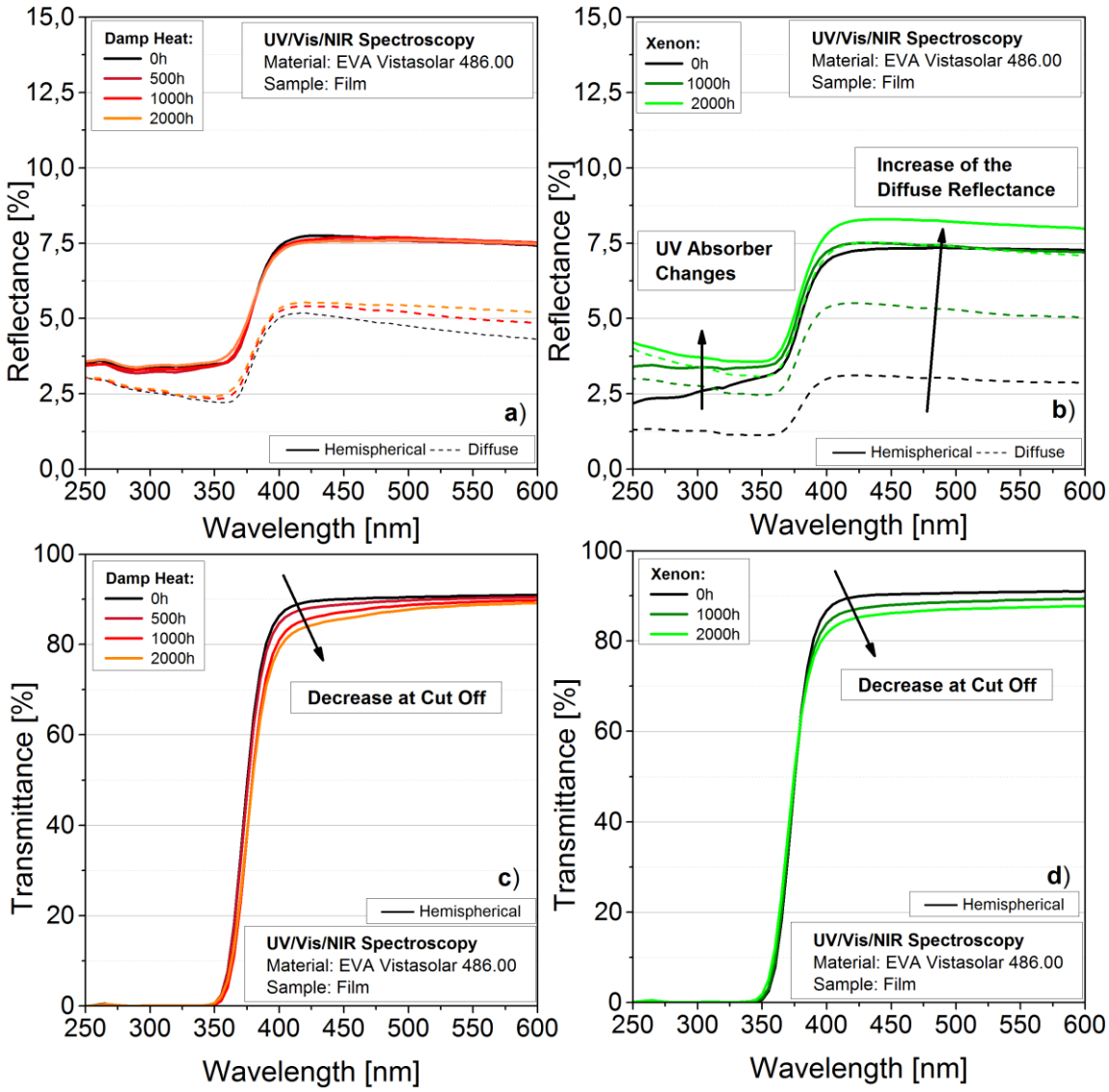

Figure 4.17: Reflectance spectra of EVA Vistasolar 486.00® films exposed to a) DH and b) XE and transmittance spectra after c) DH and d) XE exposure.

Similar observations regarding the reflectance of DH and XE exposed films were made for NovoVellum Optima MF01® in Figure 9.16 a) and b) in the appendix. EVA Vistasolar 520.00® films exposed to DH showed a broader and more undefined cut off between 300 and 400 nm as well as a higher hemispherical reflectance in the UV range of the unaged film (Figure 9.16 a). The transmittance spectra in Figure 4.17 c) and d) show a reduction in the transmittance around the cut off from about 89 to 85 % for DH and XE exposed films. A decrease in the transmittance at wavelengths above the cut off is shown

to be accompanied with the appearance of a yellow colour in the material (Pern, 1996). The NovoVellum Optima MF01® transmittance spectra in Figure 9.16 c) and d) in the appendix showed little reduction from 84 to 80 % after the exposure to DH or XE. EVA Vistasolar 520.78 films (Figure 9.14 b in the appendix)) exposed to DH showed a higher transmittance in the UV region of the unaged samples and a broader cut off. In the UV range between 250 and 400 nm (reflectance and transmittance spectra) two slight peaks at 264 and 307 nm could be observed. These peaks may probably be assigned to a UV absorber in the material.

The detailed reflectance spectra of the EVA Vistasolar 486.00 laminates exposed to DH and XE can be seen in Figure 4.18. The unaged laminates showed hemispherical reflectance of around 45 % between 400 and 600 nm with a defined cut off between 370 and 420 nm. In the UV range hemispherical reflectance dropped to around 3 %. For laminates exposed to DH for 2000 hours (Figure 4.18 a) a decrease of the hemispherical reflectance from about 41 to 38 % around the cut off could be observed. The diffuse spectra showed a similar tendency with the diffuse reflectance dropping from 38 to 34 %. The laminates exposed to XE (Figure 4.18 b) showed a significant decrease of hemispherical reflectance from 42 to 30 % at wavelengths higher than the cut off. The diffuse reflectance showed a similar decrease. No significant increase of the hemispherical reflectance in the UV region could be observed for the laminates exposed to DH and XE.

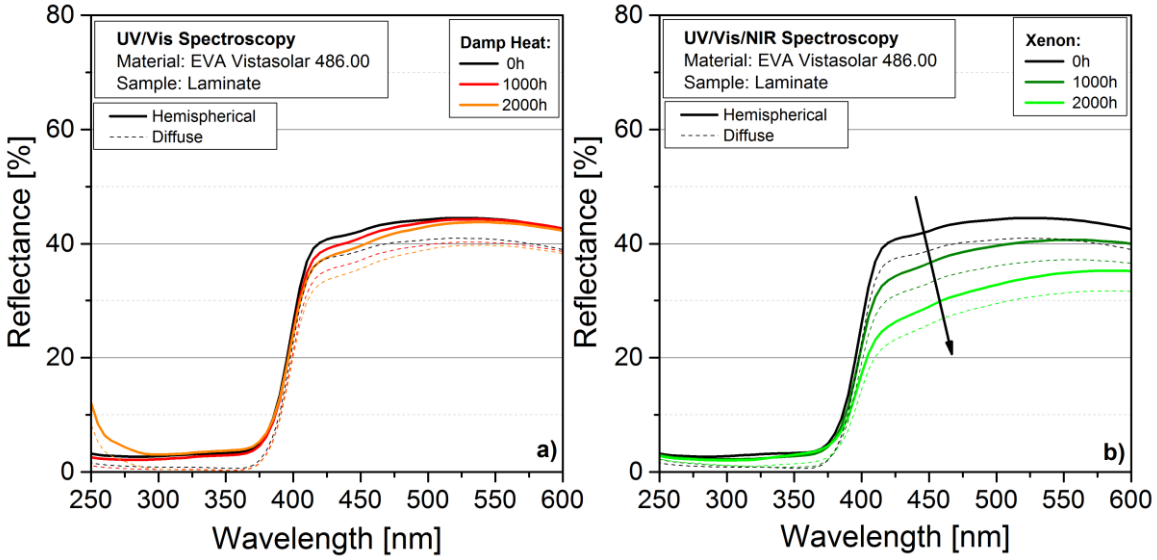

Figure 4.18: Reflectance spectra of EVA Vistasolar 486.00® laminates exposed to a) DH and b) XE for 2000 hours.

The EVA laminates exposed to XE showed a significant decrease in hemispherical reflectance while aged films only resulted in a slight decrease of the transmittance and no

significant changes in reflectance. This decrease in hemispherical reflectance of the laminates could be caused due to a stronger decrease of the transmittance of the encapsulant during ageing in a laminated structure. It also has to be considered that possible ageing of the backsheet layer might have resulted an increasing amount of light being absorbed and used for degradation reactions and heating up the material. Changes of the backsheet layer might have contributed significantly to the decrease of reflectance of the laminate. An increase in hemispherical reflectance in the UV region could only be observed for the XE exposed films while the laminates showed no significant changes. An extraction of the UV absorbers from the films could have occurred due to diffusion or washing with water during the wet cycle of the XE exposure. For the laminates the glass cover worked as a barrier against water entering the laminate and prevented the diffusion and washing of the UV absorbers. The XE exposed films also showed an increase of the diffuse reflectance while the hemispherical reflectance showed no changes. The laminated samples showed a similar decrease of diffuse and hemispherical reflectance. This might indicate changes of the polymer surface of the XE exposed films due to photo-oxidation while laminates showed no changes. Photo-oxidation reactions resulted in the formation of various functional groups (as observed in IR spectroscopy in chapter 4.1) and might have resulted in an increasing scattering of light and therefore an increasing diffuse reflectance.

In Figure 4.19 b*-values - representing the yellow and blue colour - of EVA Vistasolar 486.00® films and laminates exposed to DH and XE are shown. The b*-values of the films were evaluated from the transmittance measurements and for the laminates from the hemispherical reflectance measurements. The unaged films showed b*-values of 0.54±0.01 and an increase to 1.99±0.15 could be observed after the exposure to DH for 2000 hours. The DH exposed laminates showed a very similar increase from 0.72±0.12 to 2.81±0.08. The films measured in transmittance and exposed to XE exposure for 2000 hours showed b*-values between 0.40±0.03 and 0.91±0.09 and therefore no significant increase. The laminates had b*-values of 0.72±0.12 and increased strongly to 7.11±1.59 after exposure to XE. Considering the b*-values of the other EVA types shown in Figure 9.18 and Figure 9.19 in the appendix it seems that the DH exposure resulted in no significant yellowing of the films. Also the exposure of the films to XE resulted in no significant yellowing. Laminates showed a slight increase in the yellow colour after DH exposure for 2000 hours and a strong increase after the exposure to XE. The increase in the yellow colour therefore could not be correlated with the oxidation of the EVA as

observed in IR in chapter 4.1. The laminates showed higher discolouration that could be caused due to the formation of small chromophores that could not diffuse through the glass and backsheet layer. Additionally it is likely that discolouration of the backsheet layer took place contributing to the b*-values as well as possible interactions between the encapsulant and backsheet layer resulting in the formation of chromophores.

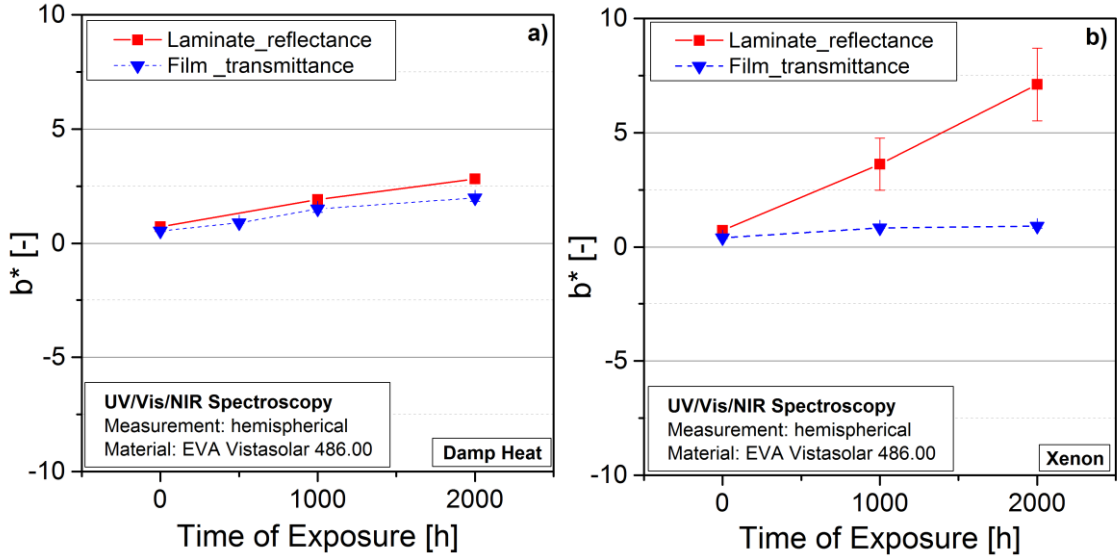

Figure 4.19: b*-values of EVA Vistasolar 486.00® films and laminates exposed to a) DH and b) XE for 2000 hours.

Polyethylene

The UV/Vis/NIR reflectance and transmittance spectra of PE PV-FS Z68® films exposed to DH and XE for 2000 hours are shown in Figure 4.20. PE PV-FS Z68® films exposed to DH for 2000 hours showed a decrease in hemispherical reflectance from 24 to 14 % at wavelengths around 420 nm. The diffuse reflectance decreased correlatively to the hemispherical reflectance. The UV region can be seen between 250 and 400 nm and showed well defined peaks at 360, 311 and around 250 nm due to the UV absorber additives in the material. When exposed to DH for 2000 hours no significant peaks could be seen in the UV region. However, the hemispherical reflectance in the UV range did not increase as seen for the XE exposed EVA films indicating a decrease in UV absorbers in the PE films during XE exposure. The films measured in transmittance mode showed values between 77 and 82 % in the visible region after DH exposure. The unaged film showed the lowest hemispherical reflectance and very similar values to the 2000 hours aged film sample. The highest reflectance values were found for the 500 hours DH exposed film. The differences in the transmittance of the DH exposed films were therefore considered standard deviation and no ageing effect. In the UV region transmittance

values around 0.3 % were found and two small peaks at 330 and 265 nm due to UV absorbers could be observed.

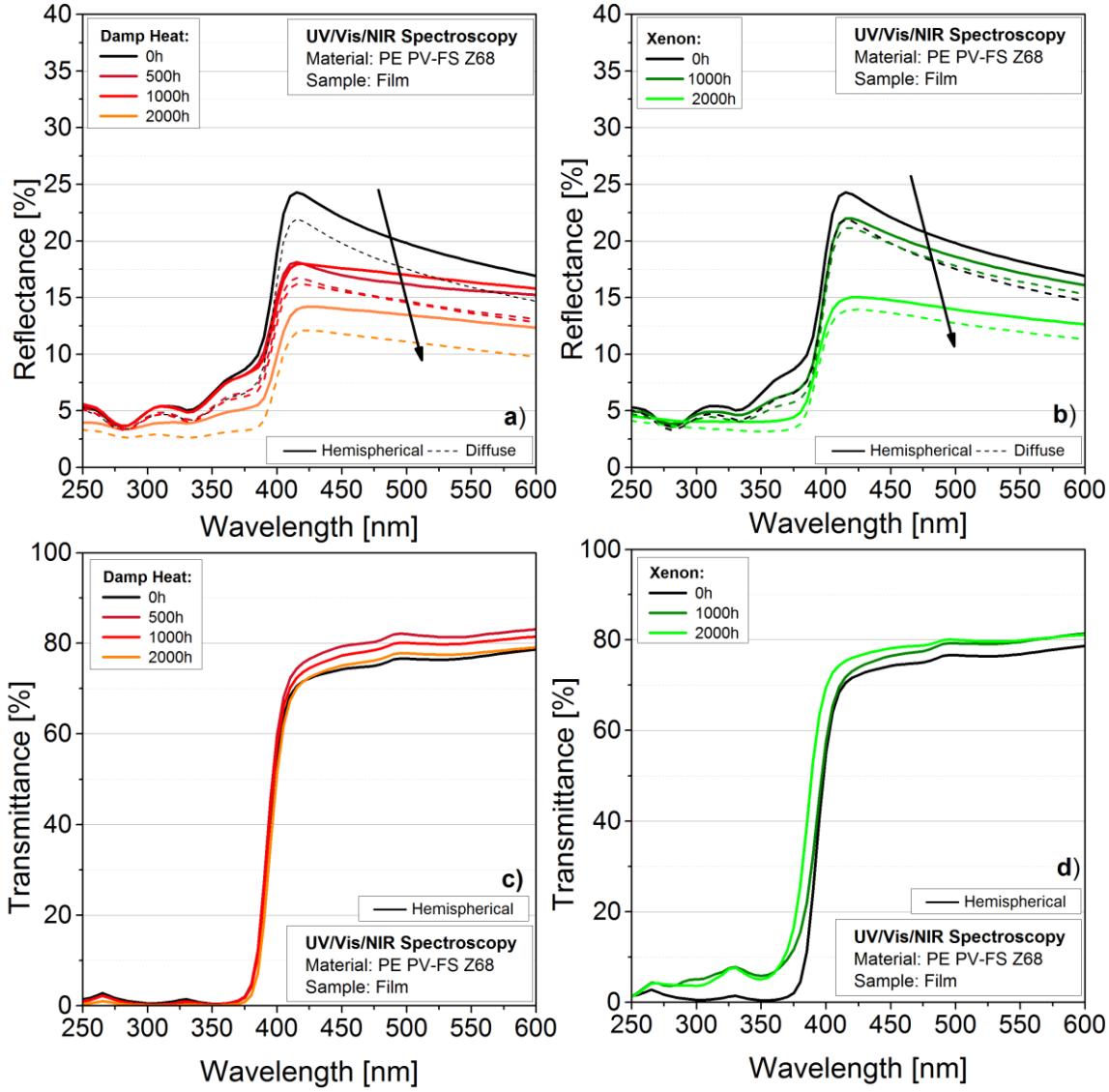

Figure 4.20: Reflectance spectra of PE PV-FS Z68® films exposed to a) DH and b) XE and transmittance spectra exposed to c) DH and d) XE.

The hemispherical reflectance of the films exposed to XE decreased from 24 to 15 % and therefore showed a similar behaviour as the DH aged films. XE exposed films showed similar transmittance values between 77 and 80 %, the unaged film showing the lowest and the 2000 hours aged film the highest transmittance. In the UV region the XE aged films showed transmittance up to 8 %, which could be due to a reduction in UV absorbers as assumed for the EVA films exposed to XE. Comparing the reflectance and transmittance spectra of the PE films exposed to DH and XE exposure it could be

observed that the reflectance values in the visible region decreased while the transmittance values showed just slight changes. Therefore an increasing absorption of visible light of the PE films during DH and XE exposure could be observed.

The UV/Vis/NIR spectra of the PE PV-FS Z68 laminates exposed to DH and XE for 2000 hours can be seen in Figure 4.21.

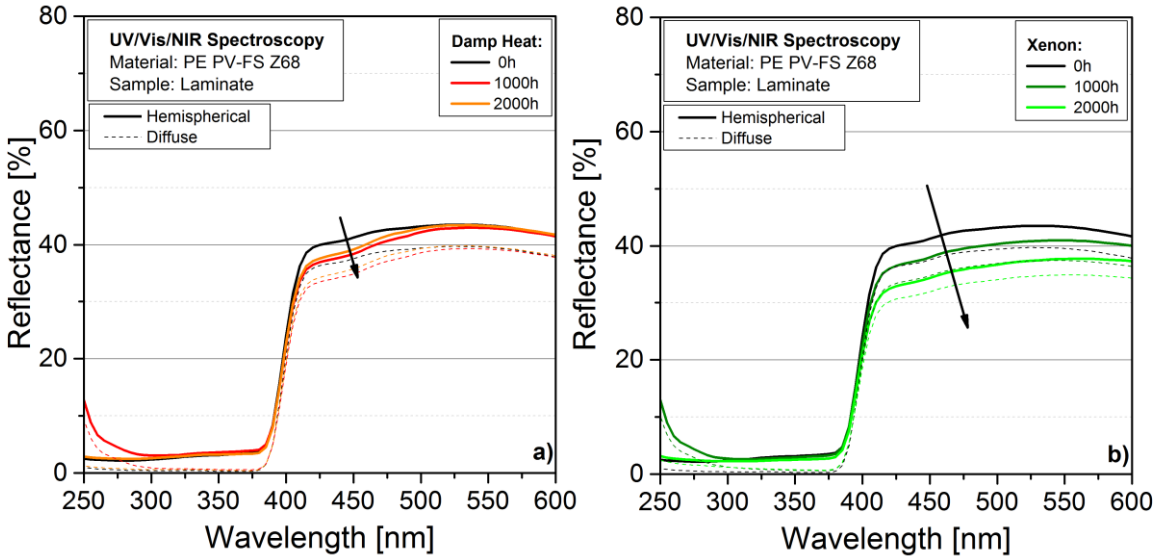

Figure 4.21: Reflectance spectra of PE PV-FS Z68® laminates exposed to a) DH and b) XE for 2000 hours.

Unaged laminates showed hemispherical reflectance values of around 40 % at the cut off and of about 3 % in the UV region. After exposure to DH for 2000 hours the reflectance decreased to 37 %. No significant changes could be observed in the UV region after DH exposure. The diffuse reflectance showed a similar tendency with values decreasing from 36 to 33 % at the cut off. The laminates showed a decrease in the reflectance values in the visible region. The laminates exposed to XE for 2000 hours showed a decrease of hemispherical reflectance from 40 to 32 % at the cut off. XE exposed laminates also showed a decrease in the visible region while the decrease in reflectance for the DH exposed laminates could only be observed around the cut off. In the UV region no significant changes could be observed for the XE exposed samples. The diffuse reflectance showed a similar tendency with values decreasing from 36 to 30 % at the cut off and in the visible region. The DH exposed PE films therefore showed a stronger decrease in hemispherical reflectance than the aged laminates suggesting a significant influence of the microclimate at the polymer film. A similar increase in absorption of the films exposed to XE and DH indicated that the presence of humidity and oxygen under increased temperatures might be the main cause for the absorbance increase of the films.

In IR spectroscopy the presence of polar groups (OH, C=O) could be observed for the modified PE encapsulants. The functional groups might have influenced the polarity of the polymer and favoured water and oxygen diffusion and resulted in interactions with these molecules. However, no significant peaks could be observed in IR or Raman spectroscopy to clarify these interactions, possibly due to an insufficient amount to be detected. Laminates showed a stronger decrease in reflectance when exposed to XE than to DH suggesting a contribution of the backsheet layer as described for the EVA laminates.

Figure 4.22 shows the b*-values of the PE PV-FS Z68® film and laminate samples exposed to DH and XE for 2000 hours. The films (transmittance mode) showed b*-values between 2.17±0.22 and 2.61±0.17 and no significant change correlated to exposure time could be observed. Laminates (reflectance mode) exposed to DH increased from 0.8±0.03 to 3.17±0.08 after 1000 hours and decreased slightly to 2.62±0.26 after 2000 hours. The PE films resulted in b*-values of 2.61±0.17 for the unaged sample and 2.9±0.15 after 1000 hours of XE exposure. Further exposure of 2000 hours led to a decrease to 1.69±0.09. The laminates showed an increase from 0.8±0.03 to 3.17±0.56 after 2000 hours of XE exposure. The b*-values of the films showed no significant changes with exposure time. The laminates exposed to DH and XE showed a slight increase in the b*-values after DH and XE exposure. When compared to the films no significantly higher b*-values were reached after 2000 hours of ageing.

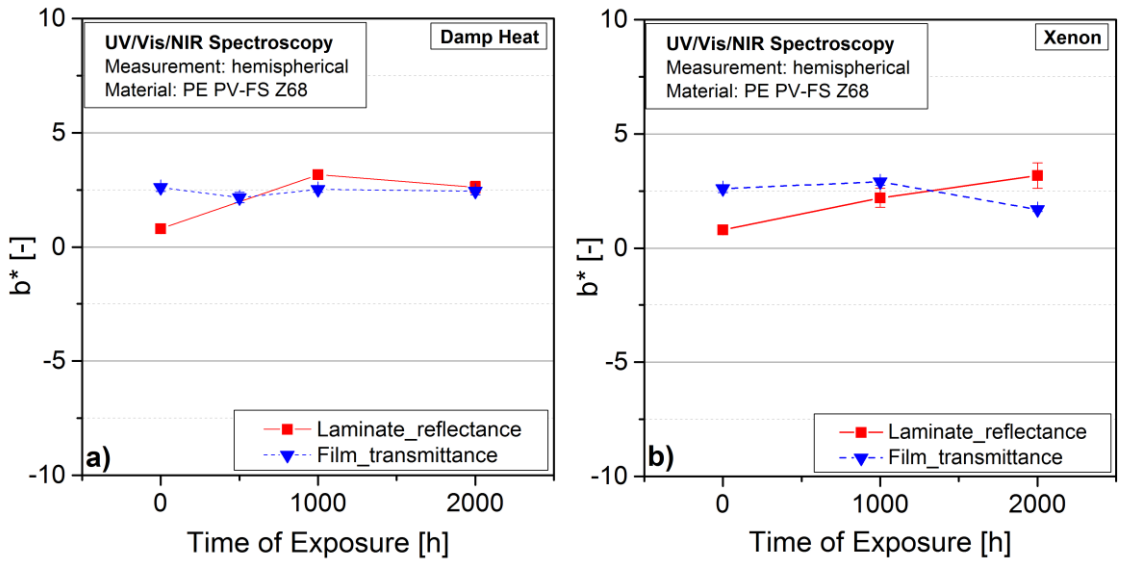

Figure 4.22: b*-values of PE PV-FS Z68® films and laminates exposed to a) DH and b) XE for 2000 hours.

The PE laminates exposed to XE resulted in a lower increase in b*-values when compared to the EVA laminates. EVA showed a stronger tendency for discolouration due to the formation of chromophores in the material. The contribution of the backsheet layer to the b*-values of the laminate might also be significantly influenced by different interactions with EVA and PE.

4.4 High Performance Liquid Chromatography (HPLC) with Mass Spectrometry (MS) and Ultraviolet (UV) Spectroscopy

Ethylene-Vinyl Acetate Copolymer

In the high performance liquid chromatography (HPLC) with mass spectrometry (MS) and ultraviolet (UV) spectroscopy experiments the additives in the encapsulants were analysed. In pretests the presence of UV absorber additives was confirmed and possible changes in the UV absorber were investigated. The results of the HPLC and MS measurements delivered information to determine additives present in the polymer as well as about the UV absorbance of the UV active additives. Additives from unaged and XE exposed film samples and laminates were tested. Laminates were tested in the centre and on the edge area. After the extraction from the EVA encapsulants an UV absorber, a hindered amine light stabilizer (HALS) and an antioxidant could be determined by their mass spectra and UV absorbance. The chemical structures and molar masses of the additives found are shown in Table 4.1.

Table 4.1: Description of the polymer additives found in the encapsulant films (Telko, 2010a; Telko, 2010b; Agilent Technologies, 2003).

Additive	Chemical Name	Chemical Structure	Molecular Weight [g/mol]
UV absorber	Methanone, [2-hydroxy-4-(octyloxy)phenyl] phenyl,-	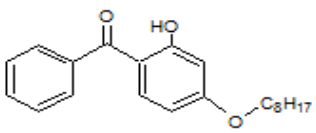	326.4
HALS	Bis(2,2,6,6,-tetramethyl-4-piperidyl) sebaceate	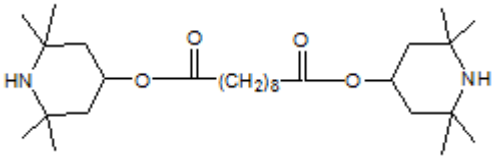	481.0
Antioxidant	Tris Nonylphenyl Phosphite	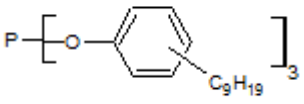	688.5

The UV absorber could be determined due to the mass spectra peaks of the molecule at 326 m/z and the peaks of the cleavage products at 248 and 213 m/z (Figure 9.20 in the appendix). Additionally the UV absorber could be identified due to the UV spectrum shown in Figure 4.23. The spectrum shows absorption peaks at 241, 287 and 314 nm. Pern and Czanderna published a similar UV absorption spectrum of Cyasorb UV 531®/Chimassorb 81® (a different trade name for the same UV absorber additive) (Pern and Czanderna, 1992a). HALS could be determined due to the mass spectrum peaks at 481 m/z of the molecule and at 356, 277 and 265 m/z of the cleavage products (Figure 9.21 in the appendix). The molecule seemed to be like the HALS Tinuvin 770®. The antioxidant had the molecule peak at 689 m/z but was determined due to its cleavage product at 501 m/z and is likely to be similar to Naugard P® (Figure 9.22 in the appendix). The described additives were found in all unaged EVA films and laminates. Publications also described these additives to be present in EVA films for PV encapsulants investigated in their research (Ezrin et al., 1995; Pern, 1993; Hintersteiner et al., 2014).

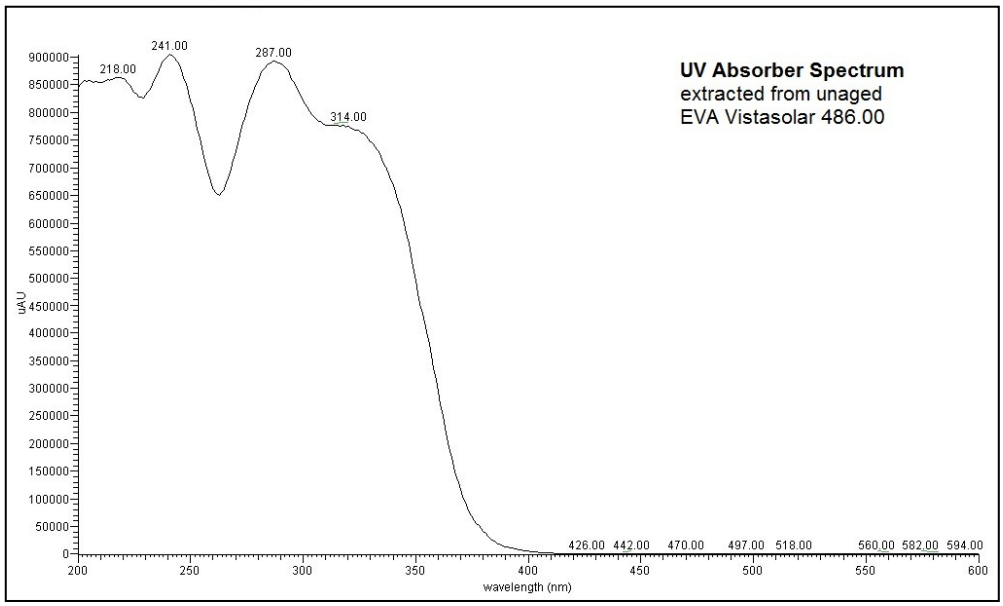

Figure 4.23: UV spectrum after extraction of unaged EVA Vistasolar 486.00®.

The described peaks of the mass spectra as well as the UV spectra of the extracted additives were analysed after the exposure to XE for 2000 hours. In Table 4.2 the determination of the additives made from mass spectra and UV spectra for the EVA Vistasolar 486.00® samples are shown. The UV absorber could be found in the mass and UV spectra of all film and laminate samples. No differences between the centre and the edge of the laminate could be observed and no significant changes could be seen after the exposure to XE for 2000 hours. The HALS could also be observed in all samples and

no significant tendencies could be found regarding time of exposure or film and laminate samples. The antioxidant was found in all samples except in the centre of the 1000 hours exposed laminate and the edge of the unaged laminate. The absence of the additive in these samples is most likely due to a low concentration, because various small peaks could be observed but no definite assignment could be made. For NovoVellum Optima MF01® similar results could be achieved (Table 9.6 in the appendix). In EVA Vistasolar 520.78® the UV absorber could be found in the unaged films and laminates. After the exposure to XE no UV absorber could be observed in the mass or UV spectra, possibly due to a low concentration. These samples turned into a sticky mass possibly due to severe material degradation. The antioxidant could also not be found in the 1000 hours XE exposed films and laminates. After 2000 hours of exposure all samples contained the antioxidant. In the UV/Vis/NIR spectra of EVA Vistasolar 486.00® and NovoVellum Optima MF01® films a decrease of the UV absorbers with XE exposure time was observed (chapter 4.3). In the HPLC-MS/UV measurement of these samples no significant decrease in UV absorbers could be detected. This indicates that possibly not all but just a certain amount of additives was extracted from the samples and therefore no changes in the amount of additives could be measured.

Table 4.2: Additive analysis of the HPLC-MS/UV measurements of EVA Vistasolar 486.00® films and laminates exposed to XE.

EVA Vistasolar 486.00	Sample Taking	Xenon Weathering [h]	Mass Spectrometry			UV Spectroscopy
			UV Absorber	HALS	Antioxidant	UV Absorber
			326, 248, 213 [m/z]	481, 356, 277, 265 [m/z]	688, 501 [m/z]	200 - 350 [nm]
Film	Centre	0	✓	✓	✓	✓
		1000	✓	✓	✓	✓
		2000	✓	✓	✓	✓
Laminate	Centre	0	✓	✓	✓	✓
		1000	✓	✓	-	✓
		2000	✓	✓	✓	✓
	Edge	0	✓	✓	-	✓
		1000	✓	✓	✓	✓
		2000	✓	✓	✓	✓

Polyethylene

The HPLC-MS/UV measurements showed that in the PE samples also UV absorbers, HALS and antioxidants were present. The HPLC showed longer elution times for the UV

absorber as in the EVA measurements indicating a different UV absorber. The UV spectrum of the UV absorber can be seen in Figure 4.24 with peaks at 303 and 342 nm. The mass spectra indicated that the UV absorber extracted from the PE samples had a molar mass of 657 g/mol, but no exact molecule could be determined (Figure 9.23 in the appendix). The HALS and antioxidant additives present in the PE samples could be determined as the similar additives found in the EVA samples. The additives found in the PE samples were analysed after the exposure to XE for 2000 hours (Table 4.3). The UV absorber could be observed in the unaged and 1000 hours exposed films but no UV absorber was measured after the exposure of 2000 hours. For PE laminates the UV absorbers could be determined in all unaged and XE exposed samples. No differences regarding the centre and the edge of the laminate could be made. The HALS and antioxidant additives were present in all unaged and XE exposed films and laminates.

Table 4.3: Additive analysis of the HPLC-MS/UV measurements of PE PV-FS Z68® films and laminates exposed to XE.

PE PV-FS Z68	Sample Taking	Xenon Weathering [h]	Mass Spectrometry			UV Spectrsocopy
			UV Absorber	HALS	Antixidant	UV Absorber
			657 [m/z]	481, 356, 277, 265 [m/z]	688, 501 [m/z]	200 - 350 [nm]
Film	Centre	0	✓	✓	✓	✓
		1000	✓	✓	✓	✓
		2000	✓	✓	✓	✓
Laminate	Centre	0	✓	✓	✓	✓
		1000	✓	✓	✓	✓
		2000	✓	✓	✓	✓
	Edge	0	✓	✓	✓	✓
		1000	✓	✓	✓	✓
		2000	-	✓	✓	-

With HPLC-MS/UV measurements UV absorbers, HALS and antioxidants present in the EVA and PE encapsulants could be determined. After the exposure to DH and XE for 2000 hours the additives were still present in the materials and therefore material ageing could not be caused due to the absence of UV absorber protection. For the EVA Vistasolar 520.78® no UV absorbers could be determined after XE exposure and these samples also showed a severe change in the mechanical properties observeable during sample taking. The samples had turned from films into a sticky mass on the sample

holder. This could indicate polymer degradation due to the absence of UV absorbers for this EVA type.

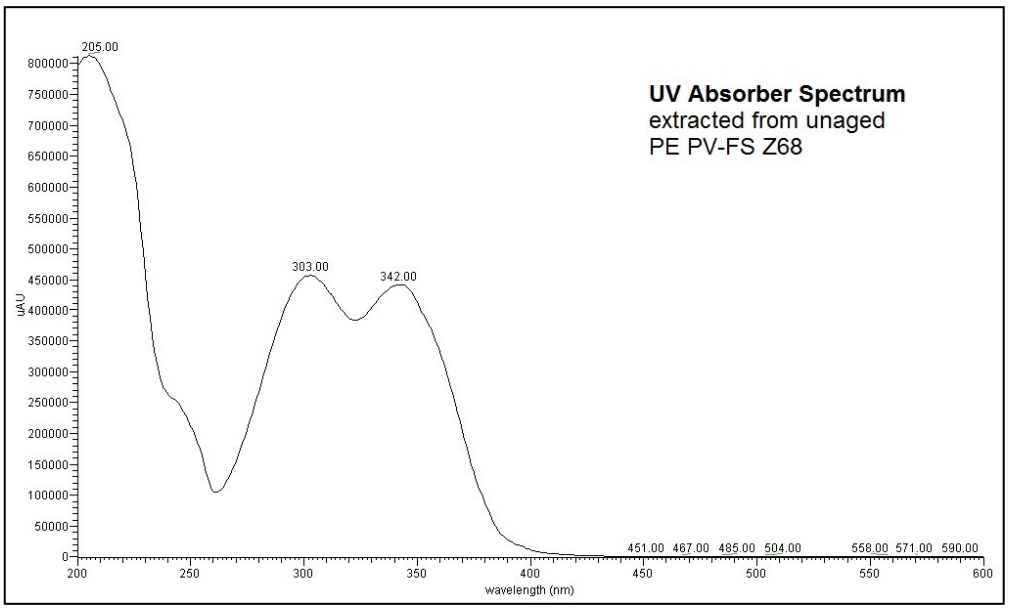

Figure 4.24: UV spectrum after extraction of unaged PE PV-FS Z68®.

4.5 Differential Scanning Calorimetry (DSC)

Ethylene-Vinyl Acetate Copolymer

The DSC was used to evaluate the crosslinking degrees of the unaged EVA types and observe crosslinking changes during artificial ageing. For the evaluation not crosslinked and unaged films of the EVA types were used to receive the curing enthalpy of an uncured material H_0. In Figure 4.25 the DSC curves of the unaged and not crossslinked films of the three EVA types can be seen. The degree of curing was calculated according to formula 3.3 with the curing enthalpy of the unaged and crosslinked samples. DSC was used in sample preparation to assure comparable crosslinking degrees of the samples prepared in the vacuum lamination press (VLP) and the laboratory oven (LO). In Table 4.4 the crosslinking data of the unaged EVA samples can be seen. The degree of curing of the films made in the VLP (82.81 %) and the LO (82.69 %) showed very similar results for the EVA Vistasolar 486.00® films. EVA Vistasolar 520.78® and EVA NovoVellum Optima MF01® showed crosslinking degrees of VLP 82 %, LO 76 % and VLP 83 %, LO 68 %, respectively. The DSC data can be seen in Table 9.7 in the appendix. The laminates were measured in the centre and on the edge. For EVA Vistasolar 486.00® the results in the centre of the laminate showed no curing peak and therefore a degree of curing of 100 %. On the edge of the laminate a degree of curing of 82.96 % could be measured.

EVA Vistasolar 520.78® laminates showed a degree of curing of 82 % in the centre and 87 % on the edge area. EVA NovoVellum Optima MF01® resulted in degrees of curing of 82 % in the centre and 77 % on the edge of the laminate. The maximum peak temperatures of the crosslinking peak were found between 165±0 and 167±1 °C.

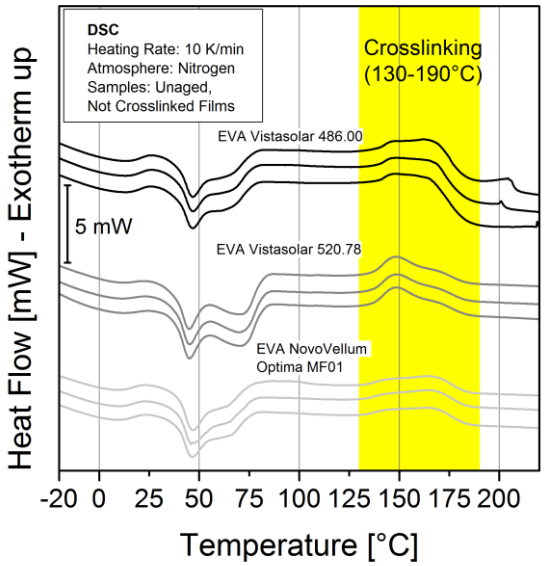

Figure 4.25: DSC measurement of unaged and not crosslinked films of the EVA types

Figure 4.26 shows the first and second heating of the DSC measurements of EVA Vistasolar 486.00® film samples. The curves of the unaged films prepared in LO (Figure 4.26 a) and in the VLP (Figure 4.26 b) were compared. In the first heating the LO samples showed a double melting peak at 40±0 and 62±1 °C and the VLP samples at 46±0 and 59±0 °C. In the second heating only the second melting peak could be observed. The first heating represents the mechanical and thermal history of the samples and the second heating gives information about the material behaviour under the given cooling conditions. The second peak of the double melting peak in the first heating could be attributed to the thermo-dynamic melting point of the material and the first peak might be caused because of a less organised crystal phase formed in the area among the primary crystals (Knausz et al., 2015). The LO samples showed the first peak at lower temperatures than the VLP samples and the second peak at just slightly shifted temperatures. The second peak of the LO prepared films was much more pronounced than for the VLP samples. The laminates (prepared in the VLP) showed similar results to the VLP films. This observation could be made for all EVA types and indicated that the different preparation conditions (temperature, pressure) might have influenced the crystallisation of the polymer when the material was cooled down after crosslinking. The

DSC results up until now described thermal properties of the unaged samples (crosslinking, crystallisation) deriving from the sample preparation but are no chemical ageing processes.

Table 4.4: Crosslinking data of unaged EVA Vistasolar 486.00® of different sample types, sample taking points and preparation.

Material	Type	Sample Taking	Crosslinking	Peak Temperature [°C]	Curing Enthalpy [J/g]	Degree of curing [%]
EVA Vistasolar 486.00	Film	Centre	not crosslinked	165±0	25.70±0.62	-
	Film	Centre	LO	167±1	4.45±0.23	83
	Film	Centre	VLP	166±1	4.42±0.17	83
	Laminate	Edge	VLP	167±0	4.38±0.20	83
	Laminate	Centre	VLP	-±-	-±-	100

To exemplarily display the effect of artificial ageing by DH and XE the curves of EVA Vistasolar 486.00® films were used (Figure 4.26). For the unaged sample the double melting peak caused by two different crystalline structures in the polymer could be measured in the first heating. Additionally a curing peak between 130 and 190 °C could be observed. In the second heating only one melting peak at 64 °C could be measured. After the exposure to DH ageing for 500 hours the melting peaks in the first and second heating remained the same but no curing peak could be observed. The same result was found after 1000 hours of XE exposure. The degrees of curing of around 80 % after the preparation process increased to 100 % due to post-crosslinking during the exposure (Bregulla et al., 2007). Post-crosslinking was found for all films and laminates (centre and edge) of all three tested EVA types exposed to DH and XE. The post-crosslinking therefore seemed not to be affected by the microclimate due to a different oxygen or water concentration. UV radiation during XE exposure might have favoured the decomposition of peroxides and caused post-crosslinking but the storage at temperatures around 85 °C for 500 hours seemed to be sufficient for the peroxides to decompose. Only the EVA Vistasolar 486.00® laminate in the centre already showed a degree of curing of 100 % without the exposure to DH or XE. Also for the XE exposed EVA Vistasolar 520.78® films no post-crosslinking could be determined because already after 1000 hours of exposure advanced degradation of the material could be observed where post-crosslinking could not be determined with certainty. The DSC curves of the DH and XE exposed films of EVA Vistasolar 520.78® and EVA NovoVellum Optima MF01® are shown in Figure 9.24 and

Figure 9.25 in the appendix. The evaluation of the peak temperatures and enthalpies of the DSC measurements of all samples and types showed no further tendencies correlating to chemical ageing. No significant differences between the exposure of a film or a laminate could be observed.

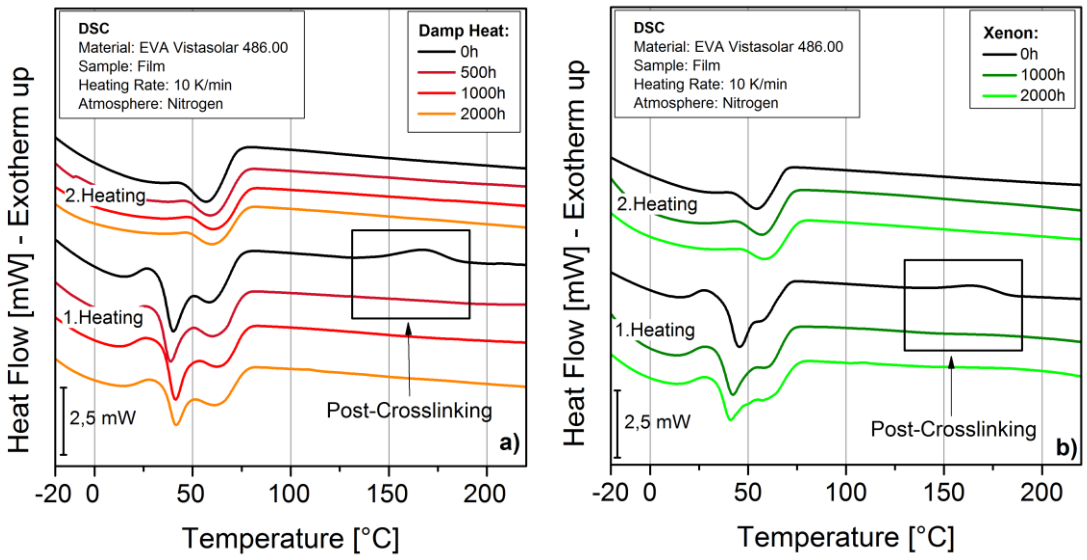

Figure 4.26: DSC curves of first and second heating of EVA Vistasolar 486.00® films exposed to a) DH and b) XE fro 2000 hours.

Polyethylene

In Figure 4.27 the DSC curves of the PE PV-FS Z68® films exposed to DH and XE for 2000 hours are shown. The unaged films showed a broad melting area between 25 and 125 °C with two peaks at 55±0 and 96±0 °C in the first heating. In the second heating one peak at 94±0 °C could be seen. After the exposure to DH for 500 hours an increase of the melting peak around 96 °C and the formation of two melting peaks at 40±0 and 69±0 °C could be seen in the first heating. In the second heating the melting peak shifted to lower temperatures (83±0 °C) and the enthalpy of the peak decreased from 97.65±10.17 to 81.12±0.49 J/g. Further exposure to DH for 1000 and 2000 hours did not result in further changes of the melting peak temperatures or enthalpies both for the first and second heating. It has to be considered that the first heating represents the thermal and mechanical history and the characteristic properties of the material while the second heating only represents the material properties (Ehrenstein et al., 2003). A change in the melting peak of the second heating therefore indicates structural changes of the polymer. The DSC curves of the PE films exposed to XE exposure can be seen in Figure 4.27 b). In the first heating four peaks were formed at 42±0, 63±0, 86±1 and 100±1 °C after

1000 hours of exposure. Further changes of the melting peaks to 43±1, 60±1, 98±6 and 105±3 °C were observed after 2000 hours of XE exposure. The second heating showed a decrease of the melting peak temperature after 1000 hours to 84±0 °C comparable to the melting peaks observed for the DH aged films exposed for 500, 1000 and 2000 hours. Further exposure of 2000 hours resulted in a shift of the melting peak in to higher temperatures (98±1 °C). Vallés-Lluch et al. investigated the effect of gamma irradiation on PE and described the decrease of the melting temperature at low irradiation due to the increase of molecular defects (e.g. C=O formation) that hinder the crystallisation process (Vallés-Lluch et al., 2003). At higher irradiation an increase in the melting temperature could occur because of the increasing chain scission reactions that allow the polymer chains to increase the lamellar thickness. Frick and Stern also described the correlation between a decreasing molar mass and an increasing crystallisation temperature during the cooling of the polymer (Frick and Stern, 2006). The crystallisation peaks of the PE are not displayed in this thesis but showed the same temperature shifts as the melting temperatures in the second heating shown in Figure 4.27. The IR measurements of the XE exposed PE films in chapter 4.1 showed an increasing number of formed C=O groups. The results do support the assumption that chain scission caused the melting temperature increase measured in the second heating of the 2000 hours XE exposed films. DH exposed films did not show oxidation in the IR measurements and the melting peak change in the second heating must therefore be caused by other structural changes that hindered the crystallisation and resulted in a broader melting peak at lower temperatures.

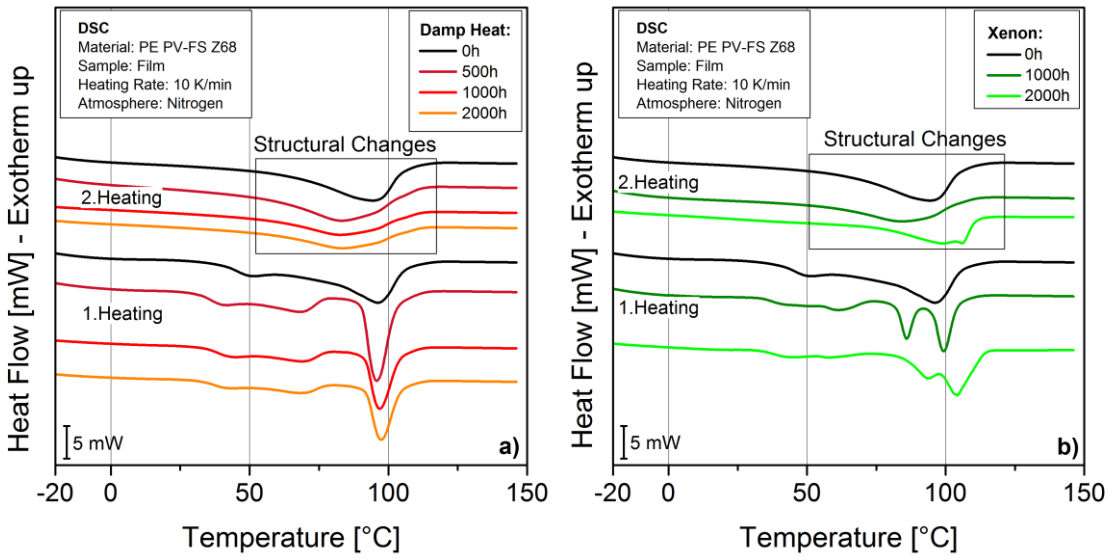

Figure 4.27: DSC curves of the first and second heating of PE PV-FS Z68® films exposed to a) DH and b) XE.

The DSC curves (1. and 2. heating) of the PE PV-FS Z68® laminates measured in the centre and on the edge and exposed to DH and XE are shown in Figure 4.28 a) and b).

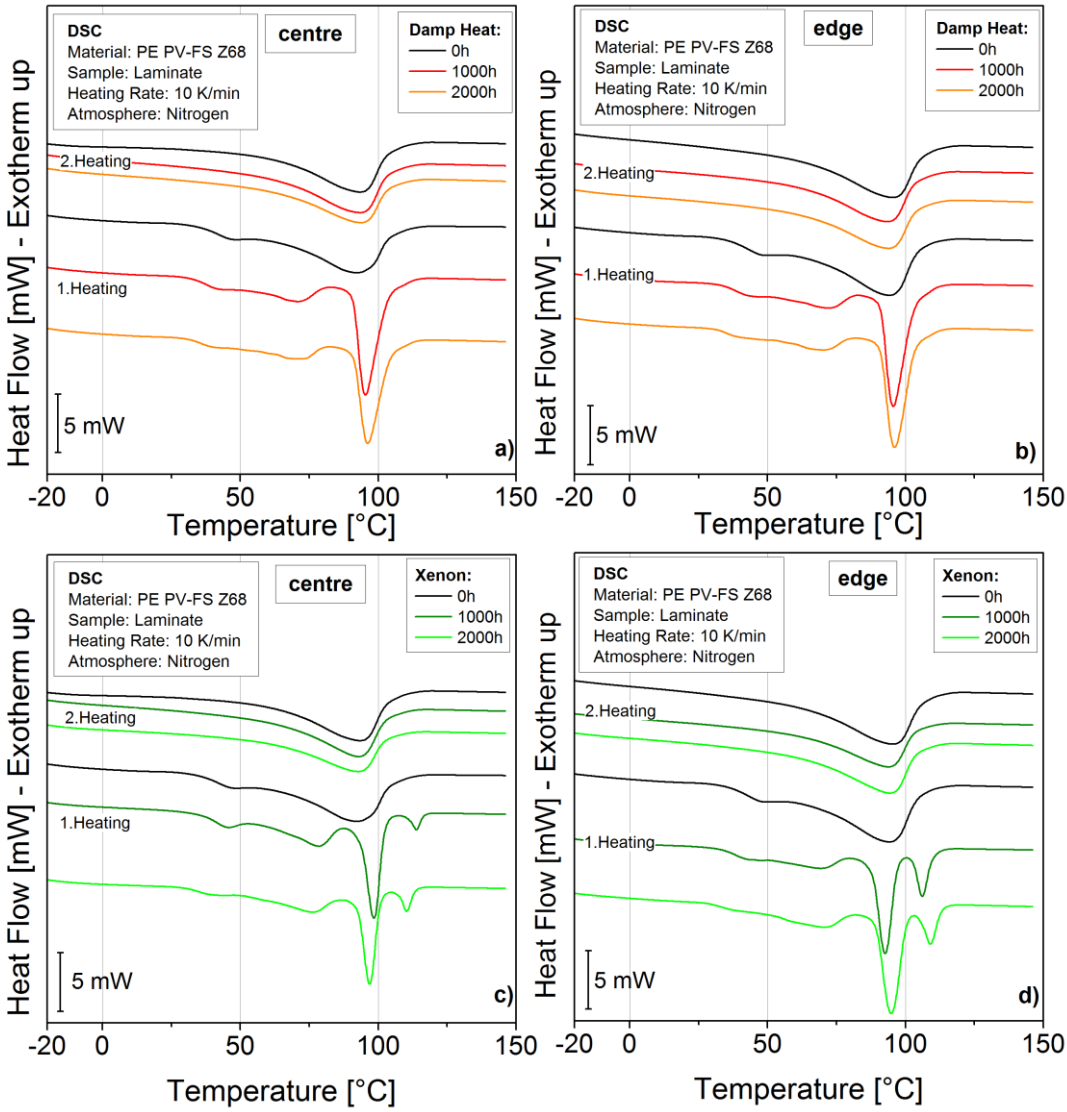

Figure 4.28: DSC curves of the first and second heating of PE PV-FS Z68® laminates exposed to DH an measured a) in the centre and b) on the edge and exposed to XE and measured c) in the centre and d) on the edge.

The unaged laminates showed similar melting peaks and enthalpies in the first and second heating as observed for the unaged films. The exposure to DH resulted in the appearance of melting peaks in the first heating as described for the film sample. The centre of the DH exposed laminate showed similar changes as found on the edge area. The second heating of the DH exposed laminate did not result in changes of the melting peak and therefore no structural changes could be observed as for the DH aged films.

The formed melting peaks measured in the first heating of the films and laminates could therefore be interpreted as post-crystallisation (physical ageing) and were not accompanied with structural changes (chemical ageing) of the material (Ehrenstein et al., 2003). The exposure of the laminate to XE for 2000 hours resulted in post-crystallisation with four melting peaks formed at 45±0, 78±1, 98±1 and 113±1 °C (Ehrenstein et al., 2003). Similar post-crystallisation with comparable peak temperatures could be found for measurements made in the centre and on the edge of the laminate. XE exposure resulted in no changes of the melting peaks in the second heating both in the centre and on the edge of the laminate (Figure 4.28 c and d). Structural changes of the PE samples were only observed for aged films while laminates aged under the same conditions did not show chemical ageing in the DSC measurements. The melting peak shift in the second heating of the films might therefore be caused due to the different microclimate at the polymer films. The exposure to XE for 1000 hours resulted in a similar shift as observed for DH aged films. Structural changes of the polymer due to the diffusion of water and oxygen and the interaction with the modifications under increased temperatures might have hindered crystallisation and resulted in a melting peak shift to lower temperatures.

5 SUMMARY AND OUTLOOK

Three commercially available EVA copolymers and a PE encapsulant were analysed. To investigate the ageing behaviour of the encapsulants under different microclimates two kinds of samples were prepared for every material. Films were laminated between a glass cover and backsheet layer to simulate a PV module and exposed to artificial ageing. Additionally plain films of the encapsulants were aged under the same conditions as the laminated samples. For artificial ageing the samples were exposed to damp heat ageing at 85 °C with 85 % relative humidity and xenon weathering with 90W/m², 60°C and wet/dry cycles for 2000 hours. The characterisation was carried out using IR spectroscopy, Raman spectroscopy, UV/Vis/NIR spectroscopy, HPLC-MS/UV and DSC. The chemical ageing processes observed in the investigation of this thesis are summarised in the overview given in Table 5.1. The table shows the EVA and PE films and laminates and the corresponding chemical changes observed with the applied analysis methods after DH and XE exposure for 2000 hours. The check symbol indicates a significant effect, an empty box says that no or no strong effect could be observed and an X means that no measurement has been carried out.

Table 5.1: Overview of the chemical ageing processes observed in the EVA and PE films and laminates and exposed to DH and XE for 2000 hours.

Chemical Ageing Process	Analysis Method	EVA				PE			
		XE		DH		XE		DH	
Oxidation	**IR**	✓				✓			
C=C double bonds	**IR, Raman**	✓				✓			
Flourescence increase	**Raman**		✓	✓	✓				
Reflectance decrease	**UV/Vis/NIR**		✓			✓	✓	✓	
Absorbance increase	**UV/Vis/NIR**		x		x	✓	x	✓	x
Increase of diffuse reflectance	**UV/Vis/NIR**	✓							
UV absorber decrease	**UV/Vis/NIR**	✓				✓			
B*-value increase	**UV/Vis/NIR**		✓		✓	✓	✓	✓	
Structural changes	**DSC**					✓			
Post-crosslinking	**DSC**	✓	✓	✓	✓				
Colour Code		Film				Laminate			

The exposure of the EVA films to XE for 2000 hours resulted in the formation of various photo-oxidation products that could be determined via IR spectroscopy. EVA films showed the formation of OH groups and hydroxyl formation of alcohols, peroxides or

hydroperoxides. Further oxidation products as lactone, ketone, ester and aldehyde groups could also be observed in the copolymer. Using variable angle ATR the depth profile of the hydroxyl formation could be determined between approximately 0.8 and 1.65 µm. The oxidation of the material increased with time of exposure to XE. A stronger increase due to photo-oxidation could be observed near the surface and with depth from the surface less UV light entered the material and thermo-oxidation seemed to dominate. The formation of C=C double bonds could be observed for EVA films exposed to XE for 2000 hours via Raman spectroscopy. The XE exposure of the films laminated between a glass cover and backsheet layer resulted in no photo-oxidation or double bond formation visible in IR or Raman spectroscopy. The glass cover and backsheet layer might have worked as a barrier against moisture and oxygen diffusion resulting in a lower oxygen concentration at the polymer film. Additionally the glass cover might have reduced the intensity of the UV radiation and therefore no photo-oxidation could be observed in the laminated samples. The DH exposure of the films and laminates resulted in no oxidation or C=C double bond formation observable with IR or Raman spectroscopy after 2000 hours of exposure. EVA samples resulted to be much more sensitive to oxidation under the influence of XE radiation.

In Raman spectroscopy an increase of the fluorescence background could be measured after ageing. XE exposed films showed no significant fluorescence increase while laminates showed a strong fluorescence background. The fluorescence could be observed to be stronger in the centre than at the edge area of the laminates. This tendency correlated with the oxygen concentration at the polymer and suggested that in oxygen rich areas the chromophores responsible for the fluorescence oxidised under the influence of UV radiation. A reduction of UV radiation due to the glass cover might have resulted in less photobleaching of the laminates compared to the film samples. Additionally the chromophores in the laminate could not evaporate or be washed out during the wet cycle of the XE exposure because of the glass cover working as a barrier against diffusion. While XE exposed films showed no significant fluorescence due to photobleaching a significant increase could be observed for the DH aged films. DH exposure also resulted in an increased fluorescence background of the EVA samples. DH exposed laminates also showed a fluorescence background and no differences between the centre and the edge of the laminate could be observed. XE exposure seemed to provoke a stronger increase in fluorescence than DH exposure but simultaneously reduce the fluorescence due to photobleaching that could not be observed after DH exposure.

In UV/Vis/NIR spectroscopy the XE exposure of EVA films resulted in a decreasing hemispherical reflectance in the UV area due a decrease in UV absorbers from the polymer. This could have occurred in the wet cycle of the XE exposure due to washing where the glass layer of the laminates worked as a barrier against water entering the laminate. The XE exposed films showed an increasing diffuse reflectance while hemispherical reflectance did not show significant changes during ageing. The photo-oxidation might have resulted in an increased scattering at the polymer surface. XE exposed laminates showed a significant decrease in reflectance above the cut off while the films showed no decrease. Ageing of the backsheet layer could have resulted in an increased absorbance and therefore contributed to the reduction in reflectance of the laminate. Laminates also showed a strong discolouration in the centre and no colour changes at the area of approximately 1 cm from the edge of the laminate. The colour measurement with UV/Vis/NIR spectroscopy showed a strong increase in the b*-value of the EVA laminates and no significant increase for the film samples. This could be caused due to the formation of small chromophores that could not diffuse through the glass and backsheet layer of the laminates as well as photobleaching in the presence of oxygen and UV radiation. Additionally it is likely that discolouration of the backsheet layer took place contributing to the b*-values as well as possible interactions between the encapsulant and backsheet layer resulting in additional formation of chromophores. The exposure to DH for 2000 hours resulted in a lower increase of the b*-values of the laminates than observed after XE exposure due to a lower tendency of the material to form chromophores without UV radiation. DH exposure caused no significant changes in the reflectance of the film and laminate samples because no photobleaching could occur.

Thermal analysis with DSC indicated post-crosslinking of all aged EVA samples. No differences between films and laminates and the exposure type could be observed. The post-crosslinking might therefore be caused due to the decomposition of the peroxides under increased temperatures during exposure time.

For the PE films exposed to XE for 2000 hours various photo-oxidation products could be determined with IR spectroscopy. The XE exposure of the PE films resulted in the formation OH, C-O, C-O-C groups and possibly salts. The presence of esters, aldehydes, ketones, lactones could also be observed. A significant formation of carboxylic acid groups was additionally observed in the PE films that could not be found in the EVA samples. An increase in photo-oxidation with exposure time could be determined. Variable angle ATR suggested a steady level of oxidation between 0.54 and 1.1 µm where EVA samples

showed a significant increase from the bulk to the material surface. The unaged PE showed a C=O and OH peak possibly due to material modifications. These polar functional groups could have favoured diffusion of the C=O groups formed due to photo-oxidation resulting in an even distribution of these groups at the polymer surface. Raman spectroscopy confirmed the presence of C=O groups in the PE films after XE exposure and in IR spectroscopy C=C double bond formation could be determined. The PE laminates exposed to XE for 2000 hours showed no indications for photo-oxidation or the formation of C=C double bonds in the polymer chain. Also DH exposure of the films and laminates did not result in oxidation of the polymer after 2000 hours of exposure. The PE samples also showed a stronger tendency to oxidise in the presence of oxygen and UV radiation as observed for the EVA samples.

For the PE film and laminate samples no significant fluorescence background could be observed in Raman spectroscopy after XE exposure. DH exposure resulted in an increased fluorescence background of the film samples. The PE might have a lower tendency to from chromophores responsible for fluorescence than EVA. A reduction in the UV intensity and oxygen concentration due to the glass cover therefore might have reduced fluorescence formation. No baseline increase could be observed for the XE exposed film samples possibly due to photobleaching of the formed chromophores in an oxygen rich environment under UV radiation.

In UV/Vis/NIR spectroscopy the exposure of the PE films and laminates to XE resulted in a decrease in the hemispherical reflectance in the visible region above the cut off. In the UV region an increase in transmittance could be observed after XE ageing due to the washing out of UV absorbers. DH exposure resulted in a decrease in hemispherical reflectance in the visible region for the film samples while laminates only showed a slight decrease at the cut off. The aged PE films therefore showed a stronger decrease in hemispherical reflectance than the aged laminates suggesting a significant influence of the microclimate at the polymer film. For the XE and DH exposed films a similar decrease in reflectance could be measured. The films showed no changes in transmittance and therefore an increasing absorbance with exposure time. The similar increase in absorption of the films might be due structural changes of the polymer chain caused by interactions of the modified polymer with water and oxygen under the influence of increased temperatures during exposure. Laminates showed a stronger decrease in reflectance when exposed to XE than to DH suggesting a contribution of the backsheet layer to these changes as described for the EVA laminates. The b*-values of the films increased after DH and XE

exposure when measured in reflectance mode changes could be observed of the b*-values measured in transmittance mode. The laminates also showed an increase after the DH and XE exposure with values comparable to the transmittance based b*-values of the films.

The thermal analysis with DSC resulted in shifts of the melting peaks in the second heating to lower temperatures. These changes could be observed for DH and XE aged films and suggested that structural changes of the polymer chain occurred that hindered the crystallisation. Laminates exposed to DH and XE did not show melting peak shifts in the second heating suggesting that an interaction of the films with moisture and oxygen at the film samples might have occurred and caused the structural changes of the polymer chain. PE films exposed to XE for 2000 hours showed a further shift of the melting peak to higher temperatures. This is most likely due to chain scission of the polymer chain.

The artificial ageing of the EVA and PE encapsulants resulted in very different results when exposed as a plain film or as a film incorporated in a laminate. The glass cover and the backsheet layer of the laminates resulted in a different concentration of oxygen and humidity as well as a reduced UV radiation on the encapsulant layer. Both polymers responded more sensitive to XE exposure than to DH exposure. Films exposed to XE therefore showed the formation of various photo-oxidation products, C=C double bonds and chain scission. Under the same exposure conditions the laminates showed no indications for these ageing processes. The occurrence of fluorescence during ageing could also be found to be influenced by the microclimate at the polymer film. Higher fluorescence occurred in the laminates where no diffusion of the chromophores could occur due to the glass cover working as a barrier. A stronger UV radiation resulted in a higher fluorescence formation and under the presence of a high oxygen concentration a reduction in the chromophores due to oxidation could be observed. XE exposed laminates showed a higher fluorescence background in the centre than at the edge area with a higher concentration of oxygen. The rain cycle during the XE exposure might have caused the washing out of UV absorbers from the film samples while UV absorbers in the laminates were protected by the glass cover. The PE laminate exposed to XE resulted in a much lower increase in the b*-values when compared to the EVA laminates. EVA has a stronger tendency for discolouration and the increase in b*-values of the EVA laminates might be due to a higher tendency to form chromophores in the material. The contribution of the backsheet layer to the b*-values of the laminate might also be

significantly influenced by interactions with the encapsulant. Aged EVA and PE encapsulants showed different changes in the reflectance properties when exposed as a film or incorporated in a laminate. This could be due to a stronger interaction of the modified PE with humidity and oxygen under increased temperatures.

The comprehensive analysis with IR spectroscopy, Raman spectroscopy, UV/Vis/NIR spectroscopy, HPLC-MS/UV and DSC showed that the artificial ageing of the encapsulants showed very different results if the samples were exposed as plain films or incorporated in a laminate. The chemical ageing processes are greatly influenced by the microclimate at the polymer surface and the influence of the other laminate layers. Further investigation would be recommended to analyse the exact influence of the backsheet layer on the ageing behaviour of the encapsulant and determine possible interactions of the two layers.

6 REFERENCES

[1]*Agilent Technologies* (2003). Homepage of Agilent Technologies http://www.chem.agilent.com/Library/applications/5988-8610EN.pdf, 16.03.2015.

[2]*Agroui, K., Collins, G. and Farenc, J.* (2012). Renewable Energy 43, 218.

[3]*Allen, N., Edge, M., Rodriguez, M., Liauw, C.M., Fontan, E.* (2000). Polymer Degradation and Stability 68, 363.

[4]*Askerland, D. and Phulé, P.* (2006). "The Science and Engineering of Materials", Thompson Learning, London.

[5]*Atlas Material Testing Solutions* (2001). "Atlas Weathering Testing Guidebook", Atlas Electric Devices Company, USA.

[6]*Avadanei, M.* (2012). Journal of Macromolecular Science, Part B: Physics Vol 51 Issue 3, 425.

[7]*Bastian, M.* (2010). "Einfärben von Kunststoffen", Hanser, Munich.

[8]*Bregulla, M., Köhl, M., Lampe, B., Oreski, G., Philipp, D., Wallner, G., Weiß, K.-A.* (2007). In Proc. "22nd European PV Solar Energy Conference", pp. 2704-2707, 3-7 Sept, Milano, Italy.

[9]*Carlsson, T., Halme, J., Lund, P., Konttinen, P.* (2006). Sensors and Actuators A 125, 281.

[10]*Carrasco, F., Pagès, P., Pascual, S., Colom, X.* (2001). European Polymer Journal 37, 1457.

[11]*Çopuroğlu, M. and Şen, M.* (2004). Polymers for Advanced Technologies 15, 393.

[12]*Czanderna, A. and Pern, F.* (1996). Solar Energy Materials and Solar Cells 43, 101.

[13]*DIN* (2012). Homepage of DIN http://www.npf.din.de/cmd?level=tpl-artikel&menuid=46862&cmsareaid=46862&cmsrubid=93979&menurubricid=93979&cmstextid=169382&2&languageid=de, 28.05.2014.

[14]*Dnpsolar* (2010). Homepage of Dnpsolar (Denmark) http://www.dnpsolar.eu/dnpsolar-encapsulant-sheets/, 20.10.2014.

[15]*Ehrenstein, G. and Pongratz, S.* (2007). "Beständigkeit von Kunststoffen", Hanser, Munich.

[16]*Ehrenstein, G., Riedel, G., Trawiel, P.* (2003). "Praxis der thermischen Analyse von Kunststoffen", Hanser, Munich.

[17]*Ezrin, M., Lavigne, G., Klemchuk, P., Holley, W., Agro, S., Galica, J., Thomas, L., Yorgensen, R.* (1995). In Proc. "ANTEC", (Society of Plastics Engineers), Boston, USA, pp. 3957.

[18]*Ferraro, J. and Nakamoto, K.* (2003). "Introductory Raman Spectroscopy". Elservier Science, USA.

[19]Frick, A. and Stern, C. (2006). "DSC Prüfung in der Anwendung", Hanser, Munich.

[20]*Gambogi, W.* (2010). In Proc. "25th European PV Solar Energy Conference and Exhibition / 5th World Conference on PV Energy Conversion", pp. 4079, 6-10 Sept, Valencia, Spain.

[21]*Gardette, M., Perthue, A., Gardette, J.-L., Janecska, T., Földes, E., Pukánszky, B., Therias, S.* (2013). Polymer Degradation and Stability 98 , 2383.

[22]*Gottwald, W. and Heinrich, K.* (1998). "UV/VIS-Spektroskopie für Anwender", Wiley-VCH, Weinheim, New York, Chichester, Brisbane, Singapore, Toronto.

[23]*Grellmann, W. and Seidler, S.* (2011). "Kunststoffprüfung", Hanser, Munich.

[24]*Gross, J.* (2013). "Massenspektrometrie - Ein Lehrbuch". Springer, Berlin, Heidelberg.

[25]*Gulmine, J. and Acelrud, L.* (2006). Polymer Testing 25, 932.

[26]*Gulmine, J., Janissek, P., Heise, H. and Akcelrud, L.* (2002). Polymer Testing 21, 557.

[27]*Gulmine, J., Janissek, P., Heise, H. and Akcelrud, L.* (2003). Polymer Degradation and Stability 79, 385.

[28]*Günzler, H. and Gremlich, H.* (2003). "IR-Spektroskopie". Wiley-VCH, Weinheim, New York, Chichester, Brisbane, Singapore, Toronto.

[29]*Haillant, O. and Lamaire, J.* (2006). Polymer Degradation and Stability 91, 2748.

[30]*Hanai, T. and Smith, R.* (1999). "HPLC - A Practical Guide"., The Royal Society of Chemistry, Cambridge.

[31]*Harvey, D.* (2008). "Analytical Chemistry 2.0", David Harvey.

[32]*Hasan, O. and Arif, A.* (2014). Solar Energy Materials and Solar Cells 122, 75.

[33]*Hintersteiner, I., Sternbauer, L., Beissmann, S., Buchberger, W.W., Wallner, G.M.* (2014). Polymer Testing 33, 172.

[34]*Hsu, H., Hsieh, H., Tuan, H. and J.L., H.* (2010). Solar Energy Materials and Solar Cells 94, 955.

[35]*Hülsmann, P. and Weiss, K.-A.* (2015). Solar Energy 115, 347.

[36]*Hummel, D.* (2002). "Atlas of Plastic Additives", Springer, Heidelberg.

[37]*International Energy Agency* (2014). http://www.iea.org/publications/

freepublications/publication/KeyWorld2014.pdf, 23.03.2015.

[38]*Jin, J., Chen, S., Zhang, J.* (2010). Polymer Degradation and Stability 95, 725.

[39] *Jorgensen, G.J., Terwilliger, K.M., DelCueto, J.A., Glick, S.H., Kempe, M.D., Pankow, J.W., Pern, F.J., McMahon, T.J.* (2006). Solar Energy Materials and Solar Cells 90, Issue 16, 2739.

[40]*Kempe, M., Jorgensen, G.J., Terwilliger, K.M., McMahon, T.J., Kennedy, C.E., Borek, T.T.* (2007). Solar Energy Materials and Solar Cells 91, 315.

[41]*Klemchuk, P., Ezrin, M., Lavigne, G., Holley, W., Galica, J., Agro, S.* (1996). Polymer Degradation and Stability 55, 347.

[42]*Klima- und Energiefonds* (2014). https://www.klimafonds.gv.at/assets/Uploads/PV-Fibel/photovoltaik-fibel2014.pdf, 24.03.2015.

[43] *Knausz, M., Oreski, G., Schmidt, M., Guttmann, P., Berger, K., Voronko, Y., Eder, G., Koch, T., Pinter, G.* (2015). Polymer Testing 44, 160.

[44]*Krimm, S., Liang, C. and Sutherland, G.* (1956). The Journal of Chemical Physics 25, 549.

[45]*Küpper, L., Gulmine, J., Janissek, P. and Heise, H.* (2004). Vibrational Spectroscopy 34, 63.

[46]*Lin-Vien, D., Colthub, N., Fateley, W. and Grasselli, J.* (1991). "The Handbook of IR and Raman Characteristic Frequencies of Organic Molecules", Academic Press, San Diego, New York, Boston, London, Tokyo, Toronto.

[47]*Liu, F., Jiang, L., Yang, S.* (2014). Solar Energy 108, 88.

[48]*Lobo, H. and Bonilla, J.* (2003). "Handbook of Plastics Analysis", Marcel Dekker, New York.

[49]*Lu, S., Russel, E., Hendra, P.* (1998). Journal of Material Science 33, 4721.

[50]*Morlier, A., Klotz, S., Sczuka, S., Kunze, I., Schaumann, I., Blankemeyer, S., Siegert, M., Döring, T., Alshuth, T., Giese, U., Denz, M., Köntges, M.* (2013). In Proc. "28th European PV Solar Energy Conference and Exhibition", pp. 2832 - 2837, 30 Sept - 4 Oct, Paris, France.

[51]*Nishikida, K., Nishio, E., Hannah, R.* (1995). "Selected Applications of Modern FT-IR Techniques". Kodansha and Gordon and Breach Science Publishers, Japan, Luxembourg.

[52]*Novopolymers NV* (2012). Hompage of Novopolymers NV (Belgium) http://www.novopolymers.com/en/node/2, 20.10.2014.

[53]*Oreski, G. and Wallner, G.* (2005). Solar Energy Materials and Solar Cells 89, 139.

[54]*Oreski, G. and Wallner, G.* (2009). Solar Energy 83, 1040.

[55]*Oreski, G., Wallner, G., Lang, R.* (2009). Biosystems Engineering 103 , 489.

[56]*Pasch, H. and Trathnigg, B.* (1999). "HPLC of Polymers", Springer, Berlin, Heidelberg.

[57]*Peacock, A.* (2000). "Handbook of Polyethylene - Structures, Properties and Applications". Marcel Dekker, USA.

[58]*Peike, C., Apin, K., Hummel, M., Weiß, K.-A., Köhl, M.* (2013a). In Proc. "6th European Weathering Symposium", pp. 381-392, 11-13 Sept, Bratislava, Slovak Republic.

[59]*Peike, C., Hoffmann, S., Hülsmann, P., Thaidigsmann, B., Weiß, K.A., Koehl, M., Bentz, P.* (2013b). Solar Energy Materials and Solar Cells 116, 49.

[60]*Peike, C., Hülsmann, P., Blüml, M., Schmid, P., Weiß, K.-A., Köhl, M.* (2012). ISRN Renewable Energy Vol 2012, pp. 459731 1-5.

[61]*Peike, C., Kaltenbach, T., Weiß, K.-A. and Koehl, M.* (2011). Solar Energy Materials and Solar Cells 95, 1686.

[62]*Peike, C., Purschke, L., Weiss, K.-A., Köhl, M., Kempe, M.* (2013c). In Proc. "39th PV Specialist Conference", pp.1579-1584, IEEE, 16-21 June, Tampa, USA.

[63]*Perkin Elmer* (2004). http://www.perkinelmer.com/Catalog/Product/ID/L950, 27.05.2014.

[64]*Pern, F.* (1993). In Proc. "23rd PV Specialists Conference", pp. 1113-1118, IEEE, 10-14 May, Louisville, USA.

[65]*Pern, F.* (1996). Solar Energy Materials and Solar Cells 41/42, 587.

[66]*Pern, F. and Czanderna, A.* (1992a). Solar Energy Materials and Solar Cells 25, 3.

[67]*Pern, F. and Czanderna, A.* (1992b). In Proc. "NREL 11th PV AR and D Review Meeting", pp. 445-452, American Institute of Physics, 13-15 May, Proc. No. 268, Denver, USA.

[68]*Plessing, A.* (2003). Einkapselung von Solarzellen, In Proc. "Polymeric Solar Materials", (Wallner, G.M. and Lang, R.W., Hrsg.) pp. XII1-XII8, Polymer Competence Center Leoben, Austria.

[69]*Pocius, A. and Dillard, D.* (2002). "Adhesion Science and Engineering I - The Mechanics of Adhesion", Elsevier, Amsterdam, Netherlands.

[70]*Quaschning, V.* (2010). "Erneuerbare Energien und Klimaschutz", Hanser, Munich.

[71]*Razykov, T., Ferekides, C.S., Morel, D., Stefanakos, E., Ullal, H.S., Upadhyaya, H.M.* (2011). Solar Energy 85, 1580.

[72]*Rodríguez-Vásquez, M., Liauw, C.M., Allen, N.S., Edge, M., Fontan, E.* (2006). Polymer Degradation and Stability 91, 154.

[73]*Salvalaggio, M., Bagatin, R., Fornaroli, M., Fanutti, S., Palmery, S., Battistel, E.* (2006). Polymer Degradation and Stability 91, 2775.

[74]*Sato, H., Shimoyama, M., Kamiya, T., Amari, T., Sasic, S., Ninomiya, T., Siesler, H.W., Ozaki, Y.* (2002). Journal of Applied Polymer Science 86, 443.

[75]*Schrader, B.* (1995). "IR and Raman Spectroscopy", Wiley-VCH, Weinheim, Germany.

[76]*Shimoyama, M., Maeda, H., Matsukawa, K., Inoue, H., Ninomya, T., Ozaki, Y.* (1997). Vibrational Spectroscopy 14, 253.

[77]*Sokrates, G.* (2001). "IR and Raman Characteristic Group Frequencies", John Wiley and Sons LTD, Chichester, GB.

[78]*Solutia Inc.* (now a subsidiary of Eastman Chemical Company, USA) (2012a). Homepage of Vistasolar http://vistasolar.com/productintro.html#VISTASOLAR%20486, 20.10.2014.

[79]*Solutia Inc.* (now a subsidiary of Eastman Chemical Company, USA) 2012b. Homepage of Vistasolar http://vistasolar.com/productintro.html#VISTASOLAR%20520.78, 20.10.2014.

[80]*Tams, C. and Enjalbert, N.* (2009). Homepage of Perkin Elmer http://www.perkinelmer.com/CMSResources/Images/4474323APP_UseofUVVisNIRinDevelopmentPV.pdf, 28.05.2014.

[81]*Telko* (2010a). Homepage of Telko http://www.telko.com/files/images/telko/ru/basf/svetostabilizator/chimassorb_81_tds.pdf, 16.03.2015.

[82]*Telko* (2010b). Homepage of Telko http://www.telko.com/files/images/telko/ru/basf/svetostabilizator/tinuvin_770_tds.pdf, 16.03.2015.

[83]*Thermo Fisher Scientific* (2007). "Surveyor MSQ Plus - Getting Started Guide", Thermo Fisher Scientific.

[84]*Urban, M.* (1996). "Attenuated Total Reflactance Spectroscopy of Polymers: Theory and Practice", American Chemical Society, Washington, USA.

[85]*Vallés-Lluch, A., Contat-Rodrigo, L., Ribes-Greus, A.* (2003). Journal of Applied Polymer Science 89, 3260.

[86]*Wang, E., Yang, H.E., Yen, J., Chi, S., Wang, C.* (2013). Energy Procedia 33, 256.

7 LIST OF FIGURES

8 LIST OF TABLES

9 APPENDIX

Table 9.1: Parameters of the IR spectroscopy measurements.

IR Spectroscopy Parameters	
Testing Device	FTIR Spektrum GX
Variable Angle Accessory	Pike Veemax II
Testing Mode	ATR
ATR Contact Crystal	ZnSe
Measuring Range	4000 - 650 cm^{-1}
Scans for one Spectrum	16
Sample size	3 x 3 cm
Angles of Incidence	35°, 45°, 50°, 60°, 70°
Software	Spectrum 10 AutoPro 5

Table 9.2: Parameters of the Raman spectroscopy measurements.

Raman Spectroscopy Parameters	
Testing Device	LabRam HR800
Laser	514 nm (green)
Hole Size	500 µm (300 µm)
Slit Size	100 µm
Grating	600 g/mm
Irradiation Time	5 s
Measuring Range	650 – 4000 cm^{-1}
Scans for one Spectrum	15
Sample size	1 x 1 cm
Software	LabSpec 5

Table 9.3: Parameters of the UV/Vis/NIR spectroscopy experiments.

UV/Vis/NIR Spectroscopy Parameters	
Testing Device	PerkinElmer Lamda 950
Integrating Sphere	150mm diameter Spectrolon coating
Measuring Range	250 – 2500 nm
Number of Measurements	3
Weighting of Spectra	AM 1.5
Testing Mode	Reflectance Transmittance (Films)
Measured Light	Hemispherical and Diffuse
Sample Size	3 x 3 cm
Colour System	CIELab
Software	Spectrum 10 Wincolor 3.1.6

Table 9.4: Parameters of the HPLC and MS spectrometry experiments.

HPLC-MS/UV Parameters	
Testing Device	Surveyor MSQ Plus
Separation Column	Reverse Phase C18
Measuring Range	150 – 600 m/z 150 – 2000 m/z
Measuring Mode	Positive and Negative
Flow Rate	300 µl/min
Solvent	Acetonitrile
Sample Injection	10 µl

Table 9.5: Parameters oft he DSC experiments.

DSC Parameters	
Testing Device	PerkinElmer DSC 4000
Heating and Cooling Rate	10°C/min
EVA Testing Method:	
1. Heating	-40°C –> 230°C
2. Cooling	230°C –> -40°C
3. Heating	-40°C –> 300°C
PE Testing Method:	
1. Heating	-40°C –> 150°C
2. Cooling	150°C –> -40°C
3. Heating	-40°C –> 150°C
Enthalpy Evaluation	ISO 11357
Sample	10 – 15 mg
Atmosphere	Nitrogen
Software	Pyris 11

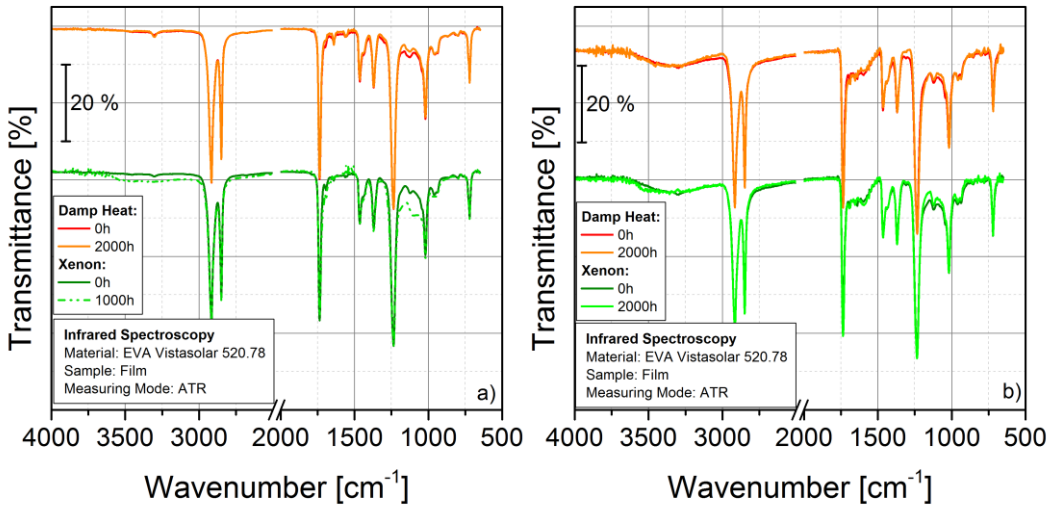

Figure 9.1: IR spectra of EVA Vistasolar 520.78® a) films and b) laminates, unaged and exposed to DH and XE.

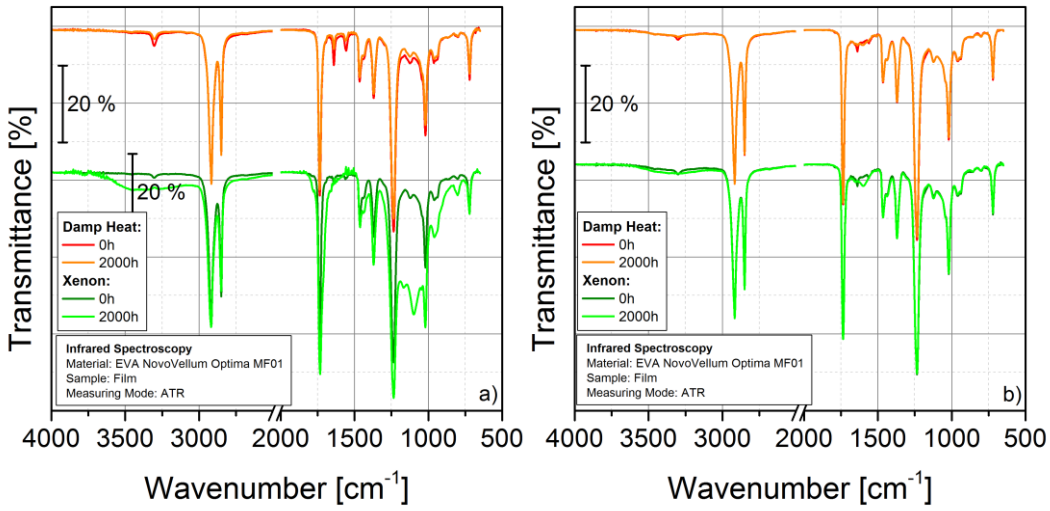

Figure 9.2: IR spectra of EVA NovoVellum Optima MF01® a) films and b) laminates, unaged and exposed to DH and XE.

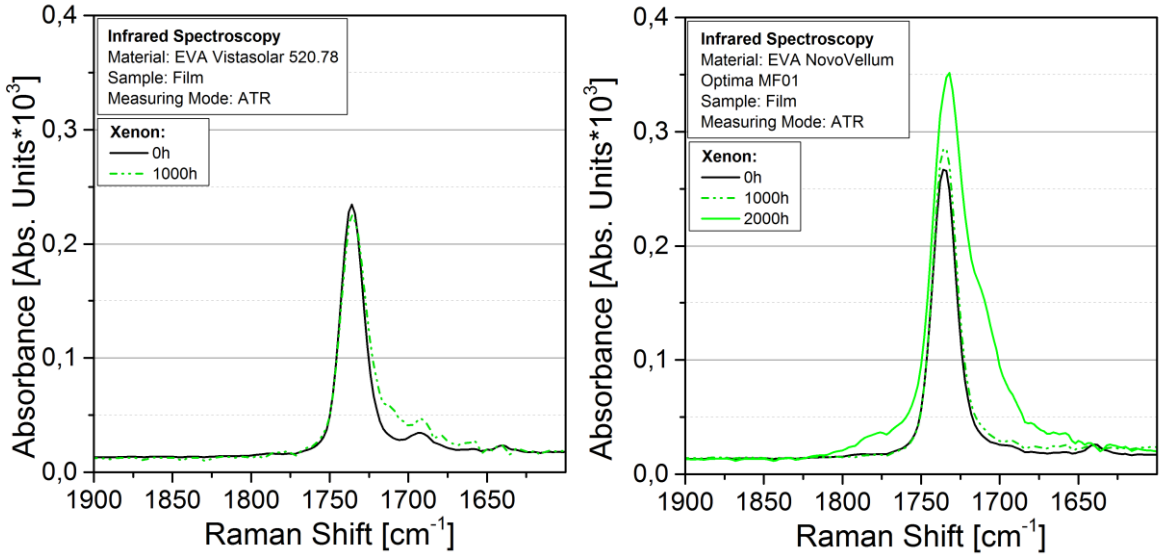

Figure 9.3: Detailed plot of the 1734 cm^{-1} peak of unaged and XE exposed a) EVA Vistasolar 520.78® and b) EVA NovoVellum Optima MF01® films.

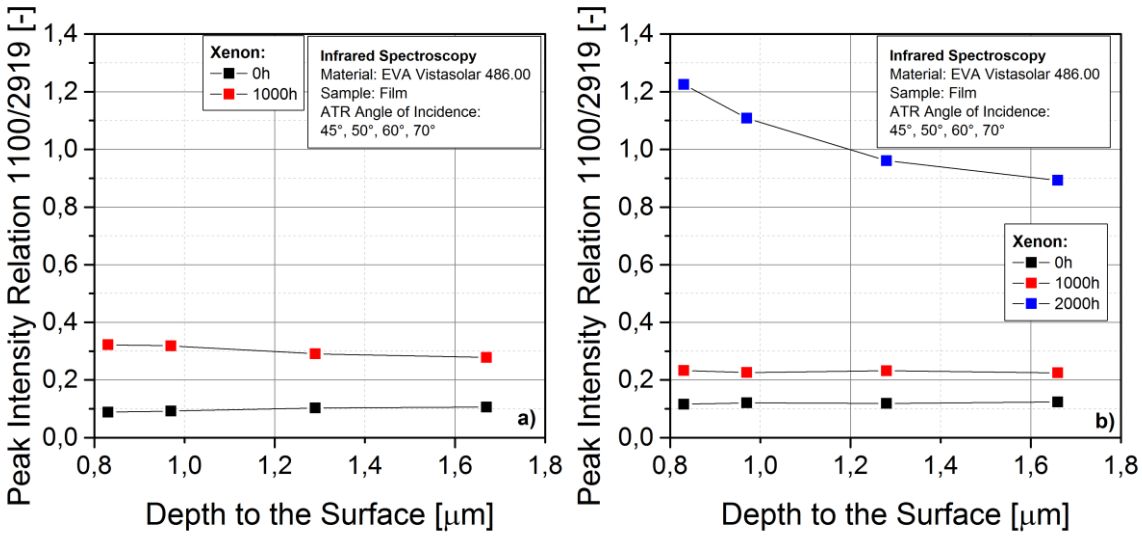

Figure 9.4: Formation of hyxdroxyl groups of a) EVA Vistasolar 520.78® and b) EVA NovoVellum Optima MF01® films exposed to XE in dependence on the depth to the material surface.

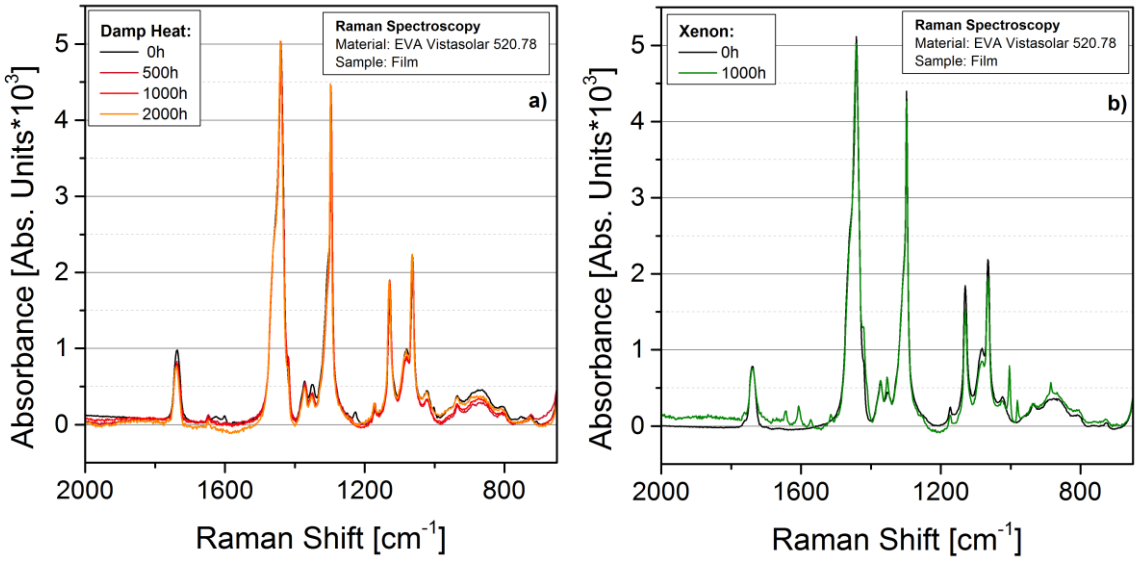

Figure 9.5: Detailed plot of baseline corrected Raman spectra of EVA Vistasolar 520.78® films exposed to a) DH and b) XE.

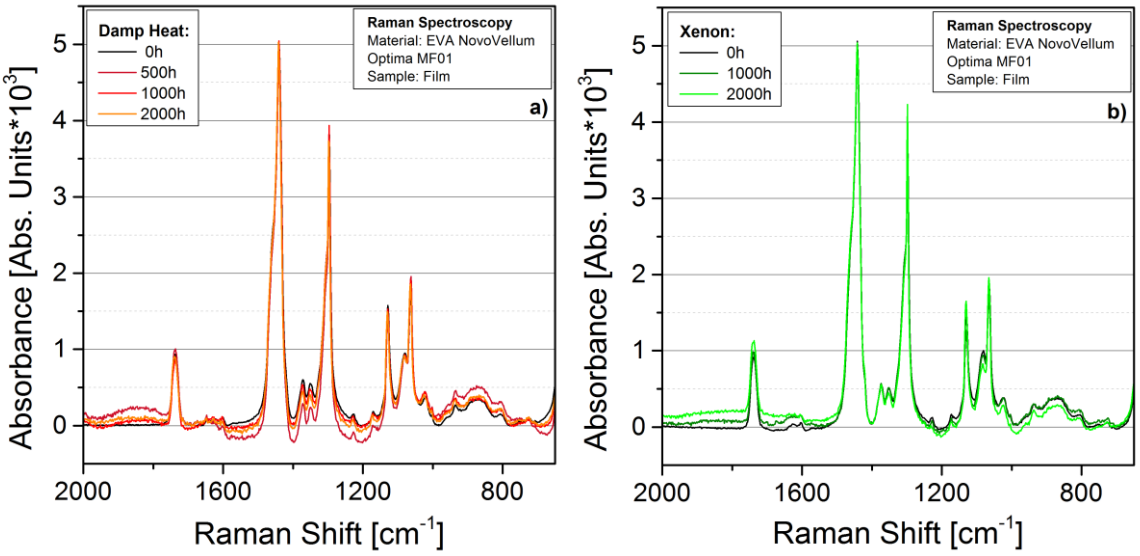

Figure 9.6: Detailed plot of baseline corrected Raman spectra of EVA NovoVellum Optima MF01® films exposed to a) DH and b) XE.

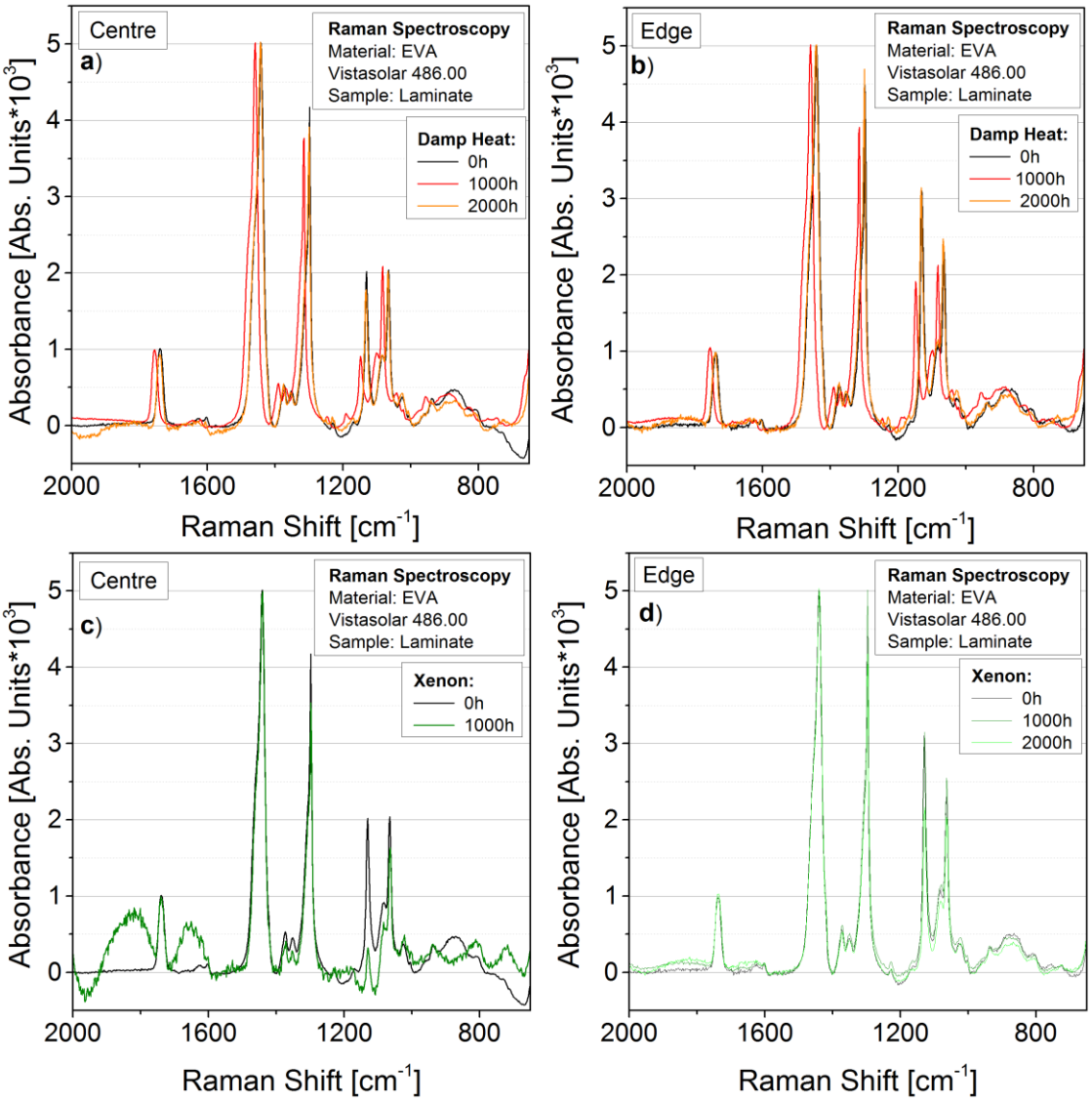

Figure 9.7: Detailed plot of baseline corrected Raman spectra of EVA Vistasolar 486.00® laminates exposured to DH and measured in the a) centre, b) edge and XE exposed and measured in the c) centre, d) edge.

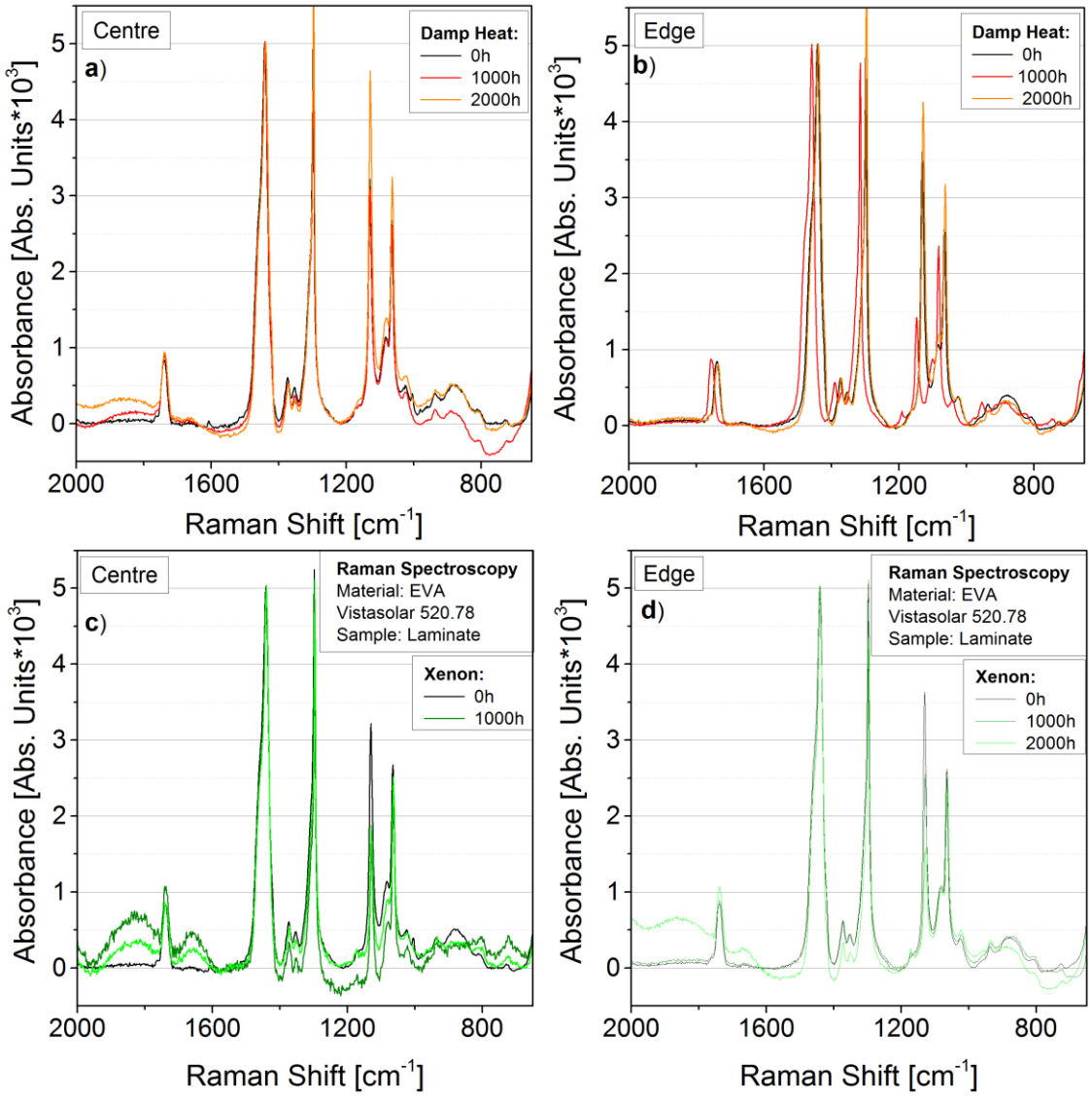

Figure 9.8: Detailed plot of baseline corrected Raman spectra of EVA Vistasolar 520.78® laminates exposured to DH and measured in the a) centre, b) edge and XE exposed and measured in the c) centre, d) edge.

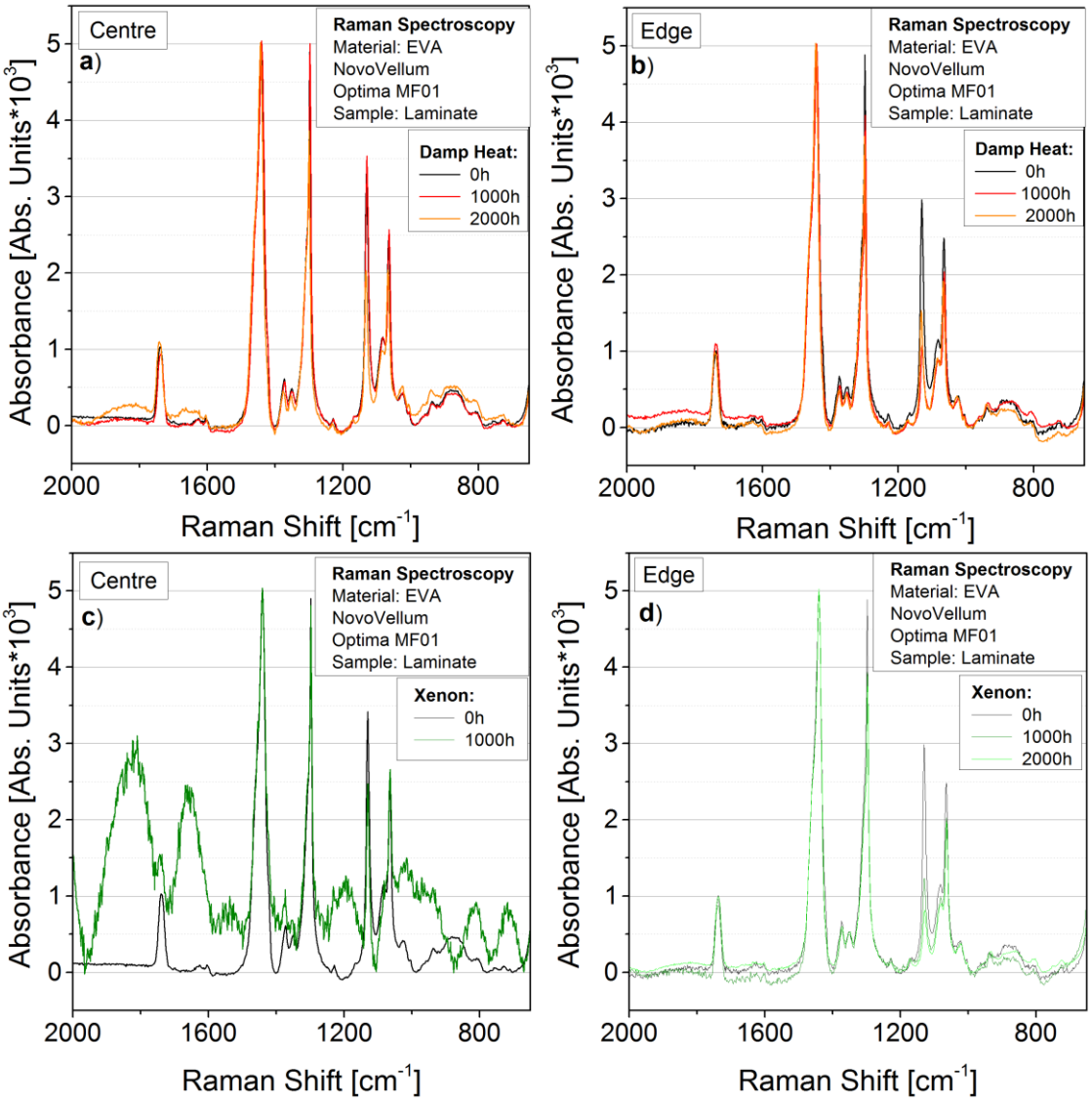

Figure 9.9: Detailed plot of Raman spectra of EVA NovoVellum Optima MF01® laminates exposured to D Hand measured in the a) centre, b) edge and XE exposed and measured in the c) centre, d) edge.

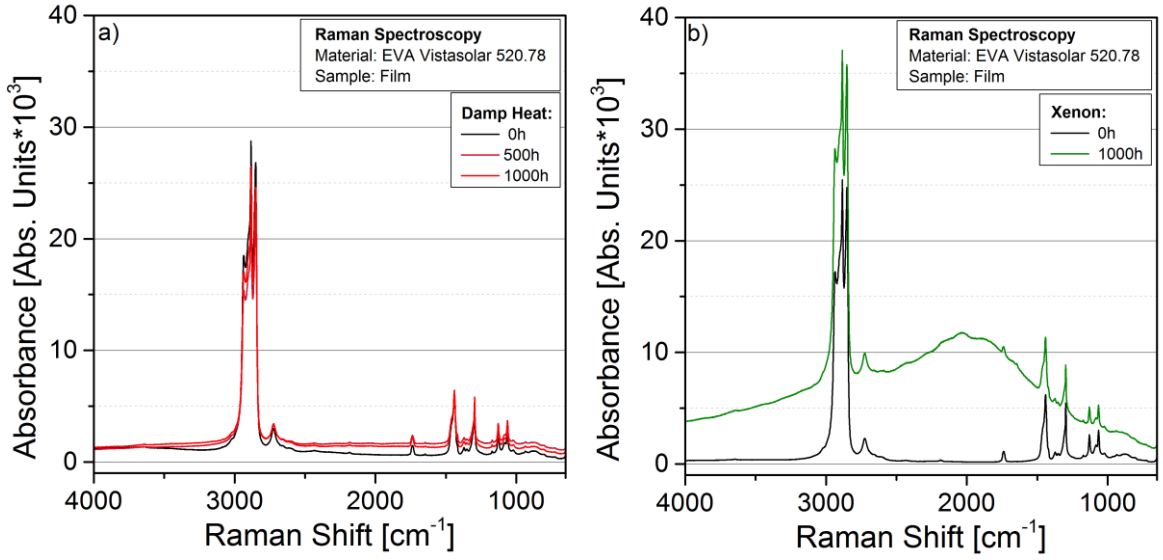

Figure 9.10: Raman spectra of EVA Vistasolar 520.78® films exposed to a) DH and b) XE for 2000 hours.

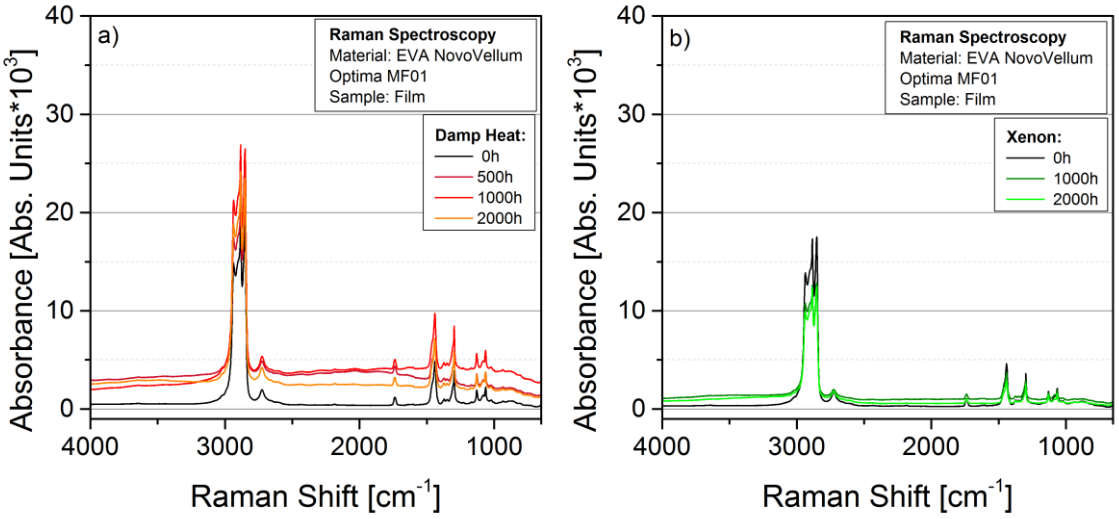

Figure 9.11: Raman spectra of EVA NovoVellum Optima MF01® films exposed to a) DH and b) XE for 2000 hours.

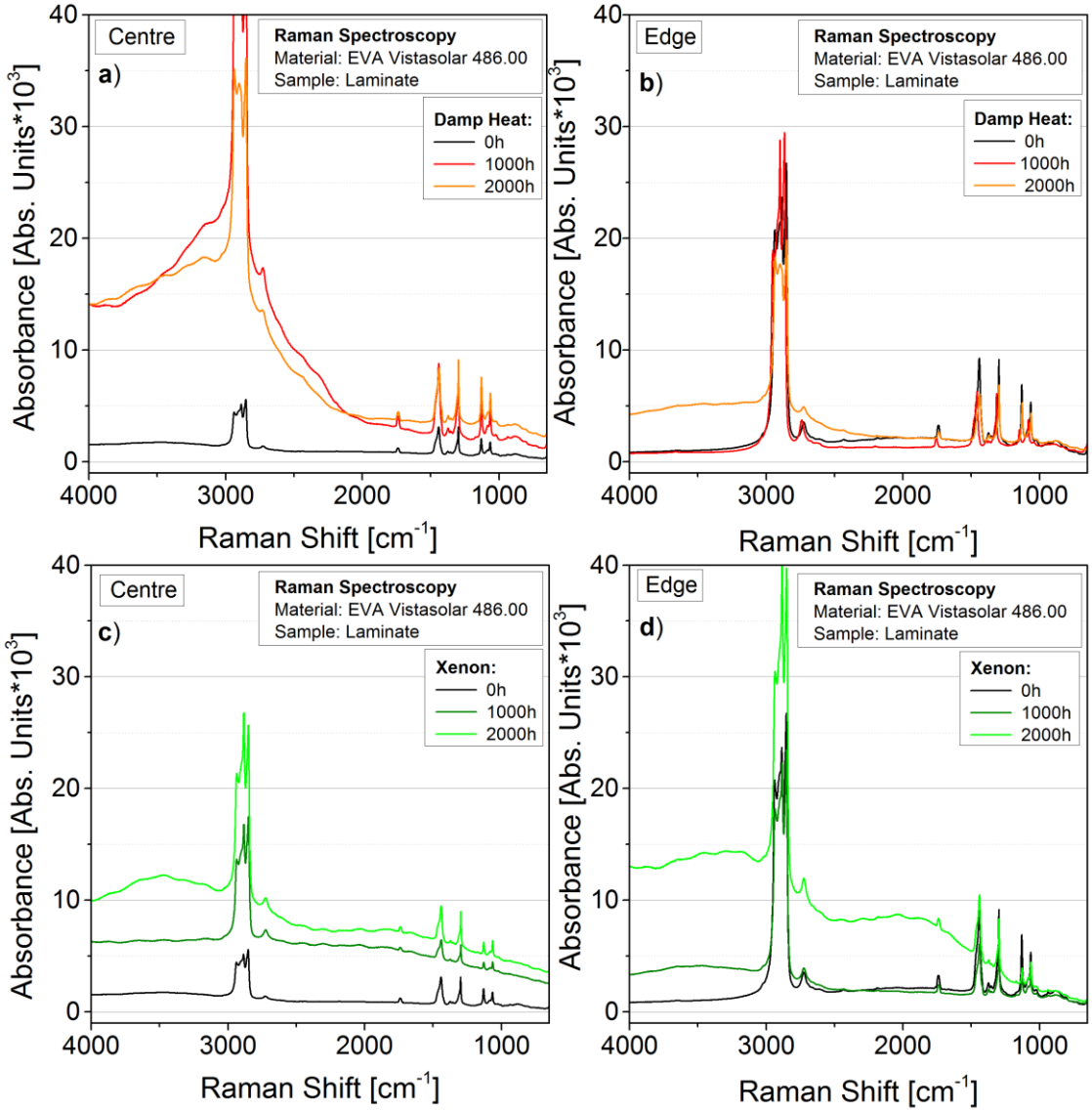

Figure 9.12: Raman spectra of EVA Vistasolar 520.78® laminates exposed to DH and measured in the a) laminate centre, b) laminate edge and XE exposed and measured in the c) laminate centre, d) laminate edge.

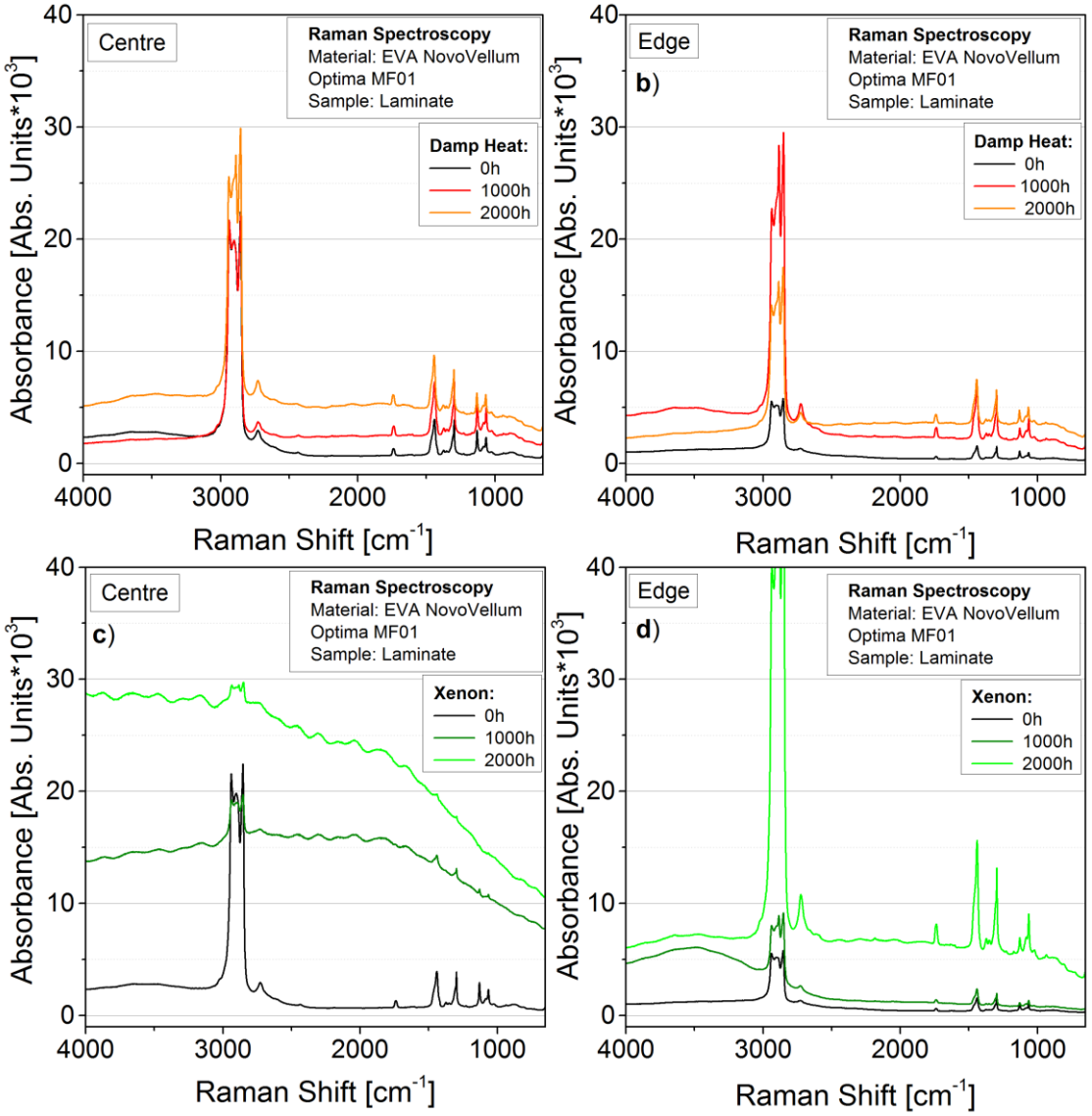

Figure 9.13: Raman spectra of EVA NovoVellum Optima MF01® laminates exposed to DH and measured in the a) laminate centre, b) laminate edge and XE exposed and measured in the c) laminate centre, d) laminate edge.

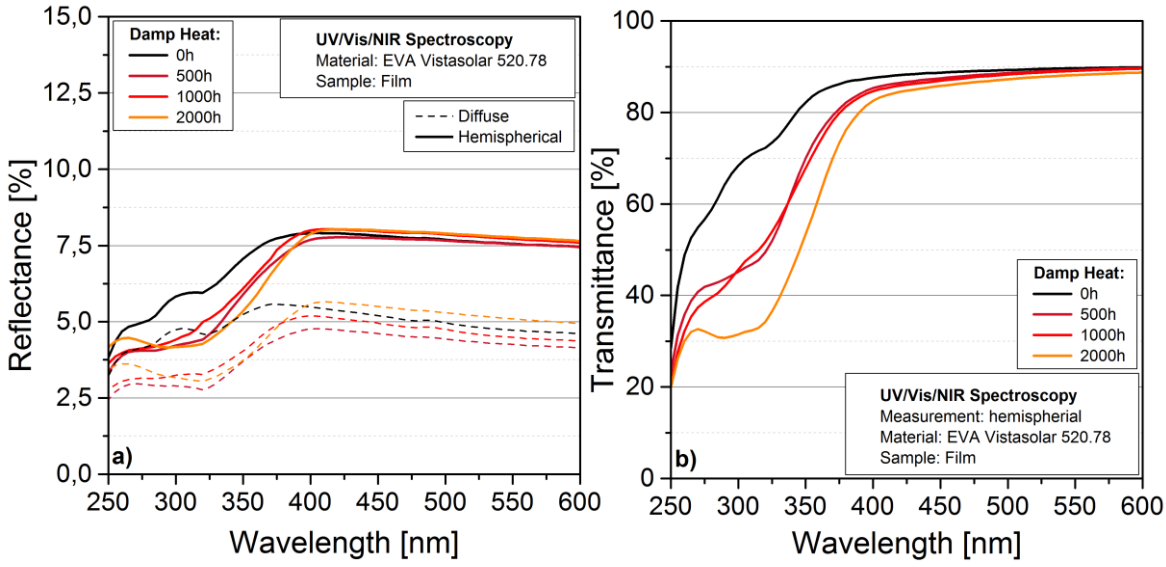

Figure 9.14: a) Reflectance and b) transmittance spectra of EVA Vistasolar 520.78® films exposed to DH.

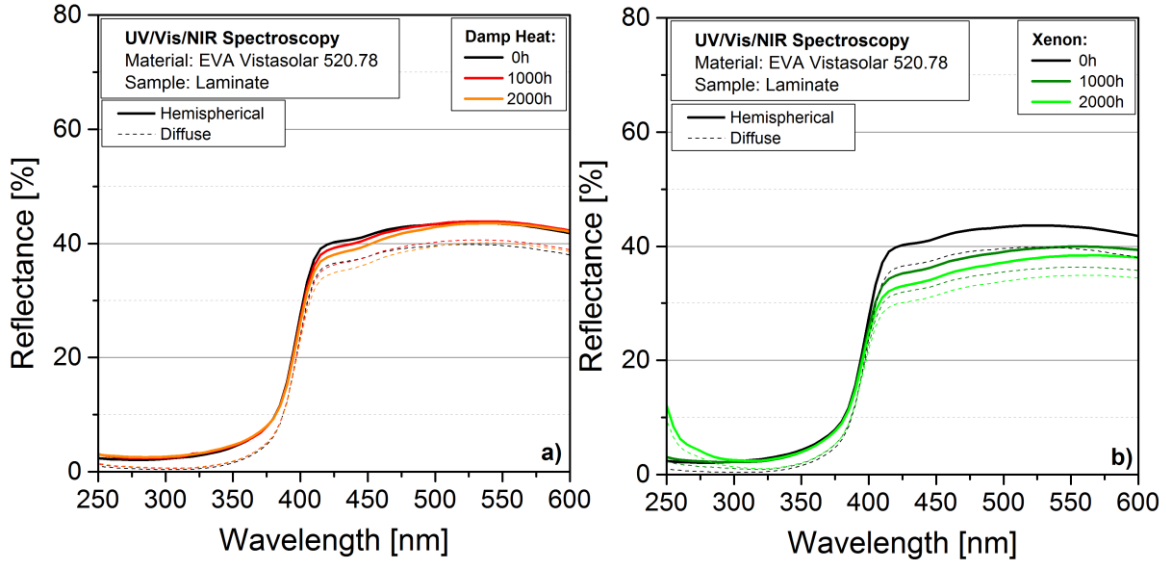

Figure 9.15 Reflectance spectra of EVA Vistasolar 520.78® laminates exposed to a) DH and b) XE.

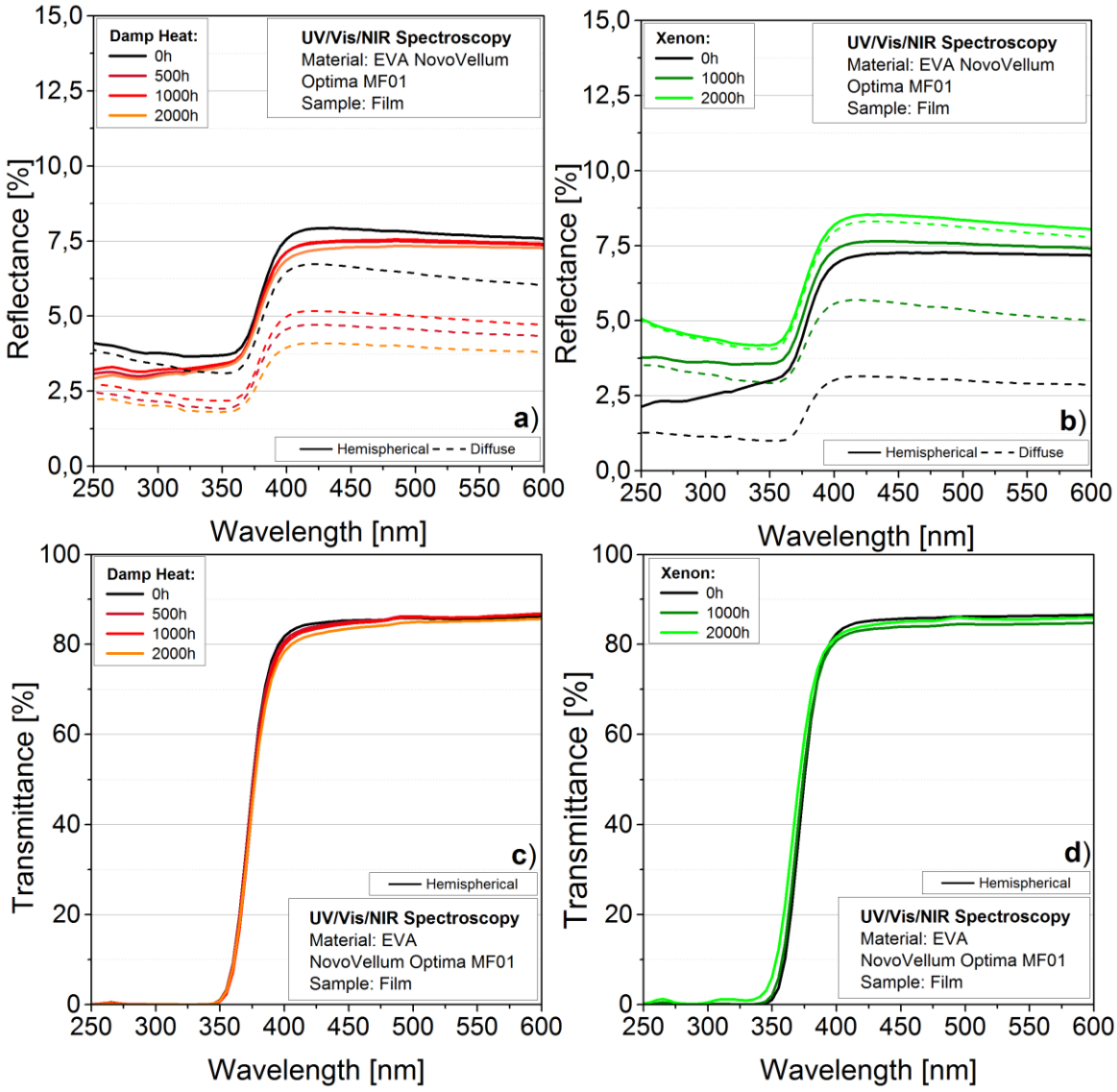

Figure 9.16: Reflectance spectra of EVA NovoVellum Optima MF01® films exposed to a) DH and b) XE and transmittance spectra exposed to c) DH and d) XE.

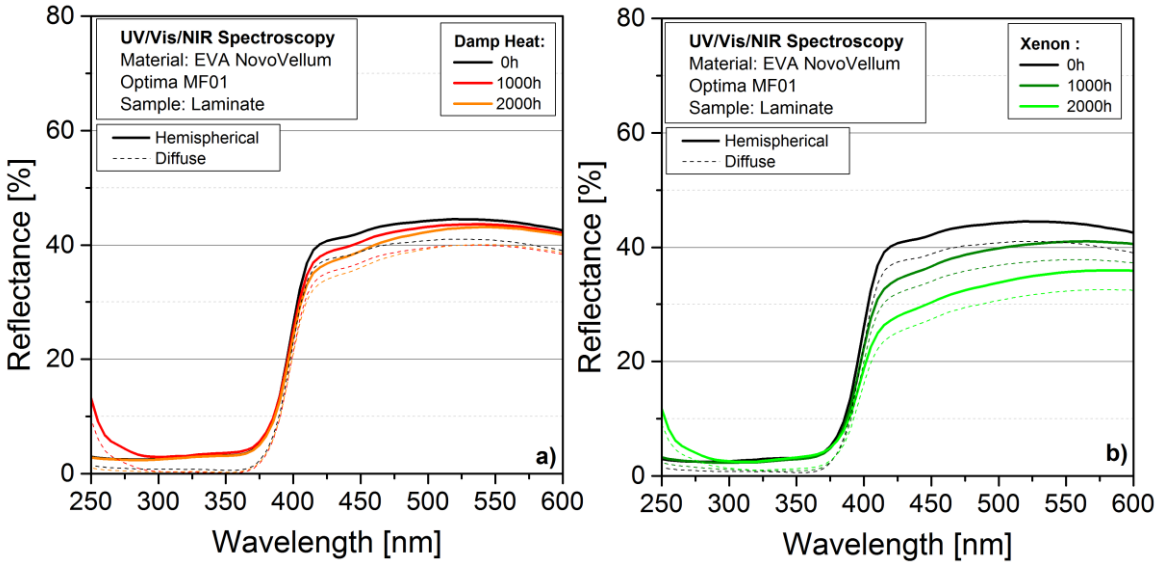

Figure 9.17: Reflectance spectra of EVA NovoVellum Optima MF01® laminates exposed to a) DH and b) XE.

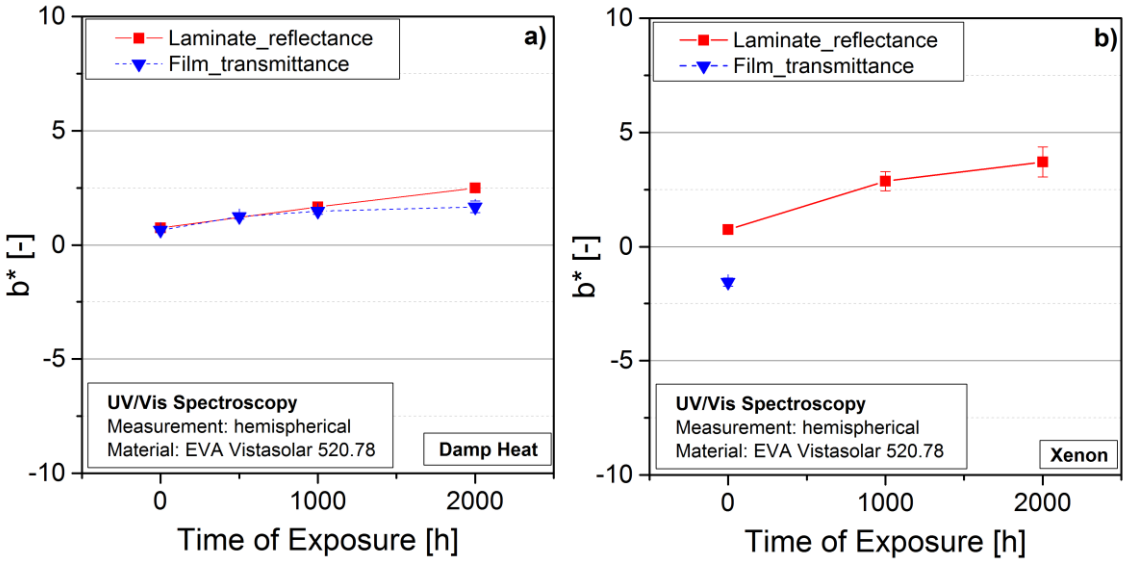

Figure 9.18: B* values of EVA Vistsolar 520.78® films and laminates exposed to a) DH and b) XE.

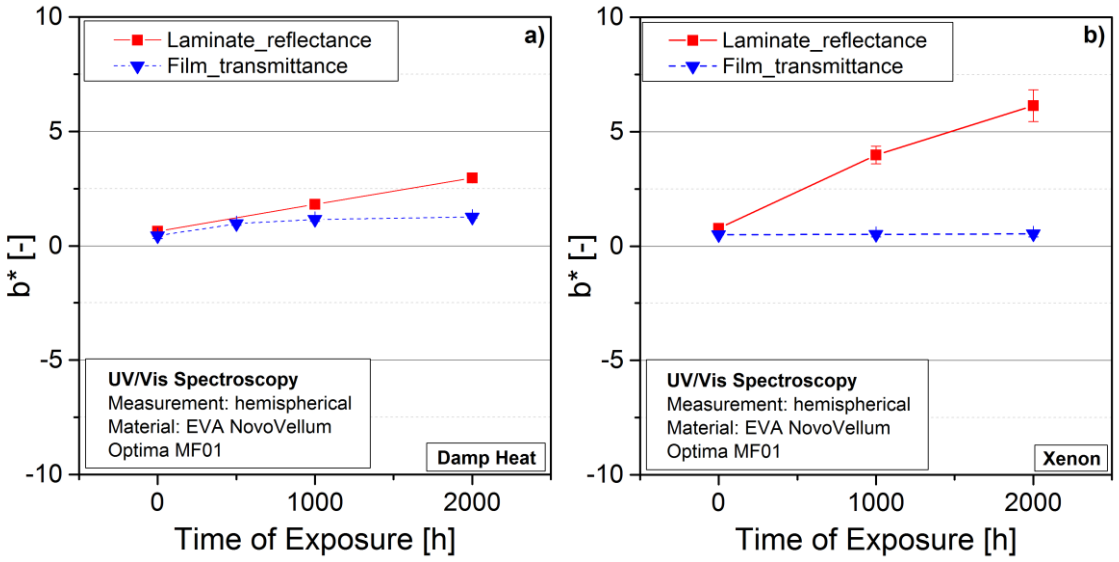

Figure 9.19: B* values of EVA NovoVellum Optima MF01® films and laminates exposed to a) DH and b) XE.

Table 9.6: Additive peaks of the HPLC-MS/UV of EVA Vistasolar 520.78® and NovoVellum Optima MF01® films and laminates exposed to XE.

Sample	Type	Sample Taking	Xenon Weathering [h]	Mass Spectrometry			UV Spectroscopy
				UV Absorber	HALS	Antioxidant	UV Absorber
				327, 248, 213 [m/z]	481, 356, 277, 265 [m/z]	688, 501 [m/z]	200 - 350 [nm]
EVA Vistasolar 520.78	Film	Centre	0	✓	✓	✓	✓
			1000	-	✓	-	-
			2000	-	-	✓	✓
	Laminate	Centre	0	✓	✓	✓	✓
			1000	-	✓	-	-
			2000	-	✓	✓	✓
		Edge	0	✓	✓	✓	✓
			1000	-	✓	✓	-
			2000	-	✓	✓	✓
EVA NovoVellum Optima MF01	Film	Centre	0	✓	✓	✓	✓
			1000	✓	✓	✓	✓
			2000	✓	✓	✓	✓
	Laminate	Centre	0	✓	✓	✓	✓
			1000	✓	✓	✓	✓
			2000	✓	✓	✓	✓
		Edge	0	✓	✓	✓	✓
			1000	✓	✓	✓	✓
			2000	✓	✓	✓	✓

Table 9.7: Crosslinking data of unaged EVA Visatasolar 520.78® and NovoVellum Optima MF01® (LO – Laboratory Oven, VLP – Vacuum lamination Press).

Material	Type	Sample Taking	Crosslinking	Peak Temperature [°C]	Curing Enthalpy [J/g]	Degree of curing [%]
EVA Vistasolar 520.78	Film	Centre	not crosslinked	149.0±0.33	17.90±0.28	-
	Film	Centre	LO	167.4±0.93	4.25±0.17	76.29
	Film	Centre	VLP	166.5±0.26	3.29±0.05	81.62
	Laminate	Edge	VLP	166.1±-	3.32±-	81.47
	Laminate	Centre	VLP	167.6±0.19	2.28±0.25	87.24
EVA NovoVellum Optima MF01	Film	Centre	not crosslinked	165.4±0.19	16.04±0.08	-
	Film	Centre	LO	167. 4±0.43	5.11±0.16	68.13
	Film	Centre	VLP	167.1±0.42	2.80±0.06	82.52
	Laminate	Edge	VLP	165.8±0.83	2.91±0.19	81.84
	Laminate	Centre	VLP	166.3±0.16	3.73±0.55	76.77

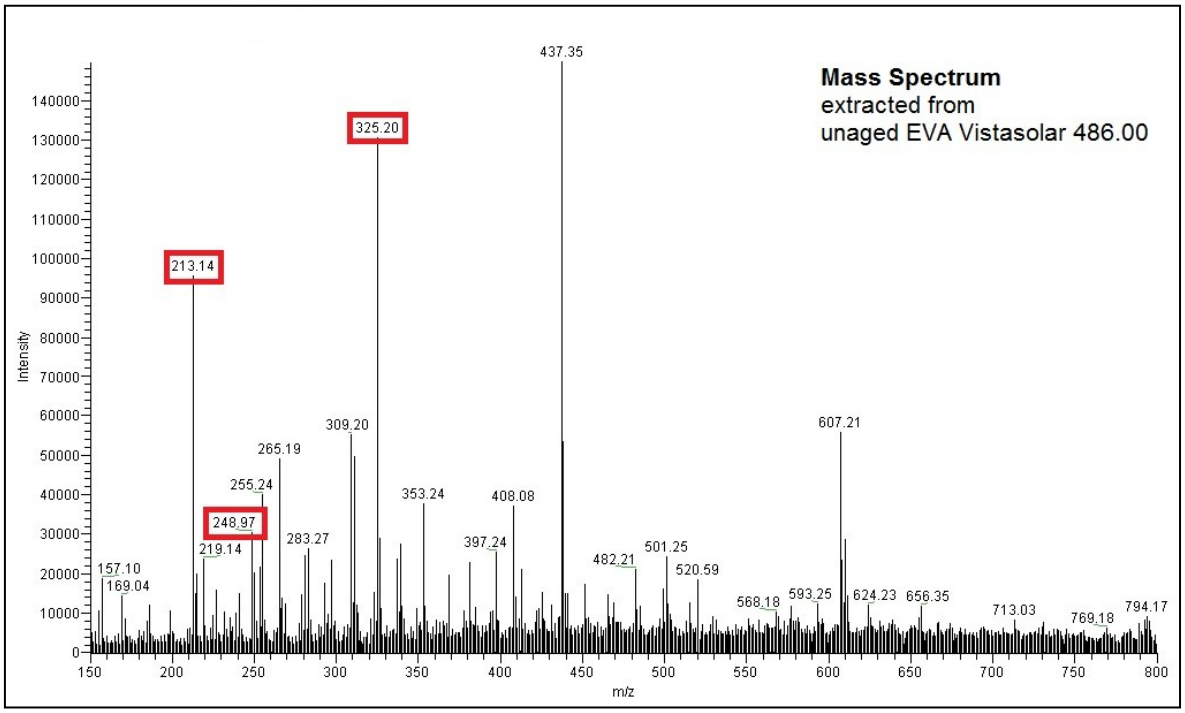

Figure 9.20: Mass spectrum of EVA Vistasolar 486.00 unaged film sample after extraction (negative mode).

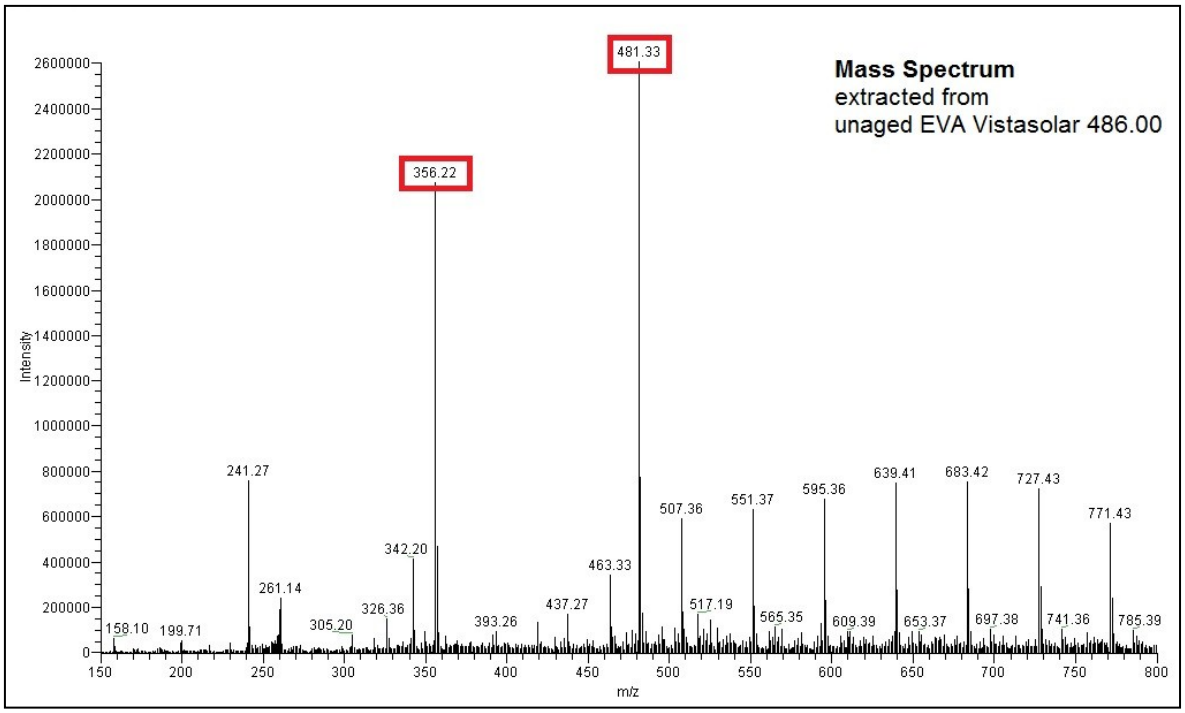

Figure 9.21: Mass spectrum of EVA Vistasolar 486.00 unaged film sample after extraction (positive mode).

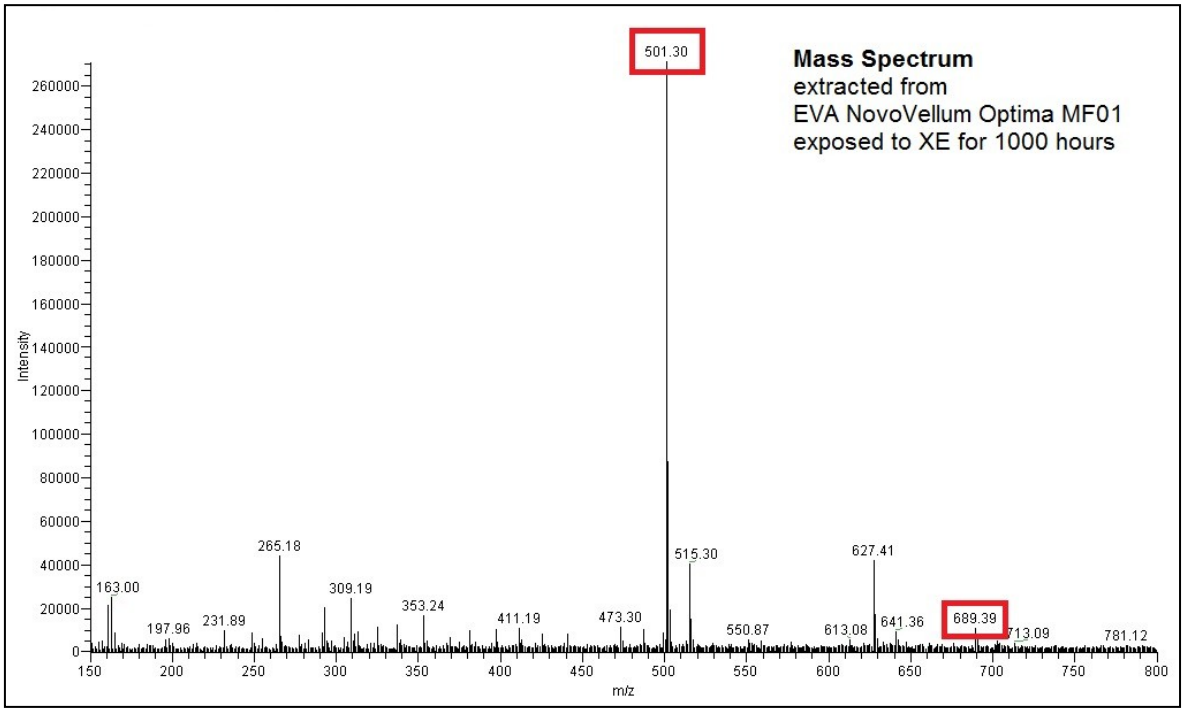

Figure 9.22: Mass spectrum of EVA NovoVellum Optima MF01 film exposed to XE for 1000 hours after extraction (negative mode).

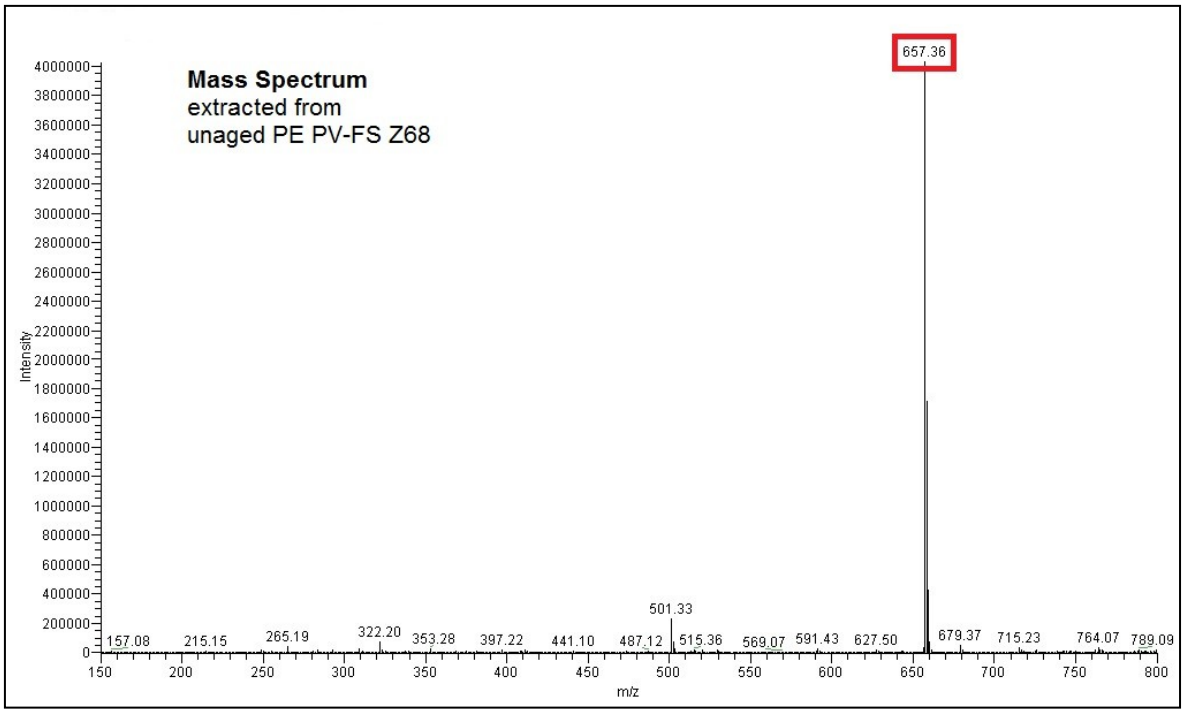

Figure 9.23: Mass spectrum of PE PV-FS Z68® unaged film sample after extraction (negative mode).

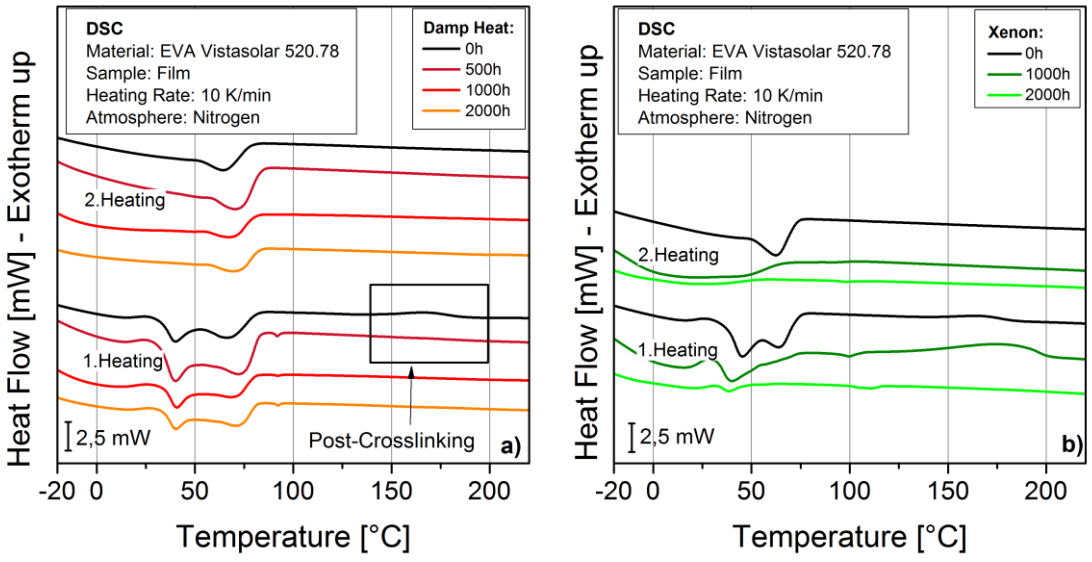

Figure 9.24: DSC curves of the first and second heating of EVA Vistasolar 520.78® films exposed to a) DH and b) XE.

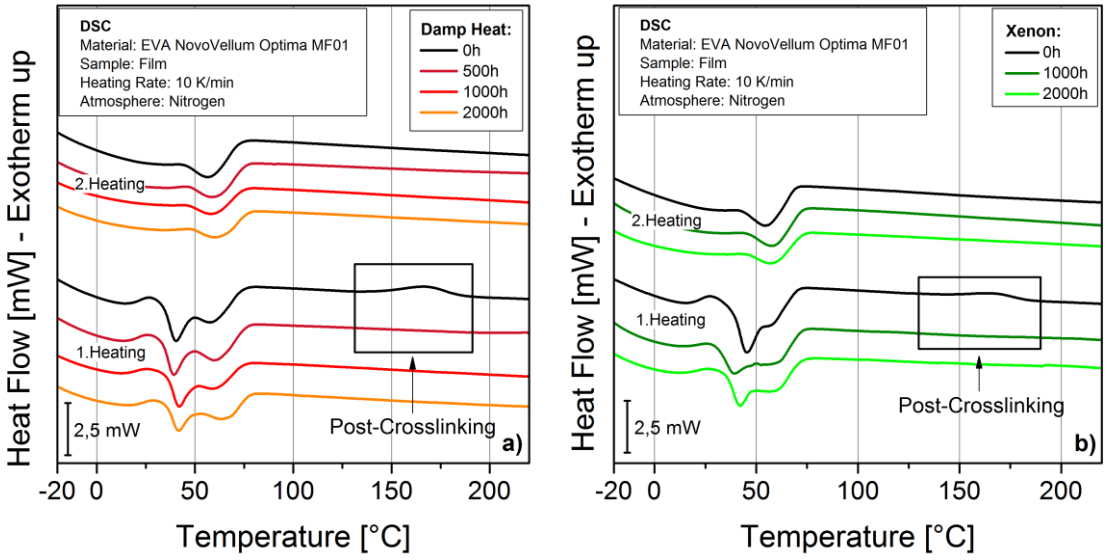

Figure 9.25: DSC curves of the first and second heating of EVA NovoVellum Optima MF01® films exposed to a) DH and b) XE.